N-alkanes phase change materials and their microencapsulation for thermal energy storage:

Peng, Hao; Zhang, Dong; Ling, Xiang; Li, Yang; Wang, Yan; Yu, Qinghua; She, Xiaohui; Li, Yongliang; Ding, Yulong

DOI:
10.1021/acs.energyfuels.8b01347

Review

n-alkanes phase change materials and their microencapsulation for thermal energy storage: a critical review

Hao Peng, Dong Zhang, Xiang Ling, Yang Li, Yan Wang, Qinghua Yu, Xiaohui She, Yongliang Li, and Yulong Ding

Energy Fuels, **Just Accepted Manuscript** • DOI: 10.1021/acs.energyfuels.8b01347 • Publication Date (Web): 30 May 2018

n-alkanes phase change materials and their microencapsulation for thermal energy storage: a critical review

Hao Peng[a*], Dong Zhang[a], Xiang Ling[a], Yang Li[a], Yan Wang[a], Qinghua Yu[b,c*], Xiaohui She[b], Yongliang Li[b], Yulong Ding[b]

[a] *Jiangsu Key Laboratory of Process Enhancement and New Energy Equipment Technology, School of Mechanical and Power Engineering, Nanjing Tech University, No. 30 Pu Zhu South Road, Nanjing 211816, P. R. China*

[b] *Birmingham Centre for Energy Storage, School of Chemical Engineering, University of Birmingham, Birmingham B15 2TT, UK*

[c] *School of Power and Mechanical Engineering, Wuhan University, Wuhan 430072, P. R. China*

[*] Corresponding author Tel: 86-25-83243112

Email address: phsight1@hotmail.com (H. Peng)

[*] Corresponding author Tel: 44-121-4146965

Email address: yqh2015@hotmail.com (Q. Yu)

Abstract: *n*-alkanes and their blends, are characterized as phase change materials (PCMs) due to their superior thermodynamic performances, for storing thermal energy in various practical applications (solar or wind energy). Such materials present some limitations, including lower thermal conductivity, supercooling, phase segregation, volume expansion, among others. To address these problems, microencapsulation of *n*-alkanes and their blends is being successfully developed. A considerable amount of works has been published in this regard. Hence, the aim of this review is focused on two aspects: summarize the pure *n*-alkanes and their blends PCMs; describe their microencapsulation. PCM-interesting characteristics (transition temperatures and enthalpies) of pure *n*-alkanes, multinary alkanes and paraffins (over 140 types) were listed, while the phase equilibrium evaluations of multinary alkanes were elaborated. The essential information: core and shell materials, crystallization and melting characteristics, encapsulation/thermal storage efficiencies, thermal conductivities and synthesis methods of microencapsulated *n*-alkanes and their blends were listed (over 200 types). A brief introduction of the synthesis methods, such as physical, chemical, physical-chemical and self-assembly processes, were presented. The characterization of microcapsules like thermal properties (phase change behaviors, thermal conductivity and thermal stability), physical properties (microcapsules size distribution & morphologies, efficiencies, mechanical strength and leakage) and chemical properties were discussed and analyzed. Finally, the practical applications of microencapsulated *n*-alkanes and their blends in the field of slurry, buildings, textiles and foam were reported.

***keywords*:** *n*-alkanes; phase change materials; microencapsulation; thermal energy storage; microencapsulated phase change materials

Nomenclature

C_n	pure *n*-alkanes	Δn_c	difference of carbon atom number
C_{2p}	even-numbered n-alkanes	*Acronyms*	
C_{2p+1}	odd-numbered n-alkanes	AFM	atomic force microscopy
d	diameter (m)	DSC	differential scanning calorimetry
E_{en}	encapsulation efficiency	FT-IR	fourier transformation infrared spectroscopy
E_{es}	energy storage efficiency	LHES	latent heat energy storage
FP	freezing point (˚C/K)	LFA	laser flash apparatus
LH	latent heat (J/g)	MPCM	microencapsulated phase change material
L_r	leakage rate	PCMs	phase change materials
M_t	mass of microcapsules after a certain time (g)	PSD	particle size distribution
M_0	mass of dried microcapsules (g)	SEM	scanning electron microscope
MP	melting point (˚C/K)	TES	thermal energy storage
n_c	carbon atom number	TGA	thermogravimetric analysis
T_{mo}	melting onset temperature (˚C)	WR	weight ratio
T_{mp}	melting peak temperature (˚C)	XRD	X-ray diffraction
T_{co}	crystallization onset temperature (˚C)	*Greek symbols*	
T_{cp}	crystallization peak temperature (˚C)	λ	thermal conductivity (W/m·K)
x	molar faction	*Subscripts*	
ΔH_m	melting enthalpy (J/g)	c	core
ΔH_c	crystallization enthalpy (J/g)	w	shell
ΔT_s	supercooling degree (˚C)	p	MPCM particles

1 Introduction

Latent heat energy storage (LHES) using phase change materials (PCMs) is one of the most efficient methods to store thermal energy, such as in the renewable energy systems (solar or wind energy), building, refrigeration, textile, among others. PCMs have the competitive merits of higher thermal storage capacity and isothermal behavior, in contrast to sensible heat energy storage. Admittedly, high energy storage density and capacity for charging and discharging are the desirable features of any heat/cold thermal energy storage (TES) systems. These systems with PCMs as thermal energy materials have been investigated for many years [1-12].

In general, the PCMs with solid-liquid phase change are mainly used to store thermal energy. Abhat [13] proposed a commonly used classification of these PCMs, organic and inorganic, as shown in Figure 1.

Among organic materials perspective for LHES, alkanes and their blends, many referred to as paraffins, are very attractive for using as PCM due to their superior thermodynamic performances, such as stable phase change, minimal supercooling, high enthalpies, among others. However, they also have limitations such as lower thermal conductivity, phase segregation and volume expansion in the process of phase transition. In addition, the leakage problem might occur during the melting process as well. These problems have been addressed by microencapsulated PCMs (MPCMs), which are named as 'PCM microcapsules'. Figure 2 shows a typical structure of microcapsules which pack the PCMs core individually with the organic or inorganic shell, and the microencapsulation working principle is introduced as well. The size of microcapsules can vary from few nanometers to microns. Microencapsulation helps to overcome low thermal conductivity by increasing the surface to volume ratio for the PCM. Microcapsules also provide a stable structure can therefore handle liquids as a solid material and prevent leakage of the melted PCMs.

Currently, even though many reviews with respect to the various PCMs for TES are available [2, 13-16], as well as the review articles related to the microencapsulation of PCMs [17-24], however, to the best of our knowledge, the literature review on the *n*-alkanes PCMs and their microencapsulation for TES is never found. Actually, the *n*-alkanes and their blends had been extensively studied for the past five decades, but only a few works were related to their PCMs utilization. In contrary, the researches in regard to microencapsulated *n*-alkanes and their blends as PCMs showed a prosperous upward tendency in recent decade. Undoubtedly, the researches on these two aspects supplement each other. Therefore, a main line to link these two aspects is essential (Materials →Microcapsules). To this end, this paper attempts to summarize the *n*-alkanes and their blends PCMs firstly (the blue dot line in Figure 1), and then describes their microencapsulation systematically. The synthesis techniques, thermal properties, physical properties and chemical properties are summarized and analyzed. Finally, the practical applications of microencapsulated *n*-alkanes and their blends in the field of slurry, buildings, textiles and foam were reported.

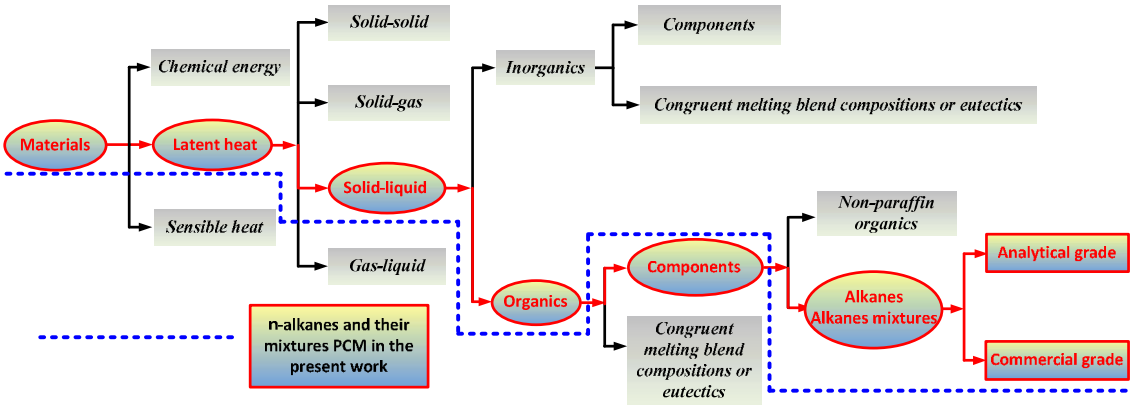

Figure 1 Classification of PCM (redrawn based on the Ref. [13])

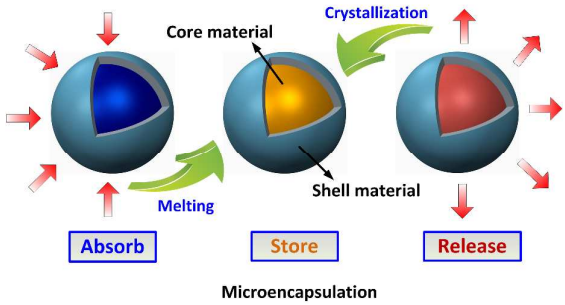

Figure 2 Structure and working principle of microencapsulation

2 Pure *n*-alkanes and their blends as PCMs

2.1 Pure *n*-alkanes

The properties of pure *n*-alkanes C_nH_{2n+2} (hereafter denoted by C_n) have been studied extensively in literatures, which include melting point, enthalpy, heat capacity, conductivity, density, among others. Among these properties, melting point and enthalpy are the PCM-interesting characteristics that predominantly affect the performance of a TES system.

In regard to these two properties, the most comprehensive review of 67 C_n (carbon number C_1~C_{390}) was presented by Dirand et al. [25]. In addition to this, a part of C_n (within the range of carbon number in Dirand et al's review) were measured by Himran et al. [26], Rajabalee et al. [27], Ventola et al. [28-29], Mondieig et al. [30] and Huang et al. [31] using DTA or DSC instruments as well.

Dirand et al [25] distinguished the thermodynamic data of the C_n into four parts: melting points, enthalpies, order-disorder (o-d) transition enthalpies and disorder-disorder (d-d) transition temperatures. This is due to the fact that the C_n have complex polymorphic nature with the existence of a mesostate, therefore, the phase change processes were very complicated and simply characterized by a solid-solid and a solid-liquid equilibrium transitions at constant temperature [25, 30]. Regardless of the complex phase change behavior of C_n, Figure 3 depicted the two dominating properties (melting points and enthalpies) of C_n from octane to pentacontane (C_8~C_{50}) by summarizing and averaging the available data obtained by the above mentioned literatures. It should be noted that the enthalpies showed in Figure 3 are the solid-solid and solid-liquid transition enthalpies. The data accuracies in Figure 3 were estimated, the melting points and the enthalpies with the deviations of ±1% and ±3%, respectively.

Except for thermodynamic properties, the thermophysical properties (specific heat capacity, density, thermal conductivity, among others) of C_n were studied by Huang et al. [31], Atkinson et al. [32], Johansen [33], Watanabe [34] and Vargaftik [35], and a summarized review with respect to these properties was conducted by Kenisarin [36].

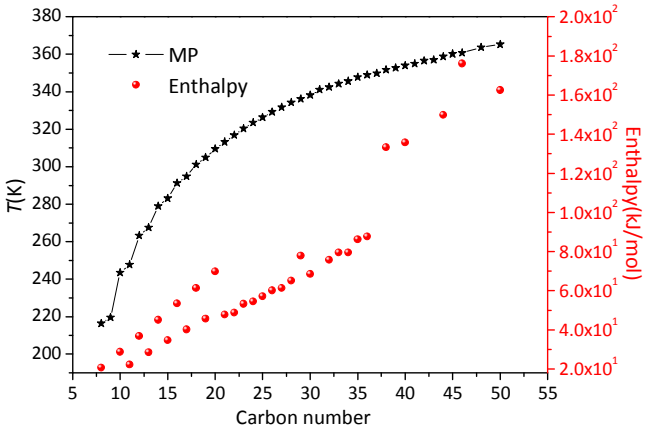

Figure 3. Melting points and enthalpies of some C_n on the basis of Dirand et al. [25] (from C_8 to C_{50})

2.2 Multinary C_n

Generally, the C_n have specific melting points and enthalpies, which limit their practical applications. However, their blends (binary, ternary or multinary systems) have proved the greater value as tunable PCMs for TES systems because the temperature range are substantially enlarged and enriched.

If following the permutation and combination theory, the binary and ternary mixtures of the C_n (41 types in the

present work) should have $C_{41}^2 + C_{41}^3 = 820 + 10660 = 11480$ groups. It is absolutely impossible to accomplish the studies for these huge groups of combination. Dirand et al. [37] pointed out that the behavior of mixtures of C_n's have to obey the four laws of thermodynamics: (a) Phase stability; (b) Miscibility in the solid state; (c) Size of molecules; and (d) Thermodynamic representation of phase equilibrium. According to these fundamental laws, the possible combinations are therefore dramatically reduced.

2.2.1 ***Binary systems***

Alkanes have complex crystalline structures for the odd and even numbers of carbons in the chain. Dirand et al. [37] and Craig et al [38] proposed the following classification with the key structures from C_{13}-C_{60}. The odd-number C_n have 'C_{23}-*Pbcm*' orthorhombic structure (C_{13}-C_{41}), as shown in Figure 4(a), the even-number C_n have 'C_{18}-*P*1' triclinic structure for C_{14}-C_{26}, as shown in Figure 4(b), 'C_{36}-$P2_1/a$' monoclinic structure for C_{28}-C_{36}, '*Pbca*' orthorhombic structure for C_{38}, C_{40} and C_{44}, and 'C_{36}-$Pca2_1$' orthorhombic structure for C_{46}, C_{50} and C_{60} [38]. These different structures will influence their solid state miscibility as well as the phase change characteristics of their mixtures. Karvchenko [39] proposed a basic rule to predict the miscibility in the binary systems of C_n from the different factor of the molecule lengths, as shown in Table 1.

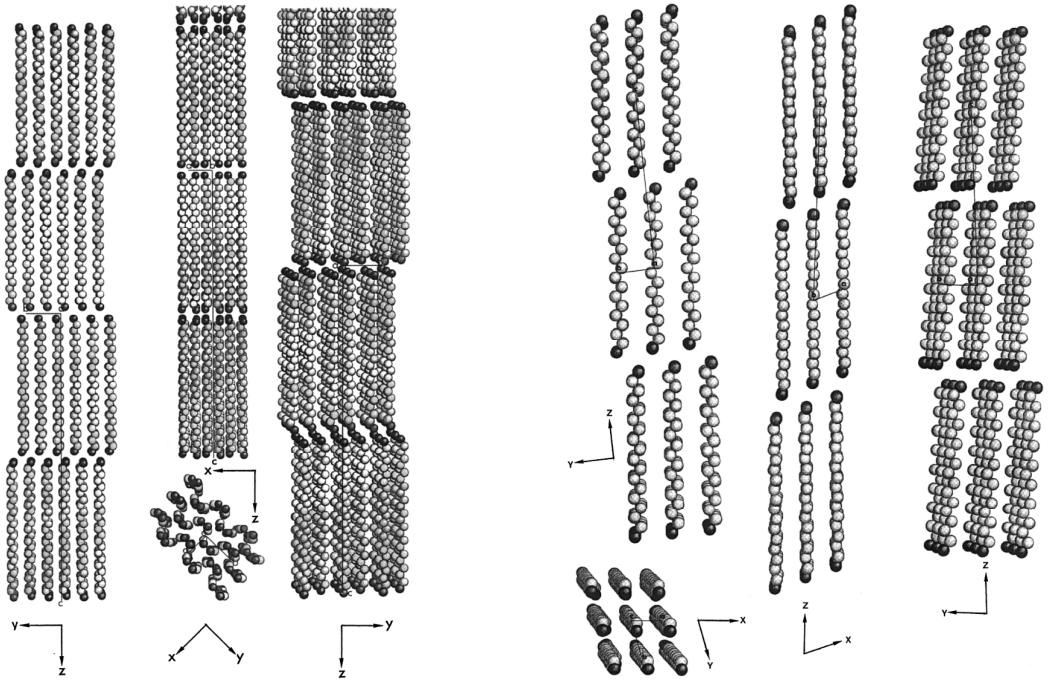

(a) 'C_{23}-*Pbcm*' key structure of odd-numbered C_{2p+1}'s (11≤2p +1≤41)

(b) 'C_{18}-*P*1' key structure of even-numbered C_{2p}'s (6≤2p ≤26)

Figure 4 Key structures of odd-numbered and even-numbered C_n [38]

Table 1. Miscibility of binary C_n mixtures versus number difference of Carbon atoms in the solid state at room temperature according to Kravchenko's predictions [39] (n_c is the carbon atoms numbers)

$\Delta n_c = n_c - n_c'$	Total miscibility	Partial miscibility	No miscibility	Comments
1	n_c>16[1]	17 > n_c > 7	n_c<8	[1] if the two consecutive C_{2p} and C_{2p+1} do not have the same crystalline structure, they cannot form a continuous solid solution.
2	n_c>33	34 > n_c > 13	n_c<14	
4	n_c>67	68 > n_c > 27	n_c<28	

Based on this rule, the studies related to binary mixtures of C_n's as PCMs were performed. The engineering blends prioritization for a specific application temperature, the blends phase equilibrium evaluation to select congruent melting or eutectic type of more suitable compositions as potential PCMs, are the primary focused issues in this review. Gunasekara et al. [40] presented a review of phase equilibrium in the design of suitable blended PCMs for TES, and summarized a series of C_n blends systems. However, some of the C_n blends were still missing. Therefore, based on their work, Table 2 summarized more comprehensive binary C_n mixtures (C_8~C_{50}) by listing the PCM-interesting characteristics, and the temperature range is from 211.7K to 359.1K (-61.5˚C~86.0˚C) [25-28, 39-61]. The compositions are either weight, molar, or volumetric percentage, while the enthalpy are either kJ/kg or kJ/mol.

Table 2. Thermodynamic characteristics of binary mixtures of C_n's PCM for TES based on Ref. [40] (NA: not available; MP: melting point)

No.	Binary	Characteristics[2]	Composition (^{w}w%, ^{a}mol%, ^{v}V%)	MP(K)	Enthalpy (^{k}kJ/kg, ^{m}kJ/mol)	Year	Ref.
1	C_8-C_{10}	E	$^{a}16C_{10}$	211.7	NA	1995	27
2	C_{10}-C_{12}	E	$^{a}20C_{12}$	238.2	NA	2002	29
3	C_{11}-C_{12}	P	$^{a}65C_{12}$	251.2	NA		
4	C_{11}-C_{13}	E	$^{a}23C_{13}$	246.1	NA		
5	C_{11}-C_{18}	IIM[3]	$^{w}21C_{18}$	279.6	NA	2015	41
6	C_{12}-C_{13}	ICM	$^{a}17.7C_{13}$	257.5	^{k}185	2017	42-43
7	C_{12}-C_{14}	E	$^{a}19C_{14}$	258.2	NA	1996	44
8	C_{12}-C_{15}	E	$^{a}24\ C_{15}$	258.6	^{m}25.8	1998	45
9	C_{13}-C_{14}	P	$^{a}25C_{13}$	272.0	^{k}212-110	2002	29
10	C_{13}-C_{15}	E	$^{a}20C_{15}$	266.4	^{m}26	1998	46
11	C_{14}-C_{15}	E	$^{a}15C_{15}$	276.2	NA	2005	47
12	C_{14}-C_{16}	E	$^{v}8.33C_{16}$	274.9	^{k}156.2	1999	48
		ICM	$^{a}6.74C_{16}$	274.9	^{k}146	2003	49
		ICM	$^{a}7.7C_{16}$	275.0	^{k}146	2004	50
		E	$^{a}17.5C_{16}$	276.2	NA	2004, 2005	30, 47
13	C_{14}-C_{18}	E	NA	275.3	^{k}227.5	2004	51
14	C_{14}-C_{21}	E	NA	278.6	^{k}200.3		
15	C_{14}-C_{22}	E	NA	278.7	^{k}234.3		
16	C_{15}-C_{16}	P	$^{a}86C_{16}$	287.2	NA	1997	52
17	C_{15}-C_{17}	ICM	$^{a}12.5C_{17}$	281.2	NA	1996, 1997	44, 52
18	C_{15}-C_{18}	E	NA	282.2	^{k}271.9	2007	53
19	C_{15}-C_{21}	E	$^{a}6.5C_{21}$	281.5	^{k}163	1996	44
20	C_{15}-C_{22}	E	NA	281.6	^{k}214.8	2004	51
21	C_{16}-C_{17}	E	$^{a}8.1C_{17}$	289.3	NA	1997, 2004	30, 52
22	C_{16}-C_{18}	E, P	$^{a}12.5C_{18}$,$^{a}78C_{18}$	288.2, 295.3	NA	2004	30
23	C_{16}-C_{28}	E	$^{a}5C_{28}$	290.4	NA	2000	54
24	C_{16}-C_{41}	E	$^{a}4C_{41}$	290.5	NA		

25	C_{17}-C_{18}	P	[a]88C_{18}	298.3	NA	2004	[30]
26	C_{17}-C_{19}	ICM	[a]5C_{19}	295.0	[m]38.9	1996	[55]
27	C_{18}-C_{19}	E	[a]6C_{19}	299.3	NA	2004	[30]
28	C_{18}-C_{20}	E, P	[a]6C_{20}, [a]90C_{20}	301.2, 308.4	NA		
29	C_{18}-C_{21}	E	NA	299.2	173.9	2004	[51]
30	C_{18}-C_{22}	E	NA	300.2	203.8		
31	C_{19}-C_{20}	P	[a]94C_{20}	308.3	NA	2004	[30]
32	C_{19}-C_{21}	ICM	[a]10C_{21}	305.5	[m]43.5	1985	[56]
33	C_{20}-C_{21}	E	[a]5C_{21}	308.5	NA	2004	[30]
34	C_{20}-C_{22}	E	[a]3C_{22}	309.5	NA	1996	[44]
35	C_{21}-C_{22}	P	[a]5C_{22}	316.8	[m]48.7	1999	[57]
36	C_{21}-C_{23}	P	[a]1.5C_{23}	313.7	NA	1996	[58]
37	C_{22}-C_{23}	IIM[3]	[a]20C_{23}	317.4	NA	1998	[59]
38	C_{22}-C_{24}	IIM[3]	[a]20C_{24}	317.9	NA	2004	[30]
39	C_{23}-C_{24}	IIM[3]	[a]20C_{24}	320.6	NA		
40	C_{23}-C_{25}	IIM[3]	[a]20C_{25}	321.9	[m]52.6	1999	[60]
41	C_{25}-C_{27}	P	[a]96C_{27}	330.3	NA	2004	[30]
42	C_{25}-C_{28}	ICM	24.6C_{28}	327.0	NA	1995, 1996	[61-62]
43	C_{26}-C_{28}	P	[a]93C_{28}	333.3	[m]62.3	2004	[63]
44	C_{28}-C_{41}	E	[a]8C_{41}	337.2	NA	2000	[54]
45	C_{32}-C_{34}	IIM[3]	[a]20C_{34}	343.0	[k]172	2005	[28]
46	C_{32}-C_{36}	ICM	[a]5C_{36}	342.2	[k]168		
47	C_{34}-C_{36}	IIM[3]	[a]20C_{36}	346.5	[k]171		
48	C_{36}-C_{40}	PIP	[a]50C_{40}	350.2	[k]223		
49	C_{40}-C_{44}	PIP	[a]52C_{44}	355.2	[k]229		
50	C_{44}-C_{50}	E	[a]9C_{50}	359.1	NA	1995, 1996	[61-62]

[2] E-eutectic; P-peritectic; ICM-isomorphous congruent minimum melting; IIM-isomorphous incongruent melting (ascendant type); PIP-partially isomorphous peritectic

[3] in IIM type, the melting point is extracted from the proposed data in literature for molar percentage of ~20 mol% in *n*-alkanes with longer chains.

As shown in Table 2, a part of studies aimed at finding the right compositions in the right C_n blends for PCM utilization. The first priority is to adjust the melting point of blends at the required temperature level in practical application, and then to choose the blends having a narrow thermal window that can store or release 95% of the total latent heat. Simultaneously, several studies with respect to the phase equilibrium were proposed as well, and potential PCM materials for TES might be found in light of some features (eutectic or peritectic point) in binary solidus-liquidus phase diagrams. Among these investigations focused on engineering or potential binary blended PCMs, systematic evaluations on a group of substantial binary mixtures were conducted by Ventola et al. and Mondieig et al. [28-30]. Mondieig et al. [30] ascertained that the group of C_n had a rich, complex polymorphic nature with the existence of mesostate. This mesostate regarded as rotator (R) is a crystalline state, having rotational freedom along their long axes, between the normal, ordered solid state and liquid. As a consequence, the C_n blends appeared

very complex phase change behaviors (melting or freezing types), and sometimes, the confusion conclusions presented by different investigators are inevitable.

Generally, as mentioned by Gunasekara et al. [40], it is accepted that the binary systems belonging to the completely or almost completely isomorphous congruent types are C_{15}-C_{17} [44, 52], C_{17}-C_{19} [55], C_{19}-C_{21} [56], C_{25}-C_{28} [61-62], C_{32}-C_{36} [28], the binary isomorphous incongruent melting systems (ascendant type) found are C_{11}-C_{18} [41], all the odd-odd and odd-even blends from C_{22} to C_{24} [30, 59], C_{23}-C_{25} [60], C_{32}-C_{34} and C_{34}-C_{36} [28]. The remainders are partially isomorphous. The phase change characteristics of these binary C_n blends include: eutectic, peritectic, isomorphous congruent melting (ICM), isomorphous incongruent melting (IIM) and partially isomorphous peritectic (PIP) [40], which are elaborated in Table 2. Actually, most of these phase change characteristics are deduced from the binary phase diagram, and hence Figure 5 depicted the typical phase diagrams of eutectic system (C_8-C_{10}), peritectic system (C_{15}-C_{16}) and ICM system (C_{15}-C_{17}) that were redrawn by extracting the figure data from the original literatures [27, 52].

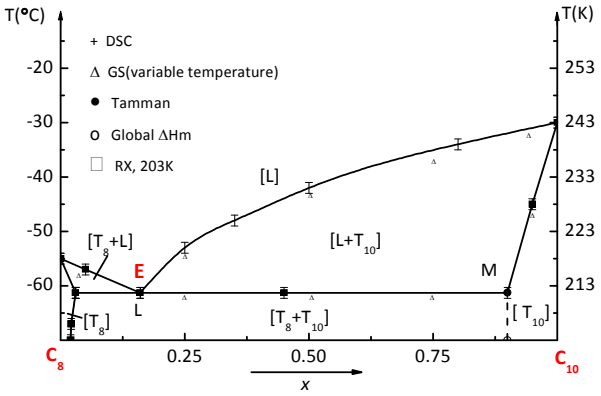

(a) C_8-C_{10} (redrawn based on Ref.[27])

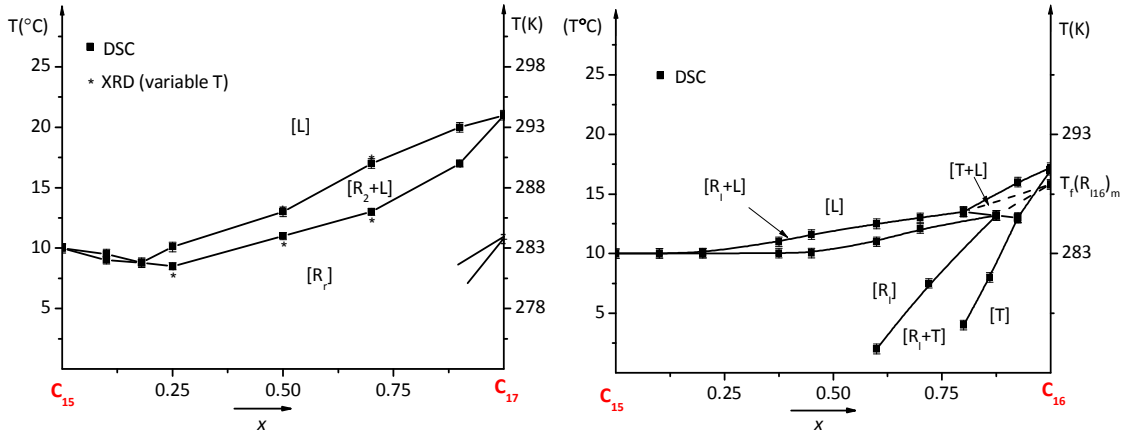

(b) C_{15}-C_{17} and C_{15}-C_{16} (redrawn based on Ref.[52])

Figure 5 Phase diagrams of binary systems C_8-C_{10}, C_{15}-C_{17} and C_{15}-C_{16} (redrawn based on Ref. [27] and Ref. [52])
(a) C_8-C_{10} (redrawn based on Ref.[27]) (b) C_{15}-C_{17} and C_{15}-C_{16} (redrawn based on Ref.[52])

The most frequently studied binary C_n system is C_{14}-C_{16} [30, 40, 47-50], however, the reported phase change characteristics of these works have discrepancies. For example, it has been reported with a eutectic [48], an isomorphous congruent minimum melting type [49 50], and as a partially isomorphous system with a eutectic and a peritectic [30]. The temperatures of these eutectic/congruent melting points are rather close, but the compositions vary from each other (in Table 2). Actually, the confusion in regard to the C_{14}-C_{16} binary system is the distinction

between a partially isomorphous eutectic and an isomorphous congruent minimum melting type. Overall evaluations including crystallography, miscibility and phase equilibrium of C_{14}-C_{16} blends were conducted by Ventolà et al. [29] and Mondieig et al. [30], which are crucial for a deep understanding of the system's phase change behaviors. As mentioned in Craig et al's work [38], both components of the C_{14} and C_{16} have '*P*1' triclinic structure. Hence, He et al. [48] pointed out that the C_{14}-C_{16} binary is an isomorphous system and found a eutectic point of the laboratory-grade C_{14}-C_{16} mixture occurs at 91.67% C_{14} (8.33% C_{16}), and the phase change temperature at this point is approximately 1.7°C. But four years later, they ascertained that this point is not a eutectic point [49]. Subsequently Mondieig et al. [30] said that the system should be partially isomorphous with a eutectic and a peritectic, and there were a eutectic three-phase equilibrium (*x* is from 0.09 to 0.30) and a perictectic one (*x* is from 0.46 to 0.93) at high temperature side. The other confused binary system is C_{12}-C_{13}. Yilmaz et al. [64] presented the liquidus line of C_{12}-C_{13} and found a maximum melting point of -3.3°C at 80% C_{13}, whereas Ventolà et al. [29] identified a eutectic composition in this system. Most recently, Gunasekara et al. [40, 42-43] carried out an overall experimental investigation of C_{12}-C_{13}, The obtained phase diagram indicated a congruent minimum-melting solid solution and polymorphs phases at lower temperatures. However, the system does not represent a eutectic, which is against to phase diagrams proposed by the Yilmaz et al. [64] and Ventolà et al. [29].

Thanks to these discrepancies and confusions, a full understanding of the phase equilibrium of binary C_n, primarily the construction of the solidus is required, for the sake of seeking the appropriate PCM for a specified TES system.

2.2.2 Multinary systems

Compared to the binary systems, a relatively small number of investigations with respect to the ternary and multinary systems were performed. Table 3 summarized the PCM-interesting characteristics of ternary mixtures of C_n (C_{11}~C_{36}). Since a set of compositions for these ternary systems were reported in the literatures, in order to select a PCM with similar phase change behavior of a pure compound [29], the compositions with narrowest thermal window were listed in Table 3. Actually, few works were related to the right compositions selection of PCM, except for Ventolà et al.[28-29]. Ventolà et al.[28-29] proposed some potential PCM compositions to cater to the application temperatures (-11˚C and 70~85˚C), within a narrow thermal window, storing or releasing 95% of the total heat. They also indicated that the thermal window should be as small as possible (just 1~2˚C) for most of practical applications. Multinary C_n systems were conducted by Craig et al. [65] (C_{18}-C_{19}-C_{20}-C_{21}-C_{22}, C_{19}-C_{20}-C_{21}-C_{22}-C_{23}, C_{20}-C_{21}-C_{22}-C_{23}-C_{24}, C_{21}-C_{22}-C_{23}-C_{24}-C_{25}, C_{22}-C_{23}-C_{24}-C_{25}-C_{26}), however, the main content was to determine the unit-cell parameters and to present the crystallographic high resolution synchrotron diffraction data, which was irrelevant to the present subject.

As a consequence, as most of ternary or multinary C_n mixtures are not directly PCM-ideal materials (like congruent melting or eutectic types), the phase change characteristics, such as phase diagrams, phase separation, among others., need to be better evaluated to confirm their potential and suitability as PCMs.

Table 3. Thermodynamic characteristics of ternary mixtures of C_n's PCM for TES(NA: not available)

No.	Ternary	Composition (mol%)	MP (K)	Thermal Window $\delta_{95\%}$(K)	Enthalpy (kJ/kg)	Year	Ref.
1	C_{11}-C_{12}-C_{13}	$3C_{11}$, $85C_{12}$, $12C_{13}$	257.1	1.2	141.3	2002	[29]
2	C_{12}-C_{13}-C_{14}	$51C_{12}$, $40C_{13}$, $9C_{14}$	261.4	1.6	144.1		

3	C_{14}-C_{15}-C_{16}	73C_{14}, 14C_{15}, 13C_{16}	276.3	0.5	NA	1999	[66]
4	C_{15}-C_{16}-C_{17}	77C_{15}, 7C_{16}, 16C_{17}	283.2	0.6	NA	1997	[52]
5	C_{16}-C_{17}-C_{18}	80C_{16}, 10C_{17}, 10C_{18}	289.5	NA	NA	1999	[66]
6	C_{18}-C_{19}-C_{20}	90C_{18},5C_{19}, 5C_{20}	300.6	0.2	NA		
7	C_{19}-C_{20}-C_{21}	90C_{19},5C_{20}, 5C_{21}	305.5	0.2	NA		
8	C_{16}-C_{28}-C_{41}	50C_{16}, 24C_{28}, 26C_{41}	347.7	NA	NA	2000	[54]
9	C_{22}-C_{23}-C_{24}	48C_{22}, 48.5C_{23}, 3.5C_{24}	319.0	NA	NA	1999	[67]
10	C_{32}-C_{34}-C_{36}	34C_{32}, 31C_{34}, 35C_{36}	345.2	1.0	NA	2005	[28]

Paraffins and paraffin waxes consist of a mixture of hydrocarbon molecules containing between twenty to forty carbon atoms (80%~95% C_n), which are produced from petroleum, coal or oil shale. Therefore, paraffins can be identified as the unrefined alkanes blends. Generally, paraffins are relatively cheap in comparison with pure C_n and have high enthalpies, which are the common PCMs utilized in practical applications. The melting points and enthalpies for laboratorial and commercial paraffins PCMs have been reported extensively nowadays [68 69 70].

2.3 Summaries and discussions

In PCM literature with C_n and their blends as a whole, it is well known that the C_n have the merits of chemically stable, noncorrosive and high enthalpies, in particular are regarded as the ideal PCMs. However, the specific melting points and relative high price limit their practical applications. Simultaneously, the C_n blends can provide suitable materials to work as PCM if two conditions are respect. The first is to find the right compositions in the right C_n blends to obtain the melting point at the required level of temperature. The second one is to choose blends having a narrow thermal window that can store or release 95% of the total latent heat.

To employ C_n blends as PCM with robust performances, an overall understanding of their phase diagrams and phase change behaviors is crucial. A narrow thermal window (phase change temperature range) with no phase separation is the properties pursued for an ideal and functional PCM.

Generally, the phase diagrams of C_n blends are complex, and previous works showed that congruent melting compositions are definitely the most expected for PCMs, with the solid and liquid in equilibrium having the same composition. Eutectics, peritectics, ICM, IMM, PIP types of phase change characteristics are elaborated through phase diagrams in this review as well. Among these phase change behaviors, eutectics and peritectics have been considered largely from a PCM selection perspective; even though peritectics are not ideal because of the supercooling and phase separation might occur in peritectics nonequilibrium cooling process. Furthermore, the literature assessment presented here, mostly focused on the binary C_n systems. Some popular systems to be considered as PCM were specified, for example, C_{14}-C_{16}, C_{15}-C_{18}, C_{15}-C_{21}, C_{18}-C_{21}, C_{20}-C_{22}, C_{26}-C_{28}, and C_{44}-C_{50}, among others. The ternary systems for PCMs were rarely involved, except for the C_{11}-C_{12}-C_{13}, C_{12}-C_{13}-C_{14} and C_{32}-C_{34}-C_{36}.

Despite numerous studies have proposed, there is still a lot to explore. First, it is interesting that the binary system with a large discrepancy in chain length ($\Delta n_c \geq 6$) still showed a eutectic characteristic (C_{11}-C_{18}, C_{14}-C_{21}, C_{14}-C_{22}, C_{15}-C_{21}, C_{15}-C_{22}, C_{16}-C_{28}, C_{16}-C_{41}, C_{28}-C_{41}), which does not respect the basic laws revealed by Dirand et al. and Karvchenko [37, 39]. Therefore, a huge amount of new combinations can be created, and then deserve further investigations. Second, ternary systems are the neglected category in the PCM-context (few works published), but are promising for exploration in the future. Finally, the phase equilibrium identification of C_n blends is done to

various levels by different works; some are very comprehensive, while some are just preliminary. The confusions in regard to the phase change characteristics of blends C_{14}-C_{16}, C_{12}-C_{13} mentioned above are attributed to this issue. To obtain PCM-design conclusions of a blend, a comprehensive phase equilibrium study is fundamental, which may require multiple testing technologies: DSC, TGA, XRD, FT-IR, and SEM, among others. C_n blends could be quite complex, e.g. with intricate metastable phases such like mesostates, that require such a combination of detection techniques. Therefore, the comprehensive studies in related to phase equilibrium of C_n blends are worth improving.

3 Microencapsulation of n-alkanes and their blends in PCMs design

This section has three sub-sections, which includes: Summarization of microencapsulated C_n and their blends, Synthesis methods for C_n and their blends microcapsules, and Characterization of microencapsulated C_n and their blends.

The first sub-section 3.1 summarized the microcapsules with various core materials: C_n, Paraffins, C_n blends and C_n mixed with other compositions (Tables 4-7). Based on the information in Tables 4-7, the sub-section 3.2 described the synthesis methods and elaborated some typical examples in regard to these methods. The last sub-section 3.3 discussed the characterization of microencapsulated C_n and their blends.

3.1 Summarization of microencapsulated C_n and their blends

This sub-section summarized the microcapsules with various core materials: C_n, Paraffins, C_n blends and C_n mixed with other compositions, for their use as PCM in practical applications from 2007 to 2017. Their most important information chosen here are: compositions of both core and shell materials, crystallization and melting characteristics, encapsulation/energy storage efficiency, thermal conductivity and synthesis method. Their remainder information, for instance, shell characterization, chemical properties, thermal reliability, applications, among others, are discussed in sub-sections 3.3 & Section 4.

An enormous amount of experimental results are available concerning the microencapsulated C_n and their blends as PCMs. To bring-about their PCM design highlights, the data in the following tables are thus chosen along certain basic concepts regarding: microcapsules synthesis methods, microcapsules modification methods, and the multinary core or shell materials respectively.

- In regard to the synthesis methods of microcapsules. There are many different synthesis methods of microcapsules, which need various chemical reagents, such as initiator, cross-linking agent, nucleating agent, monomer, surfactant, emulsifier, among others. The different mass fraction of these chemical reagents will cause various core-shell ratio, shell morphology, encapsulation efficiency (section 3.3.3.2), among others. In this situation, the information of microencapsulation with highest encapsulation efficiency are chosen and listed in the tables. Normally, the highest encapsulation efficiency microcapsules also have highest enthalpy of melting and crystallization for the same core in most of studies.
- In regard to the modification of microcapsules. For instance, nano-particles can be used to enhance the shell/core thermal conductivities or to intensify the strength of shell structure; graphene oxide can be used to prevent the leakage of microencapsulation, among others. In this circumstance, the information of microcapsules with and without modified materials are listed in the tables.
- In regard to the multinary core or shell materials. Some literatures presented the microencapsulation with multi-compositions core or shell. In this situation, all the combinations are listed in the tables.

3.1.1 C_n and modified C_n microcapsules

Table 4. Characterization of C_n and modified C_n microcapsules (NA: not available)

Shell		Core	Crystallization		Melting		E_{en} & E_{es}	λ	Synthesis method	Ref.
Components[4]	WR (w/w%)	Components	FP (˚C)	LH (J/g)	MP (˚C)	LH (J/g)	(%)	(W/m·K)		
MF		C_{12}	-29.30	187.2	-7.80	187.2	90.0	NA	*in-situ polymerization*	[71]
AS		C_{14}	[e]1.98	111.0	[e]6.02	113.5	70.2	NA	*phase separation*	[72]
ABS			[e]1.37	104.8	[e]5.91	107.1	66.3			
PC			[e]2.23	110.9	[e]7.16	113.2	74.7			
PUF		C_{14}	2.81	134.5	9.01	134.2	61.8	NA	*in-situ polymerization*	[73]
PS-co-EA	NA	C_{14}	-0.18	184.9	7.97	182.7	79.3	NA	*emulsion polymerization*	[74]
SiO_2		C_{14}	[e]-0.39	139.9	[e]2.39	140.1	62.0	0.1250~0.1510	*interfacial polymerization*	[75]
$CaCO_3$		C_{14}	[e]1.58	58.2	[e]5.35	58.5	[es]25.9	0.4920~0.6500	*self-assembly*	[76]
PMMA-co-PUF	28.8:71.2	C_{14}	3.70	183.2	9.60	185.9	87.5	NA	*in-situ polymerization*	[77]
PMMA			2.80	133.8	8.10	133.6	63.4			
PUF			3.30	159.5	8.30	171.8	78.5			
PMMA		C_{15}	[e]6.10	[e]119.0	10.00	107.0	NA	NA	*suspension polymerization*	[78]
PS-co-EA	NA	C_{15}	5.20	127.9	11.60	121.8	69.2	NA	*emulsion polymerization*	[74]
PFR		C_{16}	3.91	96.5	17.29	98.1	38.0	NA	*phase separation*	[79]
PS		C_{16}	NA	NA	22.74	80.3	NA	NA	*suspension polymerization*	[80]
GA-co-GEL	NA	C_{16}	NA	NA	21.00	144.7	NA	NA	*complex coacervation*	[81]
PMMA		C_{16}	14.85	128.2	17.34	145.6	61.4	NA	*emulsion polymerization*	[82]
PBA		C_{16}	14.54	120.6	16.58	120.2	50.7	NA	*emulsion polymerization*	[83]
PMMA		C_{16}	12.60	100.0	21.60	96.0	NA	NA	*suspension polymerization*	[84]

PODMMA			21.40	109.0	19.50	108.0	NA			
EC		C_{16}	19.51	147.1	15.25	140.8	71.7	NA	*emulsion polymerization*	[85]
PS/GO	NA	C_{16}	10.60	190.5	24.90	183.1	[es]78.5	NA	*emulsion polymerization*	[86]
PS-co-EA	NA	C_{16}	17.23	149.6	24.04	140.5	81.6	NA	*emulsion polymerization*	[74]
MUF		C_{16}	7.70	169.8	14.70	167.4	[es]84.7	0.0530	*emulsion polymerization*	[87]
MUF/GP	99.3:0.7		10.70	155.3	15.90	154.2	[es]77.8	[e]0.1030		
MUF/GP	98.7:1.3		NA	138.3	15.80	136.5	[es]69.1	0.1540		
MUF/GP	97.4:2.6		NA	103.6	14.60	104.7	[es]52.2	[e]0.1650		
PUF		C_{16}	10-12	87-116	20-23	86-115	NA	0.0557	*interfacial polymerization*	[88]
PUF/Ag NPs	93.4:6.6		10-12	73-94	19-23	83-105	NA	0.0663		
PUF/Ag NPs	87.7:12.3		4-12	76-131	22-26	73-137	NA	0.0664		
PUF/Ag NPs	78.1:21.9		7-13	70-89	21-23	71-89	NA	0.1231		
MMA-co-AA	NA	C_{16}	15.30	79.6	16.20	84.5	25.6	NA	*emulsion polymerization*	[89]
PMMA		C_{16}	8.60	NA	18.30	62.9	28.9	NA	*suspension polymerization*	[90]
BA-co-MMA	NA		7.60	NA	19.40	63.1	28.9	NA		
PMMA		C_{17}	18.40	84.2	18.20	81.5	38.0	NA	*emulsion polymerization*	[91]
PS-co-EA	NA	C_{17}	17.23	149.6	24.04	140.5	81.6	NA	*emulsion polymerization*	[74]
SiO_2		C_{17}	16.15	61.4	21.90	60.3	30.9	NA	*sol-gel process*	[92]
MF		C_{18}	28.70	145.0	40.60	144.0	59.0	NA	*in-situ polymerization*	[93]
PUF		C_{18}	26.5-17.7	17.4	26.0-33.0	18.8	NA	NA	*in-situ polymerization*	[94]
TiO_2		C_{18}	21.00	92.0	28.70	97.0	NA	NA	*spraying*	[95]
GA-co-GEL	NA	C_{18}	NA	NA	30.30	165.8	NA	NA	*complex coacervation*	[81]
MF		C_{18}	23.14	149.2	26.91	146.5	[es]69.0	NA	*in-situ polymerization*	[96]
PU		C_{18}	27.04	188.9	22.82	187.9	88.0	NA	*interfacial polymerization*	[97]
PU		C_{18}	22.60	187.9	27.00	188.9	88.0	NA	*interfacial polymerization*	[98]

PMF			23.10	149.2	26.90	146.5	68.3	NA	*in-situ polymerization*	
SiO_2		C_{18}	22.10	185.6	27.10	184.9	85.9	0.4568	*sol-gel process*	[99]
SiO_2		C_{18}	22.00	NA	27.10	NA	NA	0.3290	*interfacial polymerization*	[100]
St-co-DVB	90.7:9.3	C_{18}	16.00	127.0	29.00	125.0	56.8	NA	*suspension polymerization*	[101]
PEMA		C_{18}	29.80	197.1	32.70	198.5	89.5	0.1600	*emulsion polymerization*	[102]
PMMA			30.20	205.9	31.90	208.7	94.7	0.1400		
PMMA		C_{18}	18.30	174.4	36.80	173.7	[es]77.3	NA	*suspension polymerization*	[103]
PDVB		C_{18}	19.00	220.0	29.00	220.0	NA	NA	*suspension polymerization*	[104]
PMMA		C_{18}	4.50	182.8	35.20	156.4	[es]75.3	NA	*suspension polymerization*	[105]
PU		C_{18}	25.19	[e]159.5	28.61	[e]159.1	NA	NA	*in-situ polymerization*	[106]
PU/Fe_3O_4	NA		26.16	[e]169.7	28.81	[e]165.7	NA			
MMA-co-AMA	90.9:9.1	C_{18}	10.60	50.0	27.80	68.5	30.9	NA	*in-situ polymerization*	[107]
BMA-co-MAA	NA	C_{18}	[e]23.85	125.8	[e]21.85	130.3	[es]56.9	NA	*suspension polymerization*	[108]
PBA		C_{18}	13.40	123.7	31.60	126.4	[es]55.6	NA	*suspension polymerization*	[109]
PBMA			16.60	124.6	29.10	120.3	[es]54.4			
$CaCO_3$		C_{18}	23.43	82.2	29.19	84.4	40.4	1.2640	*self-assembly*	[110]
SiO_2		C_{18}	23.72	84.9	27.96	87.6	41.8	0.8910	*sol-gel process*	[111]
BMA-co-BA	57.1:42.9	C_{18}	12.90	125.5	30.90	116.4	[es]53.7	NA	*suspension polymerization*	[112]
BMA-co-BA-co-MAA	57.1:28.6:14.3		11.70	130.0	30.90	136.3	[es]59.2	NA		
BMA-co-MAA	57.1:42.9		12.30	152.9	32.80	144.3	[es]66.0	NA		
BMA-co-AA	57.1:42.9		16.60	143.0	27.60	141.5	[es]63.2	NA		
PSMA		C_{18}	21.50	94.8	21.80	87.9	[es]40.6	NA	*suspension polymerization*	[113]
PMMA		C_{18}	22.60	90.0	29.00	91.0	NA	NA	*suspension polymerization*	[84]
PODMMA			22.80	100.0	28.20	98.0	NA			
PODMAA		C_{18}	15.40	90.0	31.50	91.0	26.0	NA	*suspension polymerization*	[114]

PDDA		C_{18}	25.82	124.4	27.34	124.4	[es]58.0	NA	*self-assembly*	115
MPS-co-VTMS	25:75	C_{18}	17.42	169.4	27.84	166.7	[es]76.0	NA	*self-assembly*	116
PAA		C_{18}	26.50	126.0	31.80	125.0	NA	NA	*spraying*	117
PLMA		C_{18}	10.60	108.9	28.60	118.0	[es]50.4	NA	*suspension polymerization*	118
PU		C_{18}	19.40	173.2	28.60	170.4	66.7	NA	*interfacial polymerization*	119
SiO_2		C_{18}	24.27	72.2	32.56	73.5	35.6	NA	*sol-gel process*	92
PMMA		C_{18}	13.20	153.7	24.92	132.1	[es]78.0	NA	*suspension polymerization*	120
PMMA:UM-Si_3N_4	76.9:23.1		13.60	140.3	25.24	139.2	[es]76.3			
PMMA:M-Si_3N_4	97.1:2.9		15.24	151.3	24.54	150.3	[es]82.3			
PMMA:M-Si_3N_4	94.3:5.7		14.69	150.5	24.31	146.9	[es]81.1			
PMMA:M-Si_3N_4	87:13		16.37	138.2	24.27	143.0	[es]76.7			
PMMA:M-Si_3N_4	76.9:23.1		16.14	122.1	25.33	121.11	[es]66.4			
PUF		C_{18}	20-22	91-115	30-34	94-117	NA	0.0695	*interfacial polymerization*	88
PUF/Ag NPs	94.1:5.9		18-22	142-168	33-36	143-168	NA	0.0978		
MMA-co-AA		C_{18}	25.90	84.4	26.40	86.1	34.7	NA	*emulsion polymerization*	89
OSi		C_{18}	24.58	102.0	27.92	107.5	51.3		*interfacial polymerization*	121
SiO_2		C_{18}	24.17	98.85	27.35	109.5	51.5	0.4483	*interfacial polymerization*	122
SiO_2		C_{18}	26.22	226.3	28.32	227.7	NA	NA	*sol-gel process*	123
TiO_2		C_{18}	15.28	40.7	25.68	42.8	22.5	NA	*sol-gel process*	124
PMMA/SiO_2	66.7:33.3	C_{18}	13.66	131.4	24.30	129.8	66.4	NA	*emulsion polymerization*	125
PU/PUT	NA	C_{18}	23.20	141.0	28.60	143.0	NA	NA	*interfacial polymerization*	126
PU			24.00	130.0	27.90	133.0	NA			
PUF		C_{18}	20.40	175.0	30.70	176.0	81.0	NA	*in-situ polymerization*	127
MF		C_{18}	[e]21.00	137.2	NA	NA	67.5	NA	*in-situ polymerization*	128
PMMA/TiO_2	97.2:2.8	C_{18}	20.65	139.3	24.60	139.9	[es]67.6	NA	*suspension polymerization*	129

PMMA			20.56	148.3	24.99	153.8	[es]73.2			
MMA-co-MPS	75:25	C_{18}	16.91	166.1	26.20	165.3	74.9	NA	*suspension polymerization*	130
MF		C_{18}	25.26	137.9	28.22	137.1	59.3	NA	*in-situ polymerization*	131
MF/CNT-PSS	NA	C_{18}	18.81	207.4	29.85	211.2	[es]80.1	0.2500	*self-assembly*	132
MF			18.86	218.5	30.32	222.0	[es]84.2	0.1900		
MMA-co-MAA	NA	C_{18}	26.40	87.7	27.30	94.2	NA	NA	*emulsion polymerization*	133
PMMA/PIM	95.9:4.1	C_{18}	15.16	129.5	24.73	129.7	66.4	NA	*suspension polymerization*	134
PMMA			14.89	152.6	24.89	149.2	76.3			
PMMA		C_{18}	14.90	125.0	22.80	123.0	55.4	NA	*emulsion polymerization*	135
PAMA		C_{18}	11.40	106.6	31.80	104.8	51.3	NA	*suspension polymerization*	136
SF		C_{18}	14.74	90.2	22.82	88.2	46.7	NA	*self-assembly*	137
SF		C_{18}	[e]18.50	[e]70.0	[e]22.50	[e]68.0	NA	NA	*self-assembly*	138
GA-co-GEL	NA	C_{19}	NA	NA	34.00	44.1	NA	NA	*complex coacervation*	81
PMMA		C_{19}	31.03	142.9	31.23	139.2	60.3	NA	*emulsion polymerization*	139
SA		C_{19}	18.52	81.9	32.10	81.7	56.0	NA	*electro spraying*	140
SA		C_{19}	28.76	120.9	35.65	107.3	84.3	NA	*electro spraying*	141
SiO_2		C_{19}	26.24	80.8	36.89	74.8	41.1	NA	*sol-gel process*	92
PMMA		C_{20}	34.90	87.5	35.20	84.2	35.0	NA	*emulsion polymerization*	142
EC-co-MC	90.9:9.1	C_{20}	30.60	186.1	38.00	202.4	90.0	NA	*self-assembly*	143
PSX		C_{20}	[e]30.34	[e]88.8	[e]39.37	[e]160.4	NA	NA	*emulsion polymerization*	144
Fe_3O_4/SiO_2	NA	C_{20}	33.42	169.6	39.15	170.2	71.8	NA	*self-assembly*	145
$CaCO_3$		C_{20}	33.22	85.4	37.29	86.1	37.9	1.0570	*self-assembly*	146
PMMA		C_{20}	32.70	111.0	40.20	110.0	NA	NA	*suspension polymerization*	84
PODMMA			31.40	110.0	39.20	113.0	NA			
MF		C_{20}	33.60	162.4	38.40	166.6	NA	NA	*emulsion polymerization*	147

TiO_2		C_{20}	36.29	150.9	42.73	152.5	78.0	0.7490	*sol-gel process*	148
ZnO		C_{20}	[e]30.70	135.6	39.80	136.4	[e]69.5	NA	*in-situ polymerization*	149
SiO_2		C_{20}	31.86	78.6	40.48	81.2	33.0	NA	*sol-gel process*	92
ZrO_2		C_{20}	36.74	121.3	43.59	126.5	64.7	NA	*self-assembly*	150
MMA-co-AA	NA	C_{20}	33.80	88.4	31.70	90.9	32.9	NA	*emulsion polymerization*	89
TiO_2/Fe_3O_4	NA	C_{20}	32.40	144.2	38.60	144.7	53.8	NA	*self-assembly and interfacial polymerization*	151
ZrO_2		C_{20}	39.37	158.4	45.25	163.9	64.5	0.9060	*in-situ polymerization*	152
Cu_2O		C_{20}	32.52	163.1	38.71	165.3	61.6	3.6520	*self-assembly*	153
TiO_2/GP	NA	C_{20}	[e]33.00	[e]168.0	[e]40.90	[e]170.0	NA	[e]0.7000	*interfacial polymerization*	154
TiO_2			[e]32.10	[e]162.0	[e]40.95	[e]164.0	NA	[e]0.6500		
MMA-co-MAA	NA	C_{20}	35.50	101.4	36.30	107.7	NA	NA	*emulsion polymerization*	133
Ag/SiO_2	NA	C_{20}	[e]31.02	[e]166.5	[e]40.86	[e]168.2	NA	NA	*interfacial polymerization*	155
CNP/GEL/SA	NA	C_{20}	32.37	105.1	35.42	114.7	41.5	NA	*complex coacervation*	156
Ch/CNP	NA	C_{20}	32.76	114.5	35.53	120.5	43.6	NA	*complex coacervation*	157
PMMA		C_{21}	39.59	137.9	39.24	138.2	NA	0.1800	*emulsion polymerization*	158
PMMA		C_{22}	40.60	48.7	41.00	54.6	28.0	NA	*emulsion polymerization*	159
PUT		C_{22}	34.00	88.0	42.00	79.0	31.6	NA	*interfacial polymerization*	160
Fe_3O_4/SiO_2	NA	C_{22}	40.00	156.3	44.90	157.6	NA	NA	*interfacial polymerization*	161
PMMA		C_{28}	53.20	88.5	50.60	86.4	43.0	NA	*emulsion polymerization*	162
PMMA		C_{28}	60.66	156.1	60.02	152.5	NA	0.2000	*emulsion polymerization*	158
PS		C_{32}	61.80	174.8	70.90	285.5	[es]61.2	NA	*emulsion polymerization*	163

[4] Melamine-Formaldehyde (MF); Acrylonitrile-styrene copolymer (AS); Acrylonitrile-styrene-butadiene copolymer (ABS); Polycarbonate (PC); Poly(urea-formaldehyde) (PUF); Styrene-co-Ethylacrylate (PS-co-EA); Poly(methyl methacrylate) (PMMA); Phenolic resin (PFR); Polystyrene (PS); Gum arabic (GA); Gelatin (GEL); Gum arabic-co-Gelatin (GA-co-GEL); Poly(butyl acrylate) (PBA); Poly(butyl methacrylate) (PBMA); Poly(n-octadecyl acrylate-methyl methacrylate) (PODMMA); Ethyl

cellulose (EC); Graphene oxide (GO); Melamine-urea-formaldehyde (MUF); Graphene (GP); Nano particles (NPs); Poly(methyl methacrylate-co-acrylic acid) (MMA-co-AA); Poly(butyl acrylate-co-methyl methacrylate) (BA-co-MMA); Polyurea (PU); Polymelamine-Formaldehyde (PMF); Styrene-divinybenzene (St-co-DVB); Poly(ethyl methacrylate) (PEMA); Poly(divinybenzene) (PDVB); Poly(methyl methacrylate-co-allyl methacrylate) (MMA-co-AMA); Poly(n-butyl methacrylate-co-methacrylic acid) (BMA-co-MAA); Poly(n-butyl methacrylate-co-butyl acrylate) (BMA-co-BA); Poly(n-butyl methacrylate-co-butyl acrylate-co-methacrylic acid) (BMA-co-BA-co-MAA); Poly(n-butyl methacrylate-co-acrylic acid) (BMA-co-AA); Poly(stearyl methacrylate) (PSMA); Poly(n-octadecyl methacrylate-co-methacrylic acid) (PODMAA); Poly(diallyldimethylammonium chloride) (PDDA); 3-(trimethoxysilyl) propyl methacrylate-co-vinyltrimethoxysilane (MPS-co-VTMS); Polyamic acid (PAA); Poly(lauryl methacrylate) (PLMA); Unmodified Si_3N_4 (UM-Si_3N_4); Modified Si_3N_4 (M-Si_3N_4); Organosilica (OSi); Polyurethane (PUT); Poly(methyl methacrylate-co-3-(trimethoxysilyl) propyl methacrylate) (MMA-co-MPS); Carbon nanotube (CNT); Poly(4-styrenesulfonic acid) sodium (PSS); Poly(methyl methacrylate-co-methacrylic acid) (MMA-co-MAA); Pigment (PIM); Poly(Allyl methacrylate) (PAMA); Silk fibroin (SF); Sodium alginate (SA); Ethyl cellulose-co-methyl cellulose (EC-co-MC); Polysiloxane (PSX); Clay nano-particles (CNP); Chitosan (Ch)

[e] data extracted from the figures in literatures

[es] E_{es} data from the literature according to Eq.(3) in Section 3.3.2.2

3.1.2 Paraffins microcapsules

Table 5. Characterization of Paraffins microcapsules (NA: not available)

Shell		Core	Crystallization		Melting		E_{en} & E_{es} (%)	λ (W/m·K)	Synthesis method	Ref.
Components[5]	WR (w/w%)	Components	FP (˚C)	LH (J/g)	MP (˚C)	LH (J/g)				
PS		Paraffin	NA	NA	[e]42.04	[e]41.7	20.6	NA	*suspension polymerization*	[164]
PUF		Paraffin	50.40	201.2	53.30	200.4	97.9	NA	*in-situ polymerization*	[165]
SiO_2		Paraffin	58.27	107.1	58.37	165.7	87.5	NA	*sol-gel method*	[166]
St-co-MMA	20:80	Paraffin	NA	NA	[e]41.81	[e]83.7	43.2	NA	*suspension polymerization*	[167]
PMMA		Paraffin	NA	NA	28.00	101.0	61.2	NA	*emulsion polymerization*	[168]
PMMA		Paraffin	50.10	112.3	55.80	106.9	66.0	NA	*self-assembly*	[169]
MF/nano-Al_2O_3	100:0	Paraffin	47.3-28.7	106.5	33.6-54.1	112.7	[es]65.9	NA	*in-situ polymerization*	[170]
	92.3:7.7		49.1-31.8	110.6	36.9-55.5	115.3	[es]68.0			
	88.9:11.1		48.4-31.9	87.9	37.4-56.1	98.3	[es]59.0			
	78.9:21.1		43.1-26.1	89.4	38.7-60.2	101.4	[es]57.4			
	71.4:28.6		43.2-26.2	88.5	38.6-59.9	94.4	[es]55.0			
	65.2:34.8		42.6-25.2	79.1	39.9-61.6	84.1	[es]49.1			
MMA-co-AA	NA	Paraffin	NA	NA	60.00	113.0	NA	NA	*emulsion polymerization*	[171]
SiO_2		Paraffin	45.00	43.8	56.50	45.5	31.7	NA	*in-situ polymerization*	[172]
PMMA		Paraffin	NA	NA	[e]61.5	[e]140.3	60.7	NA	*emulsion polymerization*	[173]
PAM		Paraffin	14-31	121.7	29-41	122.1	87.0	NA	*interfacial polymerization*	[174]
SiO_2		Paraffin	55.78	144.1	57.96	156.9	82.2	NA	*sol-gel process*	[175]
PLA		Paraffin	50.20	170.5	58.20	176.6	NA	NA	*emulsion polymerization*	[176]
BMA-co-MAA	NA	Paraffin	[e]50.85	[e]102.0	[e]53.85	[e]99.0	[es]69.9	NA	*suspension polymerization*	[108]
TiO_2		Paraffin	56.80	147.2	58.60	164.1	87.1	NA	*sol-gel process*	[177]
PU/Fe_3O_4 NPs	NA	Paraffin	47.82	105.6	56.54	101.1	NA	[e]0.2320	*interfacial polymerization*	[178]

		Paraffin	48.90	98.2	56.32	94.3	NA	[e]0.2530		
		Paraffin	49.39	91.3	56.29	85.7	NA	[e]0.3100		
		Paraffin	49.69	87.4	55.85	83.28	NA	[e]0.3180		
PAn		Paraffin	48.95	121.0	56.63	108.9	79.9	NA	*in-situ polymerization*	[179]
PUF		Paraffin	NA	NA	26.10	74.2	52.8	NA	*in-situ polymerization*	[180]
PUF		Paraffin	NA	NA	26.20	47.7	37.4	NA	*in-situ polymerization*	[181]
MAA-co-EMA	57.1:42.9	Paraffin	26.30	103.2	29.30	102.9	[es]62.6	NA	*suspension polymerization*	[182]
PLMA		Paraffin	23.04	73.0	29.50	76.7	[es]45.5	NA	*suspension polymerization*	[118]
SiO_2		Paraffin	23.29	110.8	26.12	111.7	61.9	0.3948	*self-assembly*	[183]
PHEMA		Paraffin	48.06	167.3	57.88	168.0	97.7	NA	*redox polymerization*	[184]
PS-co-EA	NA	Paraffin	37.41	49.1	42.39	49.0	32.1	NA	*emulsion polymerization*	[185]
SiO_2		Paraffin	57.40	83.1	49.20	89.7	[es]50.8	NA	*emulsion polymerization*	[186]
SiO_2/GO	NA		57.70	81.6	49.70	87.1	[es]49.6			
PMMA:SiO_2	NA	Paraffin	19.80	71.0	26.80	69.9	[es]57.4	NA	*self-assembly*	[187]
MF/GO	NA	Paraffin	NA	NA	41.08	202.8	93.9	NA	*in-situ polymerization*	[188]
MF			NA	NA	39.85	200.3	92.7			
St-co-AA-co-BA	NA	Paraffin	[e]13.80	[e]109.7	[e]20.80	[e]112.1	NA	NA	*in-situ polymerization*	[189]
MF		Paraffin	NA	NA	47.66	126.0	65.0	NA	*in-situ polymerization*	[190]
MF/GP	NA	Paraffin	57.10	85.0	50.50	90.8	51.1	0.3120	*in-situ polymerization*	[191]
MF			57.10	94.9	49.90	102.9	57.5	0.2610		
PMMA/(BN/TiO_2)	66.7:33.3	Paraffin	51.60	141.5	53.00	140.8	72.1	0.3527~ 0.4419	*emulsion polymerization*	[192]
PMMA		Paraffin	NA	NA	59.90	137.2	89.5	NA	*suspension polymerization*	[193]
SiO_2		Paraffin	NA	NA	49.00	13.0	11.0	NA	*interfacial polymerization*	[194]
PS-co-MAA	NA	Paraffin	49.25	94.7	51.48	96.0	[es]69.5	NA	*emulsion polymerization*	[195]

EMA-co-AA-co-St-co-TMPTA	NA	Paraffin	24.90	115.3	30.70	117.8	[es]70.8	NA	*suspension polymerization*	[196]
PU		Paraffin	NA	NA	27.5	92.5	44.5	NA	*interfacial polymerization*	[197]
MR		Paraffin	NA	NA	39.8	92.2	NA	[e]0.1880~0.2660	*purchased*	[198]
MMA-co-MA/Al_2O_3NPs	90.9:9.1	Paraffin	22.54	110.0	22.47	110.4	64.3	0.2442	*emulsion polymerization*	[199]
			23.19	104.3	23.43	105.5	61.2	0.2786		
			23.32	92.4	23.75	93.4	54.2	0.3104		
			22.76	84.0	23.14	84.5	49.2	0.3409		
			22.03	75.5	23.49	76.3	44.3	0.3591		
			22.58	75.1	22.96	75.4	43.9	0.3816		
PMMA		RT21	8.0	111.9	21.90	113.4	85.6	NA	*suspension polymerization*	[200]
PMMA		RT21	7.90	111.9	22.00	113.9	86.3	NA	*suspension polymerization*	[201]
PMMA		RT25	NA	NA	20.73	113.9	NA	NA	*suspension polymerization*	[202]
LDPE-co-EVA	NA	RT27	NA	NA	28.40	98.1	49.3	NA	*spray drying*	[203]
PMMA		RT27	[e]7.50	167.0	[e]22.00	163.2	NA	NA	*suspension polymerization*	[204]
$CaCO_3$		RT28	27.41	107.2	23.33	105.8	59.0	0.714	*self-assembly*	[205]
$CaCO_3$		RT42	49.36	137.8	49.41	138.7	58.2	0.817		
$CaCO_3$		RT42	NA	NA	48.62	143.6	NA	0.814	*self-assembly*	[206]
St-co-BA	70:30	RT80	55.20	25.0	80.90	23.9	[es]80.0	NA	*emulsion polymerization*	[207]

[5] Styrene-co-methyl methacrylate (St-co-MMA); Polyamide (PAM); Polylactic acid (PLA); Polyaniline (PAn); Poly(methacrylic acid-co-ethyl methacrylate) (MAA-co-EMA); Poly(2-hydroxyethyl methacrylate) (PHEMA); Styrene-co-acrylic acid-co-n-butyl acrylate (St-co-AA-co-BA); Boron nitride (BN); Ploy(styrene -co-methylacrylic acid) (PS-co-MAA); Poly(ethyl methacrylate-co- acrylic acid-co-styrene-co-trimethylolpropane triacrylate) (EMA-co-AA-co-St-co-TMPTA); Melamine resin (MR); Poly(Methyl methacrylate-co-methacrylate) (MMA-co-MA); Poly(Styrene-co-butyl acrylate) (St-co-BA); Carbon nanofibers (CNFs)

[e] data extracted from the figures in literatures

[es] E_{es} data from the literature according to Eq.(3) in Section 3.3.2.2

3.1.3 C_n & paraffin blends microcapsules

Table 6. Characterization of C_n & paraffin blends microcapsules (NA: not available)

Shell	Core		Crystallization		Melting		E_{en} & E_{es}	λ	Synthesis method	Ref.
Components	Components	WR (w/w%)	FP (˚C)	LH (J/g)	MP (˚C)	LH (J/g)	(%)	(W/m·K)		
PUF	C_{16}:C_{20}	66:34	24.5-12.0	54.8	9.0-23.5	51.7	NA	NA	*in-situ polymerization*	94
PMMA	C_{17}:C_{24}	90:10	20.14	83.8	20.22	86.0	50.2	NA	*emulsion polymerization*	208
	C_{18}:C_{19}	95:5	26.44	112.3	26.45	117.9	65.3			
	C_{19}:C_{24}	95:5	30.96	99.0	31.22	104.9	55.8			
	C_{20}:C_{24}	90:10	35.75	165.5	35.88	169.3	65.4			
PS	C_{18}:C_{24}	90:10	16.48	152.8	25.96	156.4	64.4	NA	*emulsion polymerization*	209
MF	C_{18}:C_{20}	66.7:33.3	NA	NA	33.00	144.0	NA	NA	*in-situ polymerization*	210
PU	Paraffin (solid:liquid)	30:70	NA	NA	28.10	58.4	NA	NA	*interfacial polymerization*	211
LDPE-co-EVA	RT27:CNFs	98:2			27.60	95.6	48.1	NA	*spray drying*	203
MMA	RT21:RT58	95:5	17.51	108.3	22.28	110.4	83.6	NA	*suspension polymerization*	212
$CaCO_3$	RT28:RT42	50:50	27.67; 40.62	122.8	19.76; 34.76	82.8	57.4	0.701	*self-assembly*	205

3.1.4 Microencapsulation of C_n mixed with other compositions

Table 7. Characterization of microencapsulation of C_n mixed with other compositions (NA: not available)

Shell		Core		Crystallization		Melting		E_{en} & E_{es} (%)	λ (W/m·K)	Synthesis method	Ref.
Components[6]	WR (w/w%)	Components	WR (w/w%)	FP (˚C)	LH (J/g)	MP (˚C)	LH (J/g)				
EP		C_{14}:DMB	50:50	[e]-4.50	NA	[e]5.50	54.7	42.1	NA	*interfacial polymerization*	[213]
PUF		C_{18}:PEG600	13:87	27.0-25.2	1.6	26.0-32.5	3.9	NA	NA	*in-situ polymerization*	[94]
		C_{16}:PEG1000: $Na_2CO_3 \cdot 10H_2O$	11:50:39	15.8-13.4	42.5	13.0-23.5	44.6	NA			
MMA-co-AMA	90.9:9.1	C_{18}:PPy	89.4:10.6	11.70	29.2	28.2	141.4	63.7	NA	*in-situ polymerization*	[107]
PU/PUT	NA	Paraffin:BS	90.9:9.1-66.7:33.3	NA	NA	28-35	58.1-87.6	42.2-63.7	NA	*interfacial polymerization*	[214]
MMA-co-DVB	95:5	Paraffin:BS	90:10	28.17	33.3	34.7	117.5	85.2	NA	*in situ polymerization*	[215]
PU/PUT	NA	Paraffin:BS	83.3:16.7	NA	NA	33.70	82.6	59.4	NA	*interfacial polymerization*	[216]
			50:50	NA	NA	32.29	80.1	58.2			
			66.7:33.3	NA	NA	32.51	72.4	55.0			
DVB-co-AMA	50:50	Paraffin:BS	50:50	NA	NA	32.12	94.0	68.3	NA	*suspension polymerization*	[217]
PU		C_{18}: 1-tetradecanol	92.9:7.1	22.40	164.4	30.20	165.5	NA	NA	*interfacial polymerization*	[119]
		C_{18}:paraffin	98.3:1.7	17.50	159.9	28.10	161.9	NA			
SiO_2		Paraffin: P(GMA-EDMA)	NA	[e]53.5	[e]78.0	[e]55.5	[e]78.8	NA	NA	*sol-gel process*	[218]

[6] Epoxy polymer (EP); Dimethylbenzene (DMB); polypyrrole (PPy); poly(glycidylmethacrylate-ethylene dimethacrylate) (P(GMA-EDMA)); Butyl stearate (BS); poly(methylmethacrylate-co-divinylbenzene) (MMA-co-DVB); poly(divinylbenzene-co- allyl methacrylate) (DVB-co-AMA)

[e] data extracted from the figures in literatures

3.2 Synthesis methods for C_n and their blends microcapsules

In this sub-section, a brief description of each synthesis method (as mentioned in Table 4-7) is summarized firstly. Then, some typical examples in regard to these methods are elaborated.

Normally, the commonly used synthetic techniques for C_n and their blends microcapsules can be classified under three categories: physical, chemical and physical-chemical methods. Apart from these technologies, other methods such as self-assembly, also exist in some literatures.

3.2.1 Physical methods

The physical method retains the original chemical compositions of the shell materials, which are formed by physical processes like dehydration, adhesion, among others.

In many physical methods, Electrospraying, as the most commonly used method for microcapsules synthesis, is introduced in this sub-section.

Electrospraying

- **General processes**[117]**:** (1) preparing the PCM solution and shell material solution in two separate syringes; (2) two separated solutions are fed into different nozzles (outer and inner nozzle) at the particular feed rates; (3) the fabricated microcapsules are collected in a container and gently stirred for curing; (4) washing and drying the microcapsules.
- **A typical example:** Figure 6 shows the schematic of microencapsulation using electrospraying method according to Yuan et al.'s work [117]. At first, PAA solution and liquid C_{18} were placed in two separate plastic syringes, and then injected into the coaxial composite nozzle. The PAA solutions were extruded through outer nozzle while the C_{18} solutions were came out through the inner nozzle. Finally, the fabricated microcapsules were dripped into a container, washed and dried. The diameters of microcapsules ranged from 0.5 to 3 μm.

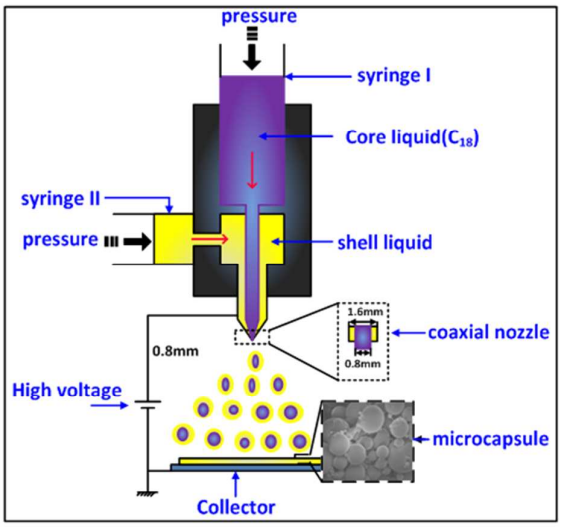

Figure 6 Schematic of electrospraying method for the C_{18} microencapsulation (redrawn based on Ref. [117])

3.2.2 Chemical method

Generally, there are 4 types of polymerization processes namely in-situ polymerization, interfacial polymerization, suspension polymerization and emulsion polymerization, which are described below.

3.2.2.1 In-situ polymerization

- **General processes** [71]**:** (1) the synthesis of the pre-polymer solution through the mixture of pre-polymers (shell materials) and solvents (water); (2) preparation of oil/water (O/W) emulsion with emulsifier (sometimes modifying agent); (3) microcapsules formation by adding this pre-polymer into the O/W emulsion; (4) microcapsules collection by rinsing, filtering and drying. This method is typically used for organic shell materials like MF and PUF.
- **A typical example:** Figure 7 shows the schematic of microencapsulation using in-situ polymerization method according to Zhu et al.'s work [71]. A pre-polymer was first synthesized by mixing melamine and formalin solution in the distilled water (formation of MF shell). Then, C_{12} was dispersed in aqueous sodium hydroxide solution to form an emulsion (O/W emulsion). The pre-polymer was added to the C_{12} emulsion by droplets to achieve polymerization. Finally, the microcapsules were rinsed and air-dried at room temperature. In this work, it was indicated that the average capsule diameters were strongly affected by the stirring rates. The size range is from 330nm to 15.69μm.

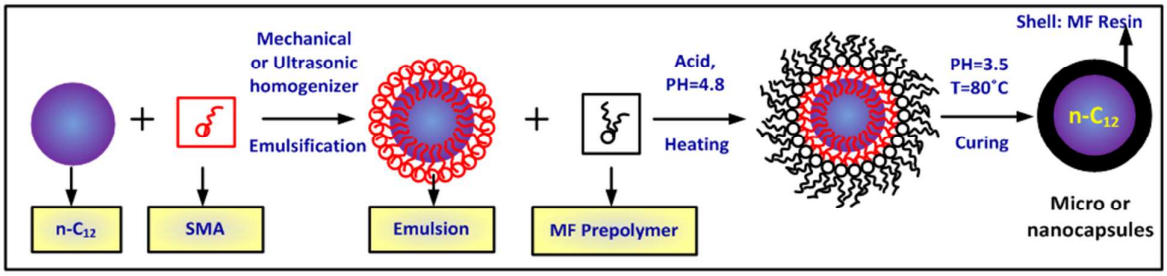

Figure 7 Schematic of in-situ polymerization for the C_{12} microencapsulation (redrawn based on Ref. [71])

3.2.2.2 Interfacial polymerization

- **General processes** [97]**:** (1) formation of the oil phase with PCM and hydrophobic monomers; (2) dissolve the hydrophilic monomers in the aqueous solution; (3) microcapsules formation the by adding hydrophilic groups in the form of droplets into oil phase; (4) microcapsules collection by filtering, washing and drying from the emulsion. This method is typically used for organic shell materials like PU and PUT.
- **A typical example:** Figure 8 shows the schematic of microencapsulation using interfacial polymerization method according to the work of Zhang and Wang [97]. Firstly, the mixed oil solution consisting of C_{18} and TDI was dispersed in an aqueous solution to form an oil-in-water microemulsion (oil phase C_{18}/TDI mixture). Then, the other requisite monomer, amine, was dropped into the emulsion and reacts with TDI. As a result, a urea-linked polymeric shell was formed at the oil-water interfaces. Finally, the resultant microcapsules were filtered, washed and dried. The particle size of the microcapsules was within a range of 3~12 μm.

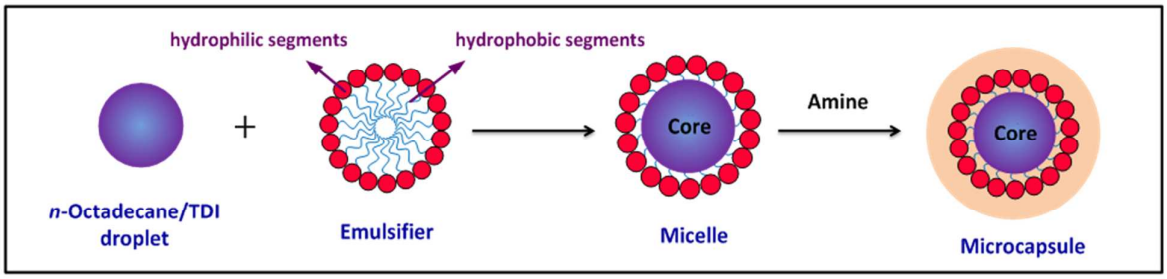

Figure 8 Schematic of interfacial polymerization for the C_{18} microencapsulation (redrawn based on Ref. [97])

3.2.2.3 Suspension polymerization

- **General processes[80]:** (1) PCM, monomers and initiators form the oil phase and suspend in the aqueous solution as discrete droplets (add surfactants); (2) initiators triggering the microcapsules polymerization from the oil phase (core materials); (3) separation of microcapsules from the emulsion. This method is typically used for organic shell materials like PMMA.
- **A typical example:** Figure 9 shows the schematic of microencapsulation using suspension polymerization method according to Ai et al.'s work [80].The first step was emulsifying the oil phase into aqueous phase. Casein molecules as the mini-reactors act to stabilize the fine oil droplets through the polymerization period. Then, The C_{16}, monomers and initiators formed the oil phase. The precipitation polymerization took place within the oil droplets after the temperature was elevated. Finally, phase separation of polymer occurred, resulting polymer particles precipitate and move to the interface of oil droplets. The size of the microcapsules was within a range of 3~15 μm.

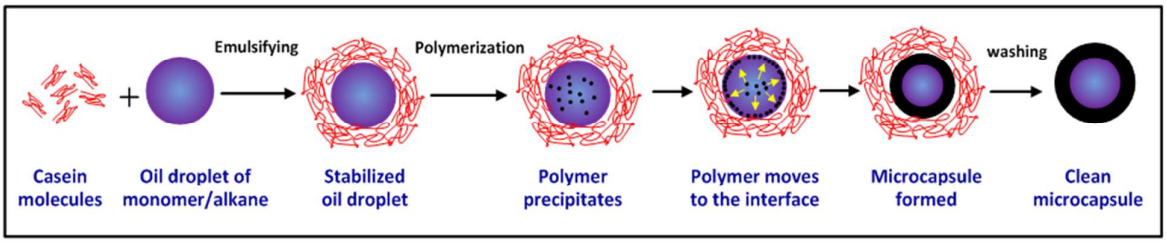

Figure 9 Schematic of suspension polymerization for the C_{16} microencapsulation (redrawn based on Ref. [80])

3.2.2.4 Emulsion polymerization

- **General processes[219]:** (1) PCM and monomers form the oil phase and suspend in the aqueous solution as discrete droplets (add surfactants); (2) initiators are dissolved in the aqueous phase; (3) initiators triggering the microcapsules polymerization; (4) separation of microcapsules from the emulsion. This method is typically used for organic shell materials like PMMA and PS.
- **A typical example:** Figure 10 shows the schematic of microencapsulation using suspension polymerization method according to Macro's work [219]. The first step was preparing the wax and monomers emulsion in hot water with stirrer and detergents, then the initiators was dissolved into aqueous solution and polymer shell grew between the interphase of wax and water, finally, a highly cross linked polymer formed the dense shell on each droplet of wax. The size of the microcapsules was within a range of 2~20 μm.

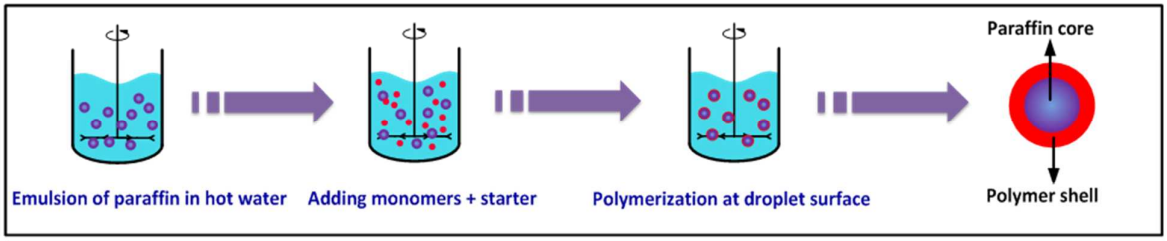

Figure 10 Schematic of emulsion polymerization for the paraffin microencapsulation (redrawn based on Ref. [219])

3.2.3 physical-chemical methods

3.2.3.1 Coacervation

- **General processes**[220-221]**:** (1) dispersion of the PCM in an aqueous solution containing the shell polymer; (2) deposition of the coating material (polymer) on the core material; (3) rigidizing of the coating material by thermal, cross linking or desolvation techniques to obtain microcapsules.
- **A typical example:** Figure 11 shows the schematic of microencapsulation using coacervation method according to the work of Uddin et al. and Fabien [220-221]. In Uddin's work, firstly, gelatine solution was prepared by dissolving in distilled water. Then, the solid paraffin was dispersed in the gelatine solution by gentle stirring and maintaining the temperature at a constant value. At this temperature, paraffin particles melted and, apparently, became coated with gelatine. Finally, the microencapsulated paraffin was hardened with cross-link agent and dehydrated by ethyl alcohol. Microencapsulated paraffin sizes are approximately 500 μm which are larger than the other synthesis methods.

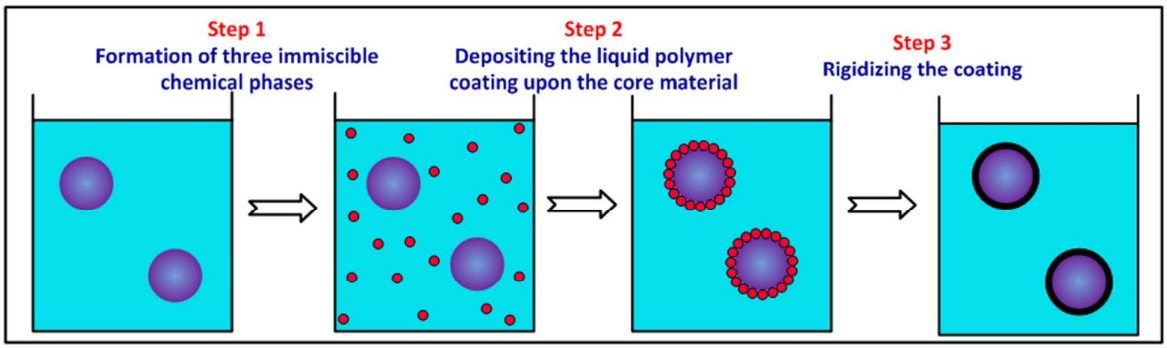

Figure 11 Schematic of coacervation method for the paraffin microencapsulation (redrawn based on Ref. [220-221])

3.2.3.2 Sol-gel process

- **General processes**[111]**:** (1) formation of oil phase with PCM and surfactants (emulsifiers) (PCM O/W emulsion) (2) preparation of sol solution by dissolving the precursor compounds in water under an acidic environment; (3) microcapsules formation through condensation polymerization by adding sol solution into the PCM O/W emulsion drop by drop; (4) separation of microcapsules from the emulsion. This method is typically used for inorganic shell materials like silica and titanium oxide.
- **A typical example:** Figure 12 shows the schematic of microencapsulation using sol-gel method according to He et al.'s works [111]. The oily C_{18} was first dispersed in an aqueous solution containing a nonionic surfactant (PEO-PPO-PEO) to form a stable O/W emulsion. Then, the silica sol was prepared by dissolving sodium silicate in water under an acidic or weakly alkaline circumstance. Afterwards, the silica sol was added into the O/W emulsion drop by drop, leading to the formation of silica gel surrounding the

C_{18} micelles. Finally, the silica wall was successfully fabricated onto the surface of the C_{18} droplets.

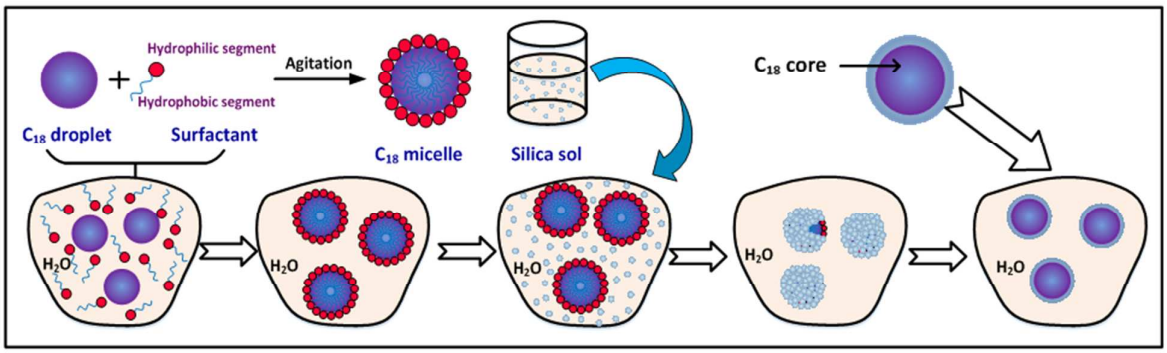

Figure 12 Schematic of sol-gel method for the C_{18} microencapsulation (redrawn based on Ref. [111])

3.2.4 Other methods

Gao et al. [153] fabricated a microencapsulated C_{20} capsules through a self-assembly process, as shown in Figure 13. First, O/W emulsion containing C_{20} micelles was built first with the aid of surfactant. Then, $CuSO_4$ was added into the emulsion system, copper ions were attracted onto the surfaces of C_{20} micelles and form a self-assemble system with copper species at the oil-water interface. Next, a $Cu(OH)_2$ layer was generated surrounding the C_{20} micelles through precipitation reaction by adding a NaOH aqueous solution into this self-assemble system. The $Cu(OH)_2$ layer was further reduced with glucose reducing agent, Finally, a well-defined Cu_2O shell encapsulating the C_{20} core was fabricated. This method actually has two key factors: the first is the selection of an appropriate surfactant template that can supply specific and local interactions among the core materials to attract precursors for self-assembly themselves, and the second one is the accurate control of a balance between the deposition and precipitation of precursors at the oil-water interface.

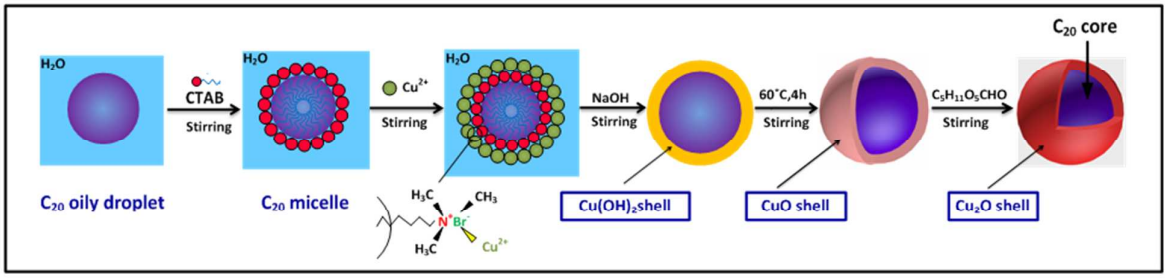

Figure 13 Schematic of self-assembly for the C_{20} microencapsulation (redrawn based on Ref. [153])

3.3 Characterization of microencapsulated C_n and their blends

The C_n and their blends microcapsules should be characterized from three aspects including thermal, physical and chemical properties to examine their microencapsulation properties, determine their application ranges, and propose improvement methods of properties. The thermal, physical and chemical properties comprise several key sub-properties, respectively. In this sub-section, the method of characterization for each property is firstly described; the corresponding microencapsulation characteristics and their improvement methods are then elaborated with some typical examples.

3.3.1 Thermal properties

3.3.1.1 Phase change properties

The phase change properties of bulk PCM and MPCM are generally measured by differential scanning calorimetry (DSC) analysis. As shown in Figure. 14, DSC testing results are presented in the form of endothermic and exothermic curves with temperature variations during heating and cooling phases, respectively. By analyzing the curves, the key phase change properties can be obtained as follows:

T_{mo}: The melting onset temperature in endothermic curves;

T_{mp}: The melting peak temperature in endothermic curves;

ΔH_m: The melting enthalpy in endothermic curves;

T_{co}: The crystallization onset temperature in exothermic curves;

T_{cp}: The crystallization peak temperature in exothermic curves;

ΔH_c: The crystallization enthalpy in exothermic curves;

ΔT_s: Supercooling degree, defined as T_{mp}-T_{cp}.

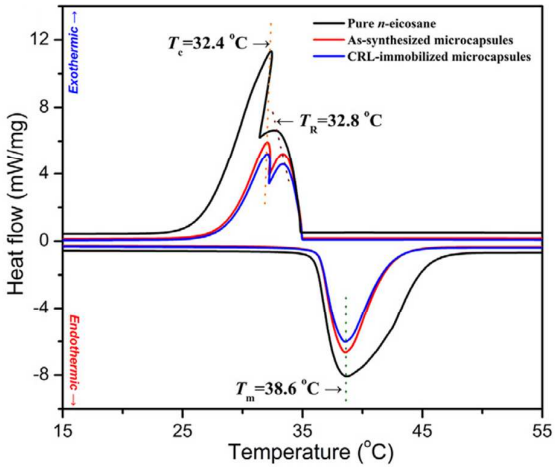

Figure 14 DSC thermograms of as-synthesized and CRL-immobilized microcapsules [151]

The thermal conductance, geometric confinement or nucleation induction of shell results in the shift of the phase change temperature [188-189]. The melting temperature of C_n in the microcapsules is generally similar to that of the bulk C_n. In contrast, the crystallization temperature of C_n in the microcapsules is significantly lowered compared to that of the bulk C_n. This means that C_n will experience severe supercooling when it is encapsulated in microcapsules, which is most likely owing to the lack of nuclei in such a tiny space [212]. Supercooling results in that the latent heat is released at a lower temperature or in a wider temperature range, which is disadvantageous for the energy storage application. Therefore, the supercooling is still a major obstacle to the widespread application of

microencapsulated C_n and hence lots of efforts have been devoted to reduce the supercooling of C_n in microcapsules. Currently, there mainly exist two types of methods to eliminate or suppress the supercooling. One is to add nucleating agents into core to promote heterogeneous nucleation, such as paraffin or alcohols with high freezing point and solid nanoparticles. Another is to modify the shell composition and structure to mediate a homogeneous nucleation by shell-induced heterogeneous nucleation. Wu et al. [119] reported that adding around 8.3 wt% paraffin or 1-tetradecanol into core materials can suppress supercooling of microencapsulated C_{18}. Similarly, Al-Shannaq et al. [212] selected 5wt% RT58 or 15 wt% 1-octadecanol as nucleating agents to decrease the supercooling of microencapsulated RT21 from 14˚C to less than 5˚C. Tang et al. [114] developed a novel microencapsulated C_{18} with ODMA-co-MAA copolymer as shell to realize low supercooling. The use of ODMA led to the formation of a number of small alkyl nanodomains on the inner wall of shell, which can act as nuclei to induce the heterogeneous nucleation of C_{18} in the microcapsules; thus the supercooling degree of microencapsulated C_{18} with the ODMA-co-MAA copolymer as shell is notably lower than that with MF as shell. Cao et al.[222] optimized the composition and structure of the adopted MF resin shell by adjusting ratio of melamine to formaldehyde, pH of pre-polymer, and pH of emulsion to achieve shell-induced nucleation of the triclinic and rotator phases and thus suppress the supercooling. Besides modified organic shell, inorganic shell also has a positive role in diminishment of supercooling. Tang et al. [123] selected SiO_2 as shell to microencapsulating C_{18} to realize extremely low supercooling, which is less than that of the bulk or pure C_{18}. This is because that the microstructure with no cross-linking on its interior wall of the silica shell is helpful for the nucleation of C_{18}. The second method is generally more advantageous in the effective latent heat of the MPCM microcapsules, because the effective latent heat will be reduced by the relatively large amount of additive in the first method.

The latent heat of MPCM is lower than that of pure PCM because of the shell existing. In order to increase the latent heat of MPCM the thinner or lighter shells are required, which will cause more challenges in the synthesis process and material selection of shell. Tang et al. [123] confirmed that the dosage reduction of the raw materials used to synthesize shell can increase the latent heats of the MPCM decrease accordingly. Wan et al. [189] found that the latent heat of fusion increases with the increase in the percentage of pentaerythritol triacrylate (PETA) which was employed as cross-linking agents. They explained it by that a higher degree of cross-linking can lead to higher core/shell size ratio. When the content of PETA was increased from 4 wt% to 22 wt%, the latent heat of melting of the PCM microcapsules measured was increased from 87.9 J/g to 112.1 J/g. Compared those microcapsules containing C18 in Table 4, it can be seen that the microcapsules using SiO_2 as shell [123] has much higher latent heat than the others, and it thus has advantages in thermal energy storage.

3.3.1.2 Thermal conductivity

Currently no sufficient information on the measurement of thermal conductivity of single MPCM particle can be found in the literature. Although the thermal conductivity of MPCM was measured using laser flash apparatus (LFA, LINSEIS LFA1000) by Chai et al. [148], an EKO HC-110 thermal conductivity meter by Yu et al. [110] or a Sweden Hot Disk thermal conductivity meter with 7577 probe by Jiang et al. [199, 205], they did not specify how to test the thermal conductivity of a single microcapsule. Pressing massive microcapsules into a tablet is likely a feasible measurement method to approximately obtain the thermal conductivity of single microcapsule [21, 198, 206]. The thermal conductivity of single microcapsule can be theoretically estimated based on the composite sphere approach as follows [223-224]:

$$\frac{1}{\lambda_p d_p} = \frac{1}{\lambda_c d_c} + \frac{d_p - d_c}{\lambda_w d_p d_c} \quad (1)$$

where λ_p, λ_c and λ_w are the thermal conductivities of the single MPCM particle, the core material and the shell material, respectively; d_p and d_c are the diameter of the single MPCM particle and core, respectively.

One of the aims of C_n or paraffin microencapsulation is to increase the heat transfer surface to overcome their low conductivities. However, the MPCMs using organic polymers as shells still exhibit poor heat transfer property due to its low thermal conductivities of the organic shells. The poor heat transfer property results in a low efficiency of thermal storage and release, which has been regarded as a dominating drawback in energy storage application [91]. Fast heat transfer in MPCMs is required to enable a prompt response during the charging and discharging processes of the thermal energy. Therefore the thermal conductivity of MPCMs needs to be enhanced. Several methods of elevating the thermal conductivity of MPCMs have been proposed by researchers recently. One is to modify the shell with inorganic nanoparticles, including Fe_3O_4 [178], Al_2O_3 [199], graphene [87, 191], CNT [132], BN/TiO_2 [192]. Jiang [199] employed emulsion polymerization to embed Al_2O_3 nanoparticles into P(MMA-co-MA) shell, which improved the thermal conductivity of the paraffin microcapsules. They reported that the thermal conductivity of the paraffin microcapsules would increase from 0.2442 W/(m·K) to 0.3816 W/(m·K) when the mass ratio of Al_2O_3 nanoparticles was increased from 0 to 38%. Another is to directly adopt inorganic materials as shells, such as TiO_2 [138, 148], SiO_2 [75, 111], $CaCO_3$ [76, 110], ZrO_2 [152] and Cu_2O [153]. Wang's research group [148] used TiO_2 as shell to microencapsulate C_{20} through sol–gel method to increase the thermal conductivity from 0.161 W/(m·K) to 0.749 W/(m·K). They also employed ZrO_2 [152] and Cu_2O [153] to microencapsulate C_{20} to obtained higher thermal conductivity of the microcapsules without decreasing thermal storage capacity. It should be noted that although the thermal conductivity of MPCM is further increased with the increase in the mass ratio of inorganic nanoparticles or shell, the latent heat of phase change correspondingly decreased. A compromise should be made between the two aspects of energy storage performances.

3.3.1.3 Thermal stability

Thermal stablitity of MPCM includes two aspects, which are thermal degradation behavior and thermal reliability. The thermal degradation behavior indicates the temperatre limit of stable operation of MCPM, which is investigated by thermogravimetric analysis (TGA) under continueously heating [166, 208]. Jiang et al. [145] conducted the thermal degradation test for C_{20} microcapsules with Fe_3O_4/SiO_2 shell using TGA. The TGA curves for pure C_{20} and C_{20} microcapsules with differnet core/shell mass ratios are shown in Figure 15. This figure shows a typical one-step thermal degradation behavior for all smaples presents and a remarkable increment in thermal degradation temperature (at which the sample undergoes the most rapid mass loss) after C_{20} was microencapsulated. They stated that the compact Fe_3O_4/SiO_2 hybrid shell hindered the decomposition of microencapsulated C_{20} and thus improved thermal degradation temperature of the microcapsules. Zhang et al. [188] reported that a two-step thermal degradation process was observed for a GO-modified MF/paraffin microcapsule. They pointed out that the first step thermal degradation is attributed to the thermal decomposition of paraffin and a decrease in the dosage of GO is helpful to elevating the thermal degradation temperature of first step due to formation of less defect shell. The increase in thermal degradation temperature ensures the stable work of MPCM at a higher temperature far above the melting point of core PCM.

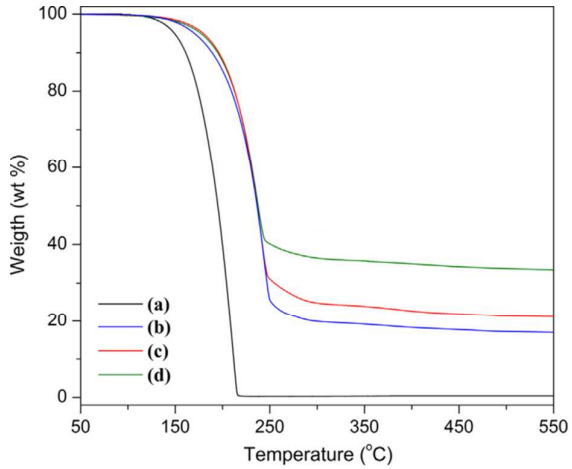

Figure 15 TGA curves of (a) pure C_{20} and the Fe_3O_4/SiO_2 hybrid shell microencapsulated C_{20} synthesiezed with core/shell mass ratios of (b) 7/3, (c) 5/5 and (d) 4/6 [145]

The thermal reliability enables long-term serving durability of MPCMs, which is analyzed by DSC based on a large number of repeated thermal cycles of alternate melting and solidification [116, 121]. If the properties of phase change exhibit tiny or even no change after sufficient thermal cycles, the MPCM is regarded as thermally reliable. Chai et al. [148]performed thermal reliability tests of a representative C_{20} microcapsule sample with TiO_2 shell using DSC. Figure 16 shows the multiple DSC curves of over 100 thermal cycles of the microcapsule. This figure indicates that their synthesized microcapsules can maintain stable phase change properties for a long-term utility period. Fourier transform infrared (FT-IR) spectroscopy can also be used to exam the thermal reliability through testing chemical composition as an auxiliary means [162]. Sarı et al. [91]demonstrated the FT-IR spectra of PMMA/C_{17} microcapsules before and after thermal cycling, which are shown in Figure 17. This figure shows that the frequencies of characteristic peaks have little change after 5000 thermal cycles, which means no effects of thermal cycling on chemical structure of the microcapsules and no chemical degradation during thermal cycling. Therefore, their synthesized microcapsules are thermally stable from the viewpoint of chemical structure.

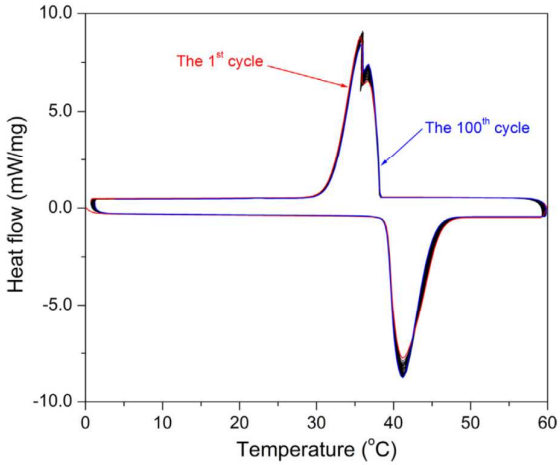

Figure 16 DSC curves over 100 cycles for the C_{20} microcapsule with TiO_2 shell [148]

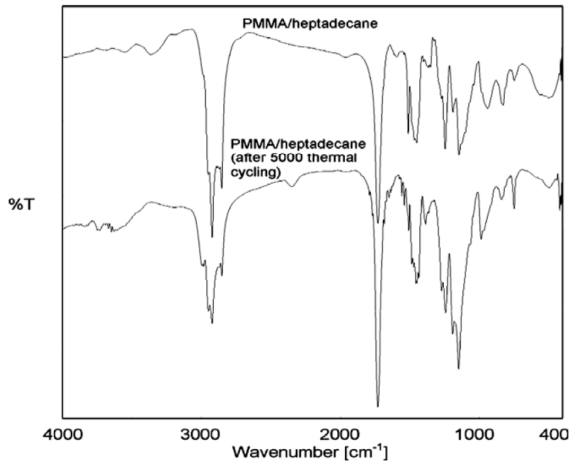

Figure 17 FT-IR Spectra of PMMA/C_{17} microcapsules before and after thermal cycling [91]

3.3.2 Physical properties

3.3.2.1 Microcapsule size distribution

The sizes of PCM microcapsules are crucial to their thermal storage performance, especially for MPCM slurry application [160, 223-224]. The particle size distribution (PSD) of microcapsules can be measured using a diameter distribution analyzer [107] or a scanning electron microscope (SEM) [90, 123]. The PSD is affected by many factors, such as viscosity of materials, shell compositions, process parameters and synthesis methods. de Cortazar et al. [173] pointed out that the average particle size increased with paraffin/MMA ratio and explained it by taking into account viscosity of the system, which affected the onset of acoustic cavitation and thus droplet size. Lashgari et al. [90] reported that the average sizes of C_{16} microcapsules using PMMA and BA-co-MMA as shells were 140 μm and 155 μm, respectively. De Castro et al. [160] found that the increase of the homogenization speed resulted in a smaller average particle size and a narrow size distribution of C_{22}/PU microcapsules through interfacial polymerization. When the homogenization speed increased from 6000 rpm to 20000 rpm, the average particle size decreased from 10 μm to 2 μm. Su et al. [21] summarized the statistics results of PSD of capsules prepared via various synthesis methods, which indicated that the size distribution range is notably different from each other for the various methods.

3.3.2.2 Efficiencies

Two types of efficiencies of microencapsulation were adopted in the literatures: encapsulation efficiency and energy storage efficiency. Generally, these two efficiencies were mainly affected by the ratio of core/shell, the mass of emulsifier and cross-link agent, as well as the synthesis methods.

The encapsulation and the energy storage efficiency are calculated using Eq. (2) and Eq.(3), where $\Delta H_{m,\mathrm{MPCM}}$ and $\Delta H_{c,\mathrm{MPCM}}$ are the melting and crystallization enthalpies of the PCM microcapsule [97, 99], $\Delta H_{m,\mathrm{PCM}}$ and $\Delta H_{c,\mathrm{PCM}}$ are the crystallization enthalpies of pure PCM. The latent heat is measured by differential scanning calorimeter (DSC).

- Encapsulation efficiency [99]

$$E_{en} = \frac{\Delta H_{m,\mathrm{MPCM}}}{\Delta H_{m,\mathrm{PCM}}} \times 100\% \quad (2)$$

- Energy storage efficiency [97]

$$E_{es} = \frac{\Delta H_{m,\mathrm{MPCM}} + \Delta H_{c,\mathrm{MPCM}}}{\Delta H_{m,\mathrm{PCM}} + \Delta H_{c,\mathrm{PCM}}} \times 100\% \quad (3)$$

Basically, these two efficiencies represent the ratio of core PCM to shell materials. In the above Tables 4-7, the values of E_{en} were listed if only E_{en} or both E_{en} and E_{es} are available in the literatures. Otherwise, the values of E_{es} were listed but marked 'es' as a superscript in front of the data.

3.3.2.3 Microcapsule morphologies

The morphologies of the fabricated microcapsules can be examined by a SEM after coating a gold layer with a thickness of several nanometres [183]. The key morphologies which need to be confirmed are as follows: (a) whether agglomeration of microcapsules exists; (b) whether the shape of microcapsules is spherical; and (c) whether cracks, dents or defects exist on shell surface. The morphologies of microcapsules are markedly affected by types of emulsifiers, types of cross-linking agents and shell compositions. Su et al. [190] compared the morphologies of paraffin microcapsules with MF shell under two different types of emulsifiers. The emulsifier with higher value of hydrophilic–lipophilic balance (HLB) led to the agglomeration of microcapsules as shown in Figure 18(a), while the emulsifier with a lower HLB value prevented the agglomeration but resulted in more obvious dents on the shell surface as shown in Figure 18(b). Qiu et al. [109] analysed the effects of cross-linking agents on the morphologies of C_{18} microcapsules with PBA shell. They found that the dimples on the surface of the microcapsules using divinylbenzene (DVB) as cross-linking agent were less in number and larger in size compared with those using pentaerythritol triacrylate (PETA) as cross-linking agent as shown in Figure 19. Meanwhile, DVB as cross-linking agent largely improved the degree of adhesions of microcapsules compared to PETA. Lashgari et al. [90] reported that the C_{16} microcapsules with PMMA shell were wrinkled although they have spherical profile as shown in Figure 20(a), while the microcapsules with BA-co-MMA polymer shell exhibited smooth surface and absence of wrinkles as shown in Figure 20(b). It was explained by that BA-co-MMA offers greater flexibility and lower interfacial tension with C_{16} compared to MMA.

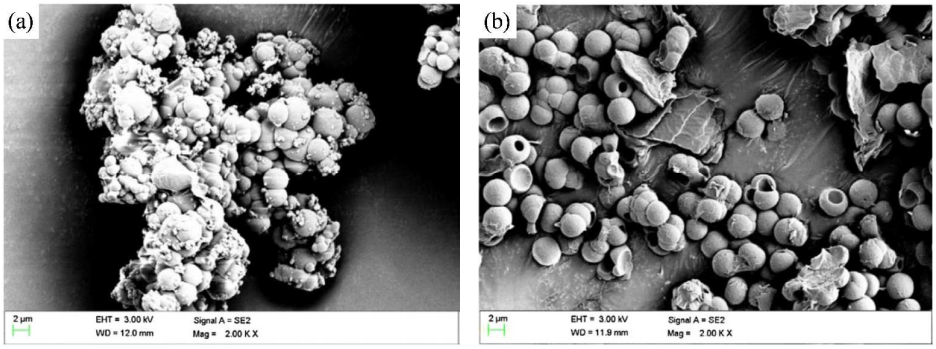

Figure 18 SEM images of paraffin microcapsules under different emulsifiers with (a) high HLB and (b) low HLB [190]

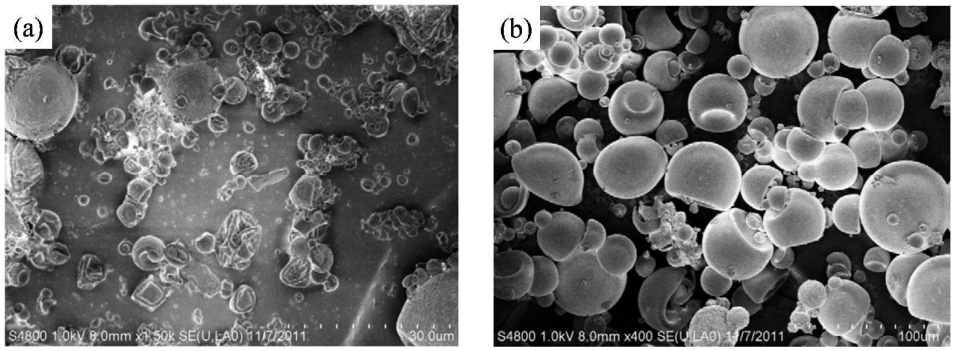

Figure 19 SEM images of C_{18} microcapsules with (a) PETA and (b) DVB as cross-linking agents [109]

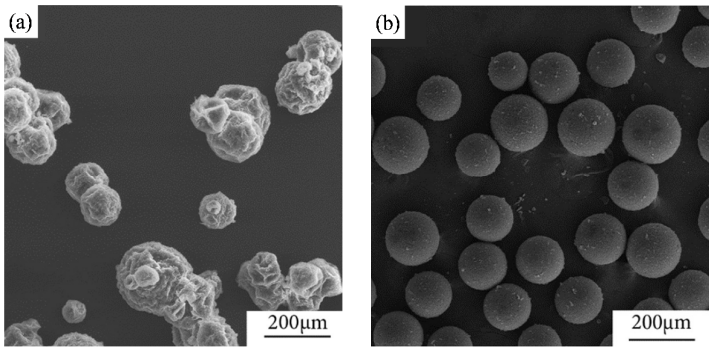

Figure 20 SEM images of C_{16} microcapsules with (a) PMMA shell and (b) BA-co-MMA polymer shell [90]

3.3.2.4 Mechanical strength

The mechanical integrity of microcapsules is the basis of successful application of microcapsules in thermal energy storage, however the PCM microcapsules are confronted with the possibility of rupture during repeated thermal charging-discharging cycling, especially in its usage as slurries because of repeatedly pumping [23]. The mechanical strength of microcapsules thus needs to be carefully considered. The mechanical properties of microcapsules can be analysed by atomic force microscopy (AFM) [203, 225-226]. Borreguero et al. [203] applied AFM probe to exert forces on RT27 microcapsules with LDPE-EVA copolymer shell and they found that the force required to produce the same deformation of microcapsules increased by approximately 83% when 2 wt% of carbon nanofibers was added into microcapsules. Giro-Paloma et al. [225] used AFM in nanoindentation mode to determine the maximum force that paraffin microcapsules with acrylate shell can afford before breakage at different temperatures. Values of effective modulus were calculated for microcapsule agglomerates of 150 μm in diameter and single microcapsule of 6 μm according to the measured results. They pointed out that values of effective Young's modulus depended on the temperature and particle size. The agglomerates presented higher effective modulus than single microcapsule and the effective Young's modulus of single microcapsule showed a remarkable decrease at 80 ℃ because this temperature is close to the acrylate shell glass transition temperature. They also compared the mechanical properties between paraffin microcapsules with acrylate and MF shells [226]. It was concluded that the acrylate shell exhibited better breakage resistance compared to MF shell, because the MF shell prepared using in-situ polymerisation tended to be more brittle and pressure-sensitive. When the temperature rose to make the paraffin become liquid state, the mechanical properties would be notably lowered.

3.3.2.5 Leakage of PCM

When the shell of PCM microcapsules possesses porous structure or cracks, leaking of liquid core PCM occurs.

And once leakage paths are formed, the core PCM will constantly leak until the PCM is depleted. Leakage rates (L_r) at different times are usually used to indicate the leakage-prevention performance of microcapsule structure. A typical measuring procedure of L_r is as follows [188]: A certain mass M_0 of dried microcapsules are individually put on filter papers. Then they are moved into an oven in which the temperature is fixed over the melting point of core PCM. The samples need to be taken out from the oven periodically at a prescribed time interval to weigh their mass which are indicated by M_t. The leakage rate is defined as

$$L_r(\%)=\frac{M_0-M_t}{M_0}\times 100 \quad (4)$$

Although the increase of shell thickness can enhance leakage-prevention performance, it will weaken the encapsulation ratio simultaneously. Zhang et al. [188] proposed a GO-modified paraffin microcapsules with MF shell to enhance leakage-prevention performance with high encapsulation ratio. They stated that the added GO nanosheets were situated at the interface between the core and the shell and successfully served as a protective screen to prevent leakage of paraffin, as shown in Figure 21. Their measured results manifested that this structure of dual protective screens comprising GO layer and MF shell slowed down the leakage of paraffin and thus could lengthen the service life of paraffin microcapsules. Al-Shannaq et al. [212] used mass loss analysis to test the permeability of core RT21 through the PMMA shell of microcapsules and compare the leakage rates of core RT21 from microcapsules with and without nucleating agent, which was used to suppress supercooling. Their testing results indicated that the leakage rate of RT21 from the microcapsules significantly decreased after RT58 was added and the increase of RT58 concentration resulted in smaller leakage. They explained it by that the RT58 may form a protective layer between the core RT21 and the PMMA shell. This suggests that the nucleating agent RT58 does not only diminish supercooling, but could also enhance leakage-prevention performance of the RT21 microcapsules with PMMA shell.

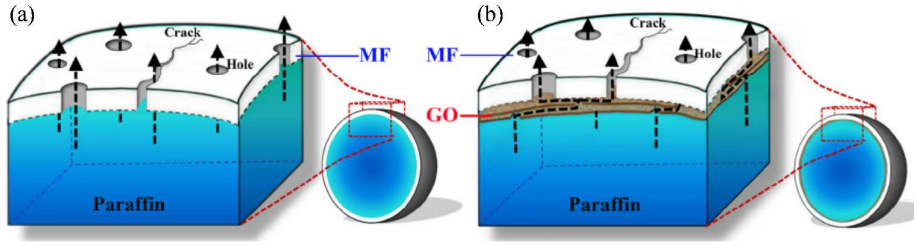

Figure 21 Schematic view for possible permeation through the shells of (a) MEPCM-00 and (b) MEPCMs with GO. [188]

3.3.3 Chemical properties

3.3.3.1 Fourier transformation infrared spectroscopy (FT-IR)

The Fourier transformation infrared spectroscopy (FT-IR) was used to identify the functional groups in organic polymers, inorganic compounds and chemical characterization of the MPCMs. Almost all of the investigations listed in Table 4-7 had performed this analysis.

Normally, the chemical compositions of PCMs before and after microencapsulation were examined by FT-IR. The obtained spectra were compared to determine whether a change occurred in chemical structures during the microencapsulation process. For example, P(MMA-co-MA) shell with nano-Al_2O_3 inlay microcapsules containing paraffin as core was synthesized through emulsion polymerization [199]. The FTIR spectra of nano-Al_2O_3, paraffin and P(MMA-co-MA) shell as well as microencapsulated paraffin modified with different percentages of nano-Al_2O_3

were shown in Figure 22. The results confirmed the successful encapsulation of paraffin within the P(MMA-co-MA) shell with no chemical interaction, and the paraffin microcapsules had been successfully modified with nano-Al_2O3 as well.

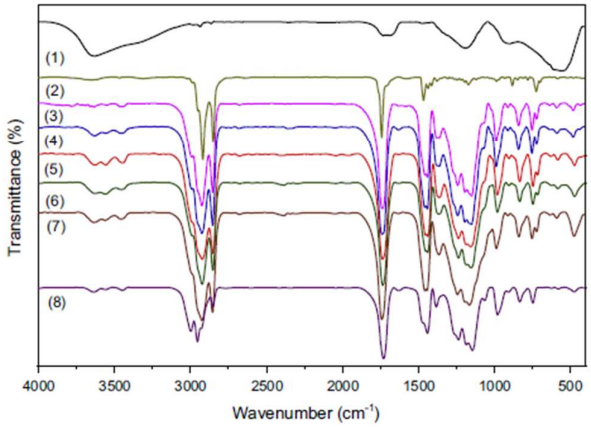

Figure 22 The FTIR spectra of nano-Al_2O_3, paraffin, copolymer shell and microcapsules modified with different amount of nano-Al_2O_3: (1) nano-Al_2O_3, (2) paraffin, (3) 0%, (4) 16%, (5) 27%, (6) 33%, (7) 38%, and (8) P(MMA-co-MA) [199]

3.3.3.2 X-ray diffraction (XRD)

The X-ray diffraction was used to determine the crystalline structures of microcapsules, which was typically suitable for the inorganic shell materials. For example, Zhang et al. [155] synthesized the microcapsules based on C_{20} core and silver/silica double-layered shell through interfacial polymerization. The XRD measurement was performed to investigate the crystalline structure of the silver/silica double-layered microcapsules, and the diffraction patterns are illustrated in Figure 23. The results suggested the sliver layer on the microcapsule surface retained good crystallinity and only an amorphous silica shell was fabricated onto the C_{20} core.

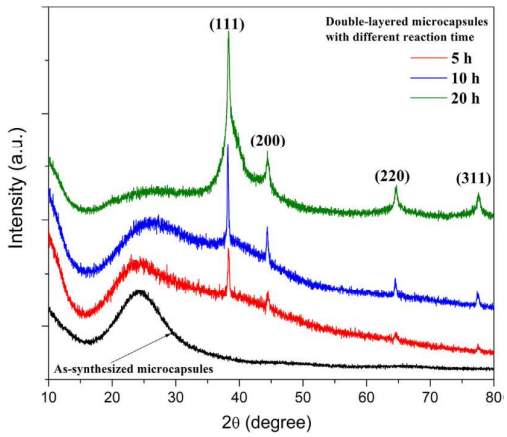

Figure 23 XRD patterns of the as-synthesized microcapsules and the silver/silica double-layered microcapsules obtained at different reaction time

3.4 Summaries and discussions

When C_n and their blends microcapsules are prepared, the characterization of these microcapsules are required to examine their microencapsulation properties, in order to further determine their application ranges and propose improvement methods of their properties. The characterization is generally conducted from three aspects including

thermal, physical and chemical properties to comprehensively evaluate the microcapsules. Multiple testing technologies such as DSC, LFA, TGA, SEM, AFM, FT-IR and XRD are used to explore these properties.

The main thermal properties are phase change temperature, latent heat, thermal conductivity and thermal stability. After PCM is microencapsulated, the shift of the phase change temperature occurs. Generally, the melting temperature slightly changes while the freezing temperature is notably decreased. The supercooling thus becomes a key barrier to the widespread application of microencapsulated C_n. In the literature, some methods to diminish or suppress the supercooling have been proposed, which can be classified into two sorts. One is to add nucleating agents into core to promote heterogeneous nucleation and another is to modify the composition and structure of shell to enable shell-induced heterogeneous nucleation. The effective latent heat in the first method will be reduced by the relatively large amount of additive and thus the second method is basically more advantageous from this point of view. It is inevitable that the latent heat decreases after microencapsulation of PCM because of shell existing. Utilization of the thinner or lighter shells can increase the latent heat of PCM microcapsules, but could cause more challenges in the synthesis process and material selection of shell. Types and dosage of shell materials and cross-linking agents should be precisely tailored to obtain the thinner or lighter shells. Due to its low thermal conductivities of the organic polymer shells, the PCM microcapsules with organic shells exhibit poor heat transfer property. The thermal conductivity of PCM microcapsules needs to be enhanced to enable a prompt response during the charging and discharging processes of thermal energy. The methods of elevating the thermal conductivity of PCM microcapsules proposed in the literature can also be classified two categories. One is to modify the organic shell using inorganic nanoparticles, such as Fe_3O_4, Al_2O_3, graphene, CNT, BN/TiO_2. Another is to directly employ inorganic shells, such as TiO_2, SiO_2, $CaCO_3$, ZrO_2 and Cu_2O. It should be noted that a compromise should be made between the thermal conductivity and the latent heat. Thermal stablitity of PCM microcapsules includes thermal degradation behavior and thermal reliability. High thermal degradation temperature ensures the stable work of PCM microcapsules at a high temperature far above the melting point of core PCM and good thermal reliability enables long-term serving durability of PCM microcapsules. Suitable shell materials or more perfect shell structure is helpful for elevating thermal degradation temperature amd achieving good thermal reliability.

The primary physical properties are microcapsule size distribution, efficiencies, microcapsule morphologies, mechanical strength, and leakage-prevention of PCM. Various microcapsule size distributions can be obtained by adjusting mass ratios of materials, shell compositions, process parameters and synthetic methods. The encapsulation efficiency and energy storage efficiency can be used to indicate the room for improvement in latent heat of PCM microcapsules. All the methods to elevate latent heat can be employed to augment the encapsulation efficiency and energy storage efficiency. The ideal morphologies of microcapsules should be spherical shape without agglomeration and without cracks, dents or defects on shell surface. Better morphologies of microcapsules can be achieved by adjusting types of emulsifiers, types of cross-linking agents and shell compositions. Excellent mechanical strength is required to maintain the integrity of microcapsules during repeated thermal charging-discharging cycling or repeatedly pumping in its usage as slurries. Additives like carbon nanofibers and adoption of shell materials with high flexibility and with glass transition temperature far away from phase change temperature is beneficial to the increase of mechanical strength. It should be noted that the mechanical strength will be decreased as PCM becomes liquid state. The leakage-prevention performance is closely related to the long term usability. A structure of dual protective screens formed by shell and additives like GO nanosheets can effectively slow down the leakage of PCM and thus lengthen the service life of PCM microcapsules.

The chemical properties are mainly chemical compositions or crystalline structures of PCM microcapsules. They can be used to indicate the chemical compatibility between core, shell and additives, and to check whether the shell has been successfully modified by nanoparticles or whether the multilayer shell has been successfully synthesized. They also can be used to aid the investigation of thermal reliability of PCM microcapsules.

Although lots of studies have been devoted to improvement of the properties of PCM microcapsules, there are still some key issues which need to be addressed: (1) Most of those prepared PCM microcapsules listed in Table 4 still have a high supercooling degree and low thermal conductivity. More effective methods are required to eliminate supercooling and increase thermal conductivity in the case of maintaining high latent heat for various PCM microcapsules. (2) The service life of PCM microcapsules need to be evaluated more precisely and be further prolonged. Thus more effective methods are required to prevent PCM in microcapsules from leaking. (3) MPCM slurry is a dominating application of PCM microcapsules, which undergoes repeatedly pumping in actual utilization. Therefore, the observed of morphologies and the measurements of mechanical strength of PCM microcapsules should be performed in repeatedly pumping conditions. (4) The microencapsulated pure C_n which can be found in the literature only refer to C_{12} to C_{32} as shown in Table 4, whereas the C_n with lower melting points such as C_8~C_{11} and higher melting points such as C_{33}~C_{50} as shown in Figure 1 have not yet been involved in the microencapsulation study or application. Table 2 and Table 3 summarize lots of binary mixtures and ternary mixtures of C_n, whose melting points are different from the corresponding pure C_n. These mixtures thus enrich the melting points of optional PCM and enable more precise solution of melting points. However, it can be found that most of these mixtures have not yet involved in the microencapsulation study or application by comparison with Table 6. Therefore, more studies should be conducted on microencapsulation of those C_n and their mixtures mentioned above.

4 Applications

4.1 Slurry

When the PCM microcapsules are dispersed into a carrier fluid (e.g. water) at the assistance of an appropriate amount of surfactant, MPCM slurry is formed. As they combine the latent heat of the PCM microcapsules and sensible heats of both the liquid and PCM microcapsules, MPCM slurry has high thermal storage capacity and strong heat transfer capacity. MPCM slurry is a multifunctional solid/liquid mixture, which can serve as both heat transfer fluids (HTFs) and thermal storage medium (TSM). MPCM slurry has various potential applications, such as cooling storage [227], solar thermal collector and storage [191, 228] and microchannel heat exchangers [229]. There are different levels of the scientific and technological issues which need to be addressed before realistic applications of MPCM slurry as HTFs and TSM.

At a material level, the thermophysical properties of MPCM slurry need to be clearly identified and predicted, such as thermal conductivity, specific heat, viscosity and density. Zhang et al. [223] studied the thermal and rheological properties of a series of MPCM slurries at low concentration of microcapsules. They measured the thermal conductivity and specific heat of MPCM slurry by the Hot Disk and the viscosity by a rheometer. Their study indicated that the predicted values of thermal conductivity and specific heat using those models adopted by Goel et al. [230] agreed well with the experimental data. The models for predicting the thermal and rheological properties of MPCM slurries are summarized and analyzed by Chen et al. [231]. These models have been widely employed as the basis of the experimental or numerical studies on heat transfer performance of MPCM slurries [224, 232-233]. There are also some studies devoted to the thermal performance improvement of MPCM slurries or development of novel PMCM slurries with excellent performances. Liu et al. [191] dispersed the paraffin@MF/graphite microcapsules into an ionic liquid to form a novel HTF. They found that this new kind of HTF exhibited an enhancement of 13% in thermal conductivity as the mass fraction of paraffin@MF/graphite was 20% and an increase by double in thermal storage capacity as compared to the base fluid.

At a component level, the heat transfer and hydrodynamic properties of MPCM slurry in ducts or channels and the thermal storage characteristics in a tank or container need to be figured out. A review on studies of heat transfer and hydrodynamic properties of MPCM slurry was conducted by Chen et al. [231]. They pointed out that wall temperature, heat transfer coefficient, Nusselt number are uesed to reflect the heat transfer properties of MPCM slurry indirectly or directly, while pressure drop and pumping power are used to estimate the degree of hydrodynamic challenge caused by high viscosity of MPCM slurry. Qiu et al. [234] reviewed the heat ransfer enhancement mechanism of MPCM slurry, which consists of microconvection caused by microencapsules, migration of microcapsules within the boudnary layer, and phase change heat latent. They also collocated and evluated the parameters that have impact on the heat transfer properties of MPCM slurry under the condition of laminar and turbulent flow, mainly including concentration of microcapslues, size of microcapsules, Stephan number, Peclet number, Reynolds number as well as Prandtl number. Song et al. [235] carried out experimental studies on laminar heat transfer of MPCM slurry using low-melting-point liqud metal as a carrier fluid. They reported that the heat transfer coefficient increases with increasing volume concentration of microcapsules and Reynolds number. Kong et al. [236] conducted pressure drop and heat transfer experiments for MPCM slurries in a helically coiled tube under turbulent flow conditions. They found that a helically coiled tube was more suitable than a straight tube for convection heat transfer of MPCM slurry, although the heat transfer enhancement was restricted by high viscosity.

Zhang et al. [237] compared the thermal storage characterisitcs of MPCM slurry storage device (coil-in-tank) and stratified water storage tank (SWST). They observed that although the thermal storage capacity of MPCM slurry was much higher than that of water, the overall charging/dischanging rates of the slurry storage device were much lower than the idealized SWST, implying that an optimized design for MPCM slurry thermal storage device was further required.

At a system level, the compatibility of selected MPCM slurry with a heat exchange system or thermal energy system and the integrated system performnce should be carefully considered. Zhang et al. [227] experimentally investigated the phase transition of MPCM slurry running in a thermal storage test system. They found that the extraction of latent heat of MPCM slurry was not entirely complete due to supercooling in a practical air conditioning system integrated with thermal storage. Therefore supercooling would lower the partical storage capacity of MPCM slurry at a limited cooling temperature or the effiency of a cooling storage system. Qiu et al. [238] conducted an experimental study concerning the overall performance of a novel PV/T thermal and power system ultilizing MPCM slurry. It was presented that the effects of various solar radiations, Reynolds numbers and concentrations of microcapsules on the performances of the PV/T system. At their recommended operational conditions, the net overall solar efficiencies of the system could achieve up to 80.8–83.9%. Kong et al. [239] performed field evaluation of ground source heat pump systems (GSHP) employing MPCM slurries as working fluids. They reported that the performance coefficient of the GSHP system was elevated by up to 4.9% due to higher heat capacity of MPCM slurries and progressive cavity pumps were more beneficial to durability of MPCM slurries than centrifugal pumps.

4.2 Buildings

For the building applications, MPCMs are always embedded into concrete mixes, cement mortar, wallboards, gypsum plasters, sandwich panels, slabs, among others, which act to increase the thermal inertia for the same mass of buildings [20]. Actually, the concrete is one of the most useful materials in buildings, and most of researchers are focused on the embedment of MPCMs into concrete to enhance the thermal and acoustic insulation of walls in recent years. However, from an economic point of view, only the lower cost of the synthesized MPCMs has potential for a pilot application.

Cabeza et al. [240] studied a new concrete with paraffin microcapsules on thermal aspects. They found that the energy storage in the walls containing paraffin microcapsules were contributed to an improved thermal inertia and smoother fluctuations of temperature, which demonstrated a commendable opportunity in energy saving for buildings. Giro-Paloma et al. [201] synthesized the microencapsulated RT21, and tested their mechanical properties like elastic modulus, load at maximum displacement, displacement at maximum load by nano-indentation technique. In addition to this, an important parameter for considering use in building, the release of volatile organic compounds (VOCs), were studied. The results indicated that the RT21 microcapsules had better mechanical resistance and stiffness, and showed better stability with less short-term emission of VOCs as well. Aguayo et al. [241] proposed a new application of paraffin microcapsules in infrastructural concrete for mitigating early-age cracking and freeze-and-thaw induced damage. Figure 24 depicted the microstructure of cement pastes incorporating MPCMs. The results ascertained that the compressive strength of cement mortars with MPCMs was noted to be strongly dependent on the encapsulation properties. Cao et al. [242] fabricated the concretes by mixing the microencapsulated RT27 into Portland cement concrete (PCC) and geopolymer concrete (GPC), it was found that the thermal performance of concrete was improved significantly by adding the microcapsules, simultaneously, the significant

loss in compressive strength was observed. However, the compressive strength still satisfied the mechanical European regulation for concrete applications. Sant et al. [243-244] synthesized the paraffin microcapsules, and applied them into cement-based composites. The results showed that the existence of MPCMs would not affect the drying shrinkage of cementitious composites, but in specific cases, it may slightly improve the durability of cementitious composites. Beyond that, the effect of MPCMs on the thermal deformation behavior was examined. The thermal deformation coefficient of microcapsules was similar to the shell materials. Finally, a rule was presented for designing the mortar composites with MPCMs which find use in built environment.

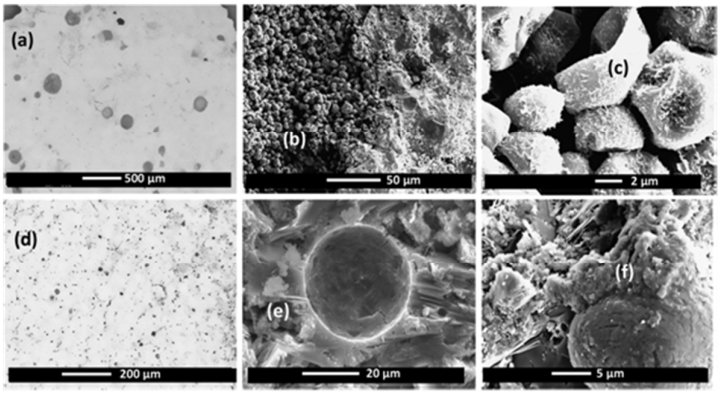

Figure 24 Microstructure of cement pastes incorporating MPCMs (a) PCM-M dispersed in cement paste, (b) breakage of PCM-M agglomerates into individual nodules in the cement paste, (c) cement hydration products on individual PCM-M nodules, (d) PCM-E dispersed in cement paste, (e) intact PCM-E microcapsule with hydration products around, and (f) dense reaction product around a PCM-E particle. [241]

4.3 Textiles

Application of microencapsulated C_n and C_n's blends in the textile industries was an old topic but had continually growing interest in recent years. Many studies have been done on microencapsulated C_n textiles materials.

As Nelson [245] reported, microcapsules can be coated on the surface of fabric or embedded within fiber. Sarier et al. [81, 94] reported that the thermal enhancement of the fabrics could be achieved by incorporating C_{16}, C_{18} and C_{19} microcapsules through coating. The energy storage capacities of the fabrics with microcapsules were found to be 2.5~4.5 times enhanced compared to the reference fabrics for particular temperature intervals. Later on, They indicated that the microencapsulated C_{16} and C_{18} with silver nanoparticles have very high thermal storage capacities, good durability, thermal stability and improved thermal conductivity, which are fairly appropriate for industrial applications in the field of textiles like sportswear and protective clothing, medical textiles and automotive and agriculture textiles [88]. Alay et al. [82-83] fabricated the C_{16} microcapsules and added to woven fabrics by cad-cure method. The results showed that the cotton, cotton/polyester, and microfiber polyester fabrics treated with microcapsules at the same concentration were capable of heat absorbing 4.95 J/g, 10.02 J/g, and 8.38 J/g, respectively. These discrepancies were attributed to the chemical compatibility of the fabric material and shell material of microcapsules. Moghaddam et al. [140-141] prepared microencapsulated C_{19} for textiles application, and they found that that C_{19} microcapsules had a high energy-storing density (>137.83 J/g) and proper temperature of solid–liquid change (30~31˚C), which were suitable for thermo-regulating textile. Most recently, Aksoy et al. [89, 133, 156-157] fabricated the microencapsulated C_{18} and C_{20} as additive used to improve thermal comfort and flame retardant

property of the textiles. SEM images demonstrated that the microcapsules could be distributed onto textile substrates homogeneously and durable to repeated washings (as shown in Figure 25). Meanwhile, thermo-regulating properties of the fabrics with microcapsules were proved via thermal history measurement results. Sun and Iqbal [210] synthesized the nanocapsules with C_{18} and C_{20} mixture as the core materials, and applied them on a cotton fabric via a pad-dry-cure process. The results indicated that nanocapsules have better durability on cotton fabric than MPCMs. The latent heat was decreasing faster for MPCM than nanoencapsulated PCM after washing.

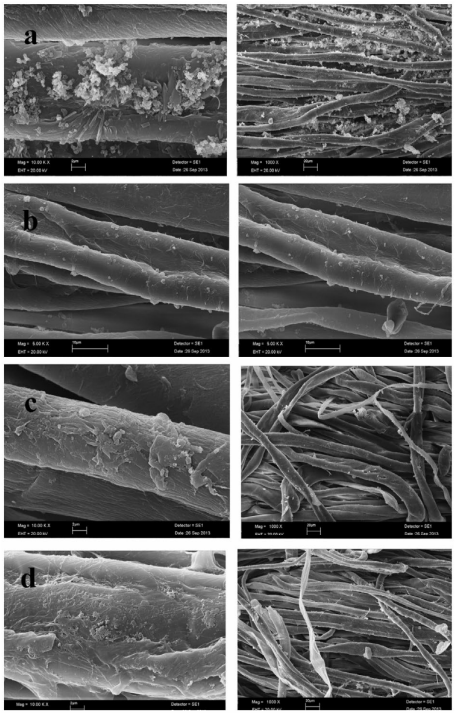

Figure 25 SEM images of the fabrics treated with P(MMA-co-MAA)/n-octadecane-3 microcapsule using Fixapret F-ECO resin (a) rubbing test applied, (b) 5 cycles washed, (c) 10 cycles washed, and (d) 20 cycles washed [133]

4.4 Foam

Integration of MPCMs into foams can improve their thermal performances, especially in thermal-insulating ability. Polyurethane, polystryrene foams with MPCMs can be applied in areas like automotive interiors, medical products, among others.

You et al. [246] fabricated the polyurethane foams containing C_{18} microcapsules. They found that the enthalpy of the foam increased with the increase of the content of MPCMs, and the maximum value of 12 J/g was achieved when the weight ratio of MPCMs/Polyurethane foam is 12.59%. Borreguero et al. [247-248] produced polyurethane foams incorporating different percentages of RT27 microcapsules. It was observed that the foam with 18 wt% of microcapsules can improve the TES capacity and hold the mechanical properties of the foam without fillers. 21 wt% of microcapsules resulted in a reduction in mechanical properties but with compressive strength and modulus higher than those exhibited by the foams containing 11 wt%. Then, 18 wt% of two types microcapsules (with different shell materials) were synthesized and added to the polyurethane foams [249], and Figure 26 illustrated the SEM images of polyurethane foams containing 18 wt % of mSP-(PS-RT27). The results indicated that the microcapsules with highest particle size from PS and the agglomeration of the microcapsules from PMMA, led to the strut rupture, damaging the final mechanical performance. Three years later, they successfully produced rigid polyurethane foams

containing up to a 40 wt% content of mSD-(LDPE-EVA-RT27) [250]. These foams as temperature-regulating materials have a latent heat of 34.4 J/g which is higher than that reported value in literature for similar materials. Qiu et al. [77, 118, 182, 196] formed the polystyrene foams containing C_{14}, C_{18} and paraffin microcapsules, and all the experimental results demonstrated that the foam treated by microcapsules had a better thermoregulatory property than the raw foam.

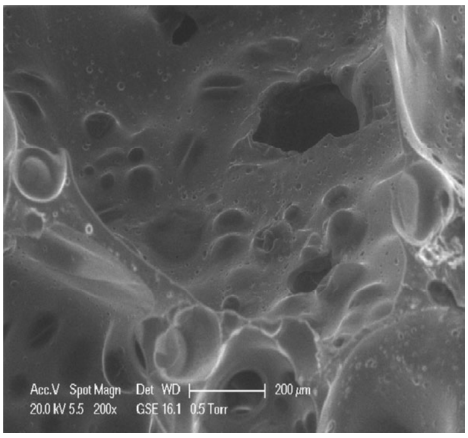

Figure 26 SEM images with 200× magnification of PU foams containing 18 wt % of mSP-(PS-RT27) [249]

5 Conclusions and outlook

A main line from materials to their microcapsules (C_n and C_n's blends to their microcapsules) as PCMs for TES systems was presented in this review. At first, PCM-interesting characteristics (transition temperatures and enthalpies) of C_n, multinary C_n and paraffins were listed, while the phase equilibrium evaluations of binary C_n were elaborated. Then, the microencapsulated C_n and C_n's blends with respect to the synthesis methods, physical properties, thermal properties and chemical properties were presented and analyzed. Finally, the practical applications of microencapsulated C_n and their blends were reported.

In this review, the temperature range of the summarized C_n and C_n's blends is from 211K to 366K (-62˚C~93˚C), while the temperature range of the summarized microencapsulated C_n and C_n's blends is from 244K to 354K (-29˚C ~81˚C).

Review demonstrated that:

(1) The fixed melting points of C_n limit their practical applications; however, the C_n's blends have proved the greater value as tunable PCMs because the temperature range are substantially enlarged and enriched. To employ C_n's blends as PCM with robust performances, a narrow thermal window with no phase separation is the properties pursued. The phase change behaviors of C_n's blends are close related to the phase equilibrium. Various types of phase change characteristics are elaborated through phase diagrams, and it is admitted that the eutectics and peritectics have been considered largely from a PCM selection perspective.

(2) The supercooling is prevalent for PCM microcapsules, which can be suppressed or eliminated by adding nucleating agents or modify the composition and structure of shell to induce heterogeneous nucleation. The thermal conductivity of PCM microcapsules can be elevated by modifying the organic shell using inorganic nanoparticles or directly employing inorganic shells. A compromise should be made between the thermal conductivity and the latent heat. Suitable shell materials or more perfect shell structure is helpful for elevating thermal degradation temperature. Better morphologies of microcapsules can be achieved by adjusting types of emulsifiers, types of cross-linking

agents and shell compositions. Suitable additives in shell or adoption of shell materials with high flexibility and glass transition temperature far away from phase change is beneficial to the increase of the mechanical strength. A structure of dual protective screens formed by shell and additives can effectively slow down the leakage of PCM and thus lengthen the service life of PCM microcapsules. The chemical compositions and crystalline structures of PCM microcapsules should be tested to certify the chemical compatibility between materials and success of shell modification or hybrid shell synthesis.

Outlook:

(1) For materials (C_n and C_n's blends) level: Firstly, the published studies indicated that the binary system with a large discrepancy in chain length ($\Delta n_c \geq 6$) still showed a eutectic characteristic, which does not respect the basic thermodynamic and miscible laws. Therefore, a huge amount of new combinations can be created, and deserve further investigations. Secondly, ternary systems are the neglected category in the PCM-context (few works published), but are promising for exploration in the future. Finally, a comprehensive phase equilibrium analysis is a fundamental way to indentify the phase change characteristics of C_n's blends, but now it is still insufficient, the relative studies are worth improving.

(2) For microcapsules level: Firstly, more effective methods are required to eliminate supercooling and increase thermal conductivity in the case of maintaining high latent heat for various PCM microcapsules. Secondly, the service life of PCM microcapsules need to be evaluated more precisely and be further prolonged. Thirdly, the observed of morphologies and the measurements of mechanical strength of PCM microcapsules should be performed in repeatedly pumping conditions for slurry application. Finally, microencapsulation of more C_n and their mixtures which are not involved in the literature should be studies to enrich the optional range or values of melting points of PCM microcapsules. Except for the application areas in slurry, building, textiles and foam, the PCM microcapsules may also have the potential to be applied in solar air heater, refrigeration, liquid air thermal energy storage systems, among others.

Acknowledgements

The authors acknowledge the financial support provided by National Natural Science Foundation of China (Grant Nos. 51776095 and 51606135), Natural Science Foundation of Jiangsu Province (Grant No. BK20151539), and Natural Science Foundation of Hubei Province (Grant No. 2016CFB156).

References:

1. Chen, H.; Cong, T. N.; Yang, W.; Tan, C.; Li, Y.; Ding, Y., Progress in electrical energy storage system: A critical review. *Progress in Natural Science* **2009,** *19* (3), 291-312.

2. Mehling, H., Cabeza, LF., *Heat and cold storage with PCM. An up to date introduction into basics and applications*. Springers-Verlag Berlin Heidelberg: 2008.

3. Zhao, B.; Li, C.; Jin, Y.; Yang, C.; Leng, G.; Cao, H.; Li, Y.; Ding, Y., Heat transfer performance of thermal energy storage components containing composite phase change materials. *IET Renewable Power Generation* **2016,** *10* (10), 1515-1522.

4. Wang, P.; Wang, X.; Huang, Y.; Li, C.; Peng, Z.; Ding, Y., Thermal energy charging behaviour of a heat exchange device with a zigzag plate configuration containing multi-phase-change-materials (m-PCMs). *Applied Energy* **2015,** *142*, 328-336.

5. Peng, H.; Dong, H.; Ling, X., Thermal investigation of PCM-based high temperature thermal energy storage in packed bed. *Energy Conversion and Management* **2014,** *81*, 420-427.

6. Peng, H.; Li, R.; Ling, X.; Dong, H., Modeling on heat storage performance of compressed air in a packed bed system. *Applied Energy* **2015,** *160*, 1-9.

7. Peng, H.; Yang, Y.; Li, R.; Ling, X., Thermodynamic analysis of an improved adiabatic compressed air energy storage system. *Applied Energy* **2016,** *183*, 1361-1373.

8. Peng, H.; Shan, X.; Yang, Y.; Ling, X., A study on performance of a liquid air energy storage system with packed bed units. *Applied Energy* **2018,** *211*, 126-135.

9. Chang, C.; Wu, Z.; Navarro, H.; Li, C.; Leng, G.; Li, X.; Yang, M.; Wang, Z.; Ding, Y., Comparative study of the transient natural convection in an underground water pit thermal storage. *Applied Energy* **2017,** *208*, 1162-1173.

10. She, X.; Peng, X.; Nie, B.; Leng, G.; Zhang, X.; Weng, L.; Tong, L.; Zheng, L.; Wang, L.; Ding, Y., Enhancement of round trip efficiency of liquid air energy storage through effective utilization of heat of compression. *Applied Energy* **2017,** *206* (Supplement C), 1632-1642.

11. Yu, Q.; Romagnoli, A.; Al-Duri, B.; Xie, D.; Ding, Y.; Li, Y., Heat storage performance analysis and parameter design for encapsulated phase change materials. *Energy Conversion and Management* **2018,** *157*, 619-630.

12. Yu, Q.; Tchuenbou-Magaia, F.; Al-Duri, B.; Zhang, Z.; Ding, Y.; Li, Y., Thermo-mechanical analysis of microcapsules containing phase change materials for cold storage. *Applied Energy* **2018,** *211*, 1190-1202.

13. Abhat, A., Low temperature latent heat thermal energy storage: Heat storage materials. *Solar Energy* **1983,** *30* (4), 313-332.

14. Oró, E.; de Gracia, A.; Castell, A.; Farid, M. M.; Cabeza, L. F., Review on phase change materials (PCMs) for cold thermal energy storage applications. *Applied Energy* **2012,** *99* (Supplement C), 513-533.

15. Li, G.; Hwang, Y.; Radermacher, R.; Chun, H.-H., Review of cold storage materials for subzero applications. *Energy* **2013,** *51* (Supplement C), 1-17.

16. Pereira da Cunha, J.; Eames, P., Thermal energy storage for low and medium temperature applications using phase change materials – A review. *Applied Energy* **2016,** *177* (Supplement C), 227-238.

17. Zhao, C. Y.; Zhang, G. H., Review on microencapsulated phase change materials (MEPCMs): Fabrication, characterization and applications. *Renewable and Sustainable Energy Reviews* **2011,** *15* (8), 3813-3832.

18. Jamekhorshid, A.; Sadrameli, S.; Farid, M., A review of microencapsulation methods of phase change materials (PCMs) as a thermal energy storage (TES) medium. *Renewable and Sustainable Energy Reviews* **2014,** *31*, 531-542.

19. Khadiran, T.; Hussein, M. Z.; Zainal, Z.; Rusli, R., Encapsulation techniques for organic phase change materials as thermal energy storage medium: A review. *Solar Energy Materials and Solar Cells* **2015,** *143* (Supplement C), 78-98.

20. Konuklu, Y.; Ostry, M.; Paksoy, H. O.; Charvat, P., Review on using microencapsulated phase change materials (PCM) in building applications. *Energy and Buildings* **2015,** *106* (Supplement C), 134-155.

21. Su, W.; Darkwa, J.; Kokogiannakis, G., Review of solid–liquid phase change materials and their encapsulation technologies. *Renewable and Sustainable Energy Reviews* **2015,** *48*, 373-391.

22. Giro-Paloma, J.; Martínez, M.; Cabeza, L. F.; Fernández, A. I., Types, methods, techniques, and applications for microencapsulated phase change materials (MPCM): A review. *Renewable and Sustainable Energy Reviews* **2016,** *53* (Supplement C), 1059-1075.

23. Alva, G.; Lin, Y.; Liu, L.; Fang, G., Synthesis, characterization and applications of microencapsulated phase change materials in thermal energy storage: A review. *Energy and Buildings* **2017,** *144* (Supplement C), 276-294.

24. Milián, Y. E.; Gutiérrez, A.; Grágeda, M.; Ushak, S., A review on encapsulation techniques for inorganic phase change materials and the influence on their thermophysical properties. *Renewable and Sustainable Energy Reviews* **2017,** *73* (Supplement C), 983-999.

25. Dirand, M.; Bouroukba, M.; Briard, A.-J.; Chevallier, V.; Petitjean, D.; Corriou, J.-P., Temperatures and enthalpies of (solid + solid) and (solid + liquid) transitions of n-alkanes. *The Journal of Chemical Thermodynamics* **2002,** *34* (8), 1255-1277.

26. Himran, S.; Suwono, A.; Mansoori, G. A., Characterization of Alkanes and Paraffin Waxes for Application as Phase Change Energy Storage Medium. *Energy Sources* **1994,** *16* (1), 117-128.

27. Rajabalee, F.; Espeau, P.; Haget, Y., n-Octane + n-Decane: a Eutectic System in the n-Alkane Family; Experimental Phase Diagram and Thermodynamic Analysis. *Molecular Crystals and Liquid Crystals Science and Technology. Section A. Molecular Crystals and Liquid Crystals* **1995,** *269* (1), 165-173.

28. Ventolà, L.; Cuevas-Diarte, M. A.; Calvet, T.; Angulo, I.; Vivanco, M.; Bernar, M.; Bernar, G.; Melero, M.; Mondieig, D., Molecular alloys as phase change materials (MAPCM) for energy storage and thermal protection at temperatures from 70 to 85°C. *Journal of Physics and Chemistry of Solids* **2005,** *66* (10), 1668-1674.

29. Ventolà, L.; Calvet, T.; Cuevas-Diarte, M. Á.; Métivaud, V.; Mondieig, D.; Oonk, H., From concept to application. A new phase change material for thermal protection at -11 °C. *Materials Research Innovations* **2002,** *6* (5), 284-290.

30. Mondieig, D.; Rajabalee, F.; Metivaud, V.; Oonk, H. A. J.; Cuevas-Diarte, M. A., n-Alkane Binary Molecular Alloys. *Chemistry of Materials* **2004,** *16* (5), 786-798.

31. Huang, D.; Simon, S. L.; McKenna, G. B., Chain length dependence of the thermodynamic properties of linear and cyclic alkanes and polymers. *The Journal of Chemical Physics* **2005,** *122* (8), 084907.

32. Atkinson, C. M. L.; Larkin, J. A.; Richardson, M. J., Enthalpy changes in molten n-alkanes and polyethylene. *The Journal of Chemical Thermodynamics* **1969,** *1* (5), 435-440.

33. Johansen, A. V., Density of hydrocarbons in liquid state as a function of temperature. *Physico-Chemical Properties of Individual Hydrocarbons* **1960**, 85-112.

34. Watanabe, H.; Seong, D. J., The Thermal Conductivity and Thermal Diffusivity of Liquid n-Alkanes: C n H2n+2 (n=5 to 10) and Toluene. *International Journal of Thermophysics* **2002,** *23* (2), 337-356.

35. Vargaftik, N. B., *Handbook of Thermal Conductivity of Liquids and Gases*. CRC Press: 1994.

36. Kenisarin, M. M., Thermophysical properties of some organic phase change materials for latent heat storage. A review. *Solar Energy* **2014,** *107* (Supplement C), 553-575.

37. Dirand, M.; Bouroukba, M.; Chevallier, V.; Petitjean, D.; Behar, E.; Ruffier-Meray, V., Normal Alkanes, Multialkane Synthetic Model Mixtures, and Real Petroleum Waxes: Crystallographic Structures, Thermodynamic Properties, and Crystallization. *Journal of Chemical & Engineering Data* **2002,** *47* (2), 115-143.

38. Hastie, G. P.; Roberts, K. J., Investigation of inter- and intra-molecular packing in the solid state for crystals of normal alkanes and homologous mixtures using FT-IR spectroscopy. *Journal of Materials Science* **1994,** *29* (7), 1915-1919.

39. Kravchenko, V., The eutectics and solid solutions of paraffins. *Acta Physicochim. URSS* **1946,** *21*, 335-344.

40. Gunasekara, S. N.; Martin, V.; Chiu, J. N., Phase equilibrium in the design of phase change materials for thermal energy storage: State-of-the-art. *Renewable and Sustainable Energy Reviews* **2017,** *73* (Supplement C), 558-581.

41. Parsa, S.; Javanmardi, J.; Aftab, S.; Nasrifar, K., Experimental measurements and thermodynamic modeling ofwax disappearance temperature for the binary systems n-C14H30 + n-C16H34, n-C16H34 + n-C18H38 and n-C11H24 + n-C18H38. *Fluid Phase Equilibria* **2015,** *388*, 93-99.

42. Gunasekara, S. N. Phase Equilibrium-aided Design of Phase Change Materials from Blends : For Thermal Energy Storage. Doctoral thesis, comprehensive summary, KTH Royal Institute of Technology, Stockholm, 2017.

43. Gunasekara, S. N.; Kumova, S.; Chiu, J. N.; Martin, V., Experimental phase diagram of the dodecane–tridecane system as phase change material in cold storage. *International Journal of Refrigeration* **2017,** *82* (Supplement C), 130-140.

44. Espeau, P.; Robles, L.; Cuevas-Diarte, M. A.; Mondieig, D.; Haget, Y., Thermal cycling of molecular alloys and eutectics containing alkanes for energy storage. *Materials Research Bulletin* **1996,** *31* (10), 1219-1232.

45. Espeau, P.; Rajabalee, F.; Haget, Y., Binary Phase Diagram with Non Isomorphous n-Alkanes: C12H266 – C15H32. Implication of the Rotator Phase R, in the Melting Behaviour of Odd - Even and Even – Odd Phase Diagrams. *Molecular Crystals and Liquid Crystals Science and Technology. Section A. Molecular Crystals and Liquid Crystals* **1998,** *323* (1), 145-153.

46. Oonk, H. A. J.; Mondieig, D.; Haget, Y.; Cuevas-Diarte, M. A., Perfect families of mixed crystals: The rotator I N-alkane case. *The Journal of Chemical Physics* **1998,** *108* (2), 715-722.

47. Milhet, M.; Pauly, J.; Coutinho, J. A. P.; Dirand, M.; Daridon, J. L., Liquid–solid equilibria under high pressure of tetradecane + pentadecane and tetradecane + hexadecane binary systems. *Fluid Phase Equilibria* **2005,** *235* (2), 173-181.

48. Bo, H.; Gustafsson, E. M.; Setterwall, F., Tetradecane and hexadecane binary mixtures as phase change materials (PCMs) for cool storage in district cooling systems. *Energy* **1999,** *24* (12), 1015-1028.

49. He, B.; Martin, V.; Setterwall, F., Liquid–solid phase equilibrium study of tetradecane and hexadecane binary mixtures as phase change materials (PCMs) for comfort cooling storage. *Fluid Phase Equilibria* **2003,** *212* (1), 97-109.

50. He, B.; Martin, V.; Setterwall, F., Phase transition temperature ranges and storage density of paraffin wax phase change materials. *Energy* **2004,** *29* (11), 1785-1804.

51. Dotsenko, S.; Martsinkovskii, A.; Danilin, V., Thermal storage properties of n-paraffins, fatty acids and multicomponent systems on their basis. *e-Journal: Fiziko-khimicheskii analiz svoistv mnogokomponentnykh system*

2004.

52. Stolk, R.; Rajabalee, F.; Jacobs, M. H. G.; Espeau, P.; Mondieig, D.; Oonk, H. A. J.; Haget, Y., The RI-liquid equilibrium in the ternary system n-pentadecane + n-hexadecane + n-heptadecane. Calculation of liquidus surface and thermal windows comparison with experimental data. *Calphad* **1997,** *21* (3), 401-410.

53. Kenisarin, M.; Mahkamov, K., Solar energy storage using phase change materials. *Renewable and Sustainable Energy Reviews* **2007,** *11* (9), 1913-1965.

54. Paunovic, I.; Mehrotra, A. K., Liquid–solid phase transformation of C16H34, C28H58 and C41H84 and their binary and ternary mixtures. *Thermochimica Acta* **2000,** *356* (1), 27-38.

55. Robles, L.; Espeau, P.; Mondieig, D.; Haget, Y.; Oonk, H. A. J., Polymorphisme et alliages moleculaires dans le systeme C17H36□C19H40. *Thermochimica Acta* **1996,** *274* (Supplement C), 61-72.

56. Maroncelli, M.; Strauss, H.; Snyder, R., Structure of the n-alkane binary solid n-C19H40/n-C21H44 by infrared spectroscopy and calorimetry. *The Journal of Physical Chemistry* **1985,** *89* (24), 5260-5267.

57. Metivaud, V.; Rajabalee, F.; Mondieig, D.; Haget, Y.; Cuevas-Diarte, M. A., Solid−Solid and Solid−Liquid Equilibria in the Heneicosane−Docosane Binary System. *Chemistry of Materials* **1999,** *11* (1), 117-122.

58. Jouti, B.; Provost, E.; Petitjean, D.; Bouroukba, M.; Dirand, M., Phase diagram of n-heneicosane and n-tricosane molecular alloys. *Journal of Molecular Structure* **1996,** *382* (1), 49-56.

59. Nouar, H.; Petitjean, D.; Bouroukba, M.; Dirand, M., Binary phase diagram of the system: n-docosane-n-tricosane. *Journal of Molecular Structure* **1998,** *443* (1), 197-204.

60. Rajabalee, F.; Métivaud, V.; Mondieig, D.; Haget, Y.; Oonk, H. A. J., Thermodynamic Analysis of Solid−Solid and Solid−Liquid Equilibria in Binary Systems Composed of n-Alkanes: Application to the System Tricosane (C23H48) + Pentacosane (C25H52). *Chemistry of Materials* **1999,** *11* (10), 2788-2795.

61. Hammami, A.; Mehrotra, A. K., Liquid-solid-solid thermal behaviour of n-C44H90 + n-C50H102 and n-C25H52 + n-C28H58 paraffinic binary mixtures. *Fluid Phase Equilibria* **1995,** *111* (2), 253-272.

62. Hammami, A.; Mehrotra, A. K., Non-isothermal crystallization kinetics of binary mixtures of n-alkanes: ideal eutectic and isomorphous systems. *Fuel* **1996,** *75* (4), 500-508.

63. Rajabalee, F.; Métivaud, V.; Mondieig, D.; Haget, Y.; Oonk, H. A., Structural and Energetic Behavior of Mixed Samples in the Hexacosane (n-C26H54)/Octacosane (n-C28H58) System; Solid-Solid and Solid-Liquid Equilibria. *Helvetica chimica acta* **1999,** *82* (11), 1916-1929.

64. Yilmaz, S.; Sayin, K.; Gök, Ö.; Yilmaz, M. Ö.; Beyhan, B.; Sahan, N.; Paksoy, H.; Evliya, H. In *New binary alkane mixtures as pcms for cooling applications*, 11th International Conference on Thermal Energy Storage for Energy Efficiency and Sustainability, Stockholm International Fairs. Stockholm, Sweden, 2009.

65. Craig, S.; Hastie, G.; Roberts, K.; Gerson, A.; Sherwood, J.; Tack, R., Investigation into the structures of binary-, tertiary-and quinternary-mixtures of n-alkanes and real diesel waxes using high-resolution synchrotron X-ray powder diffraction. *Journal of Materials Chemistry* **1998,** *8* (4), 859-869.

66. Metivaud, V.; Rajabalee, F.; Oonk, H. A. J.; Mondieig, D.; Haget, Y., Complete determination of the solid (RI)-liquid equilibria of four consecutive n-alkane ternary systems in the range C14H30-C21H44 using only binary data. *Canadian Journal of Chemistry* **1999,** *77* (3), 332-339.

67. Nouar, H.; Petitjean, D.; Bouroukba, M.; Dirand, M., Isothermal Sections of Ternary Mixtures: n-docosane + n-tricosane + n-tetracosane. *Molecular Crystals and Liquid Crystals Science and Technology. Section A. Molecular Crystals and Liquid Crystals* **1999,** *326* (1), 381-394.

68. Ukrainczyk, N.; Kurajica, S.; Šipušić, J., Thermophysical comparison of five commercial paraffin waxes as latent heat storage materials. *Chemical and biochemical engineering quarterly* **2010,** *24* (2), 129-137.

69. Dincer, I.; Rosen, M., *Thermal energy storage: systems and applications*. John Wiley & Sons: 2002.

70. https://www.rubitherm.eu/en/index.php/productcategory/organische-pcm-rt.

71. Zhu, K.; Qi, H.; Wang, S.; Zhou, J.; Zhao, Y.; Su, J.; Yuan, X., Preparation and Characterization of Melamine-Formaldehyde Resin Micro- and Nanocapsules Filled withn-Dodecane. *Journal of Macromolecular Science, Part B* **2012,** *51* (10), 1976-1990.

72. Yang, R.; Zhang, Y.; Wang, X.; Zhang, Y.; Zhang, Q., Preparation of n-tetradecane-containing microcapsules with different shell materials by phase separation method. *Solar Energy Materials and Solar Cells* **2009,** *93* (10), 1817-1822.

73. Fang, G.; Li, H.; Yang, F.; Liu, X.; Wu, S., Preparation and characterization of nano-encapsulated n-tetradecane as phase change material for thermal energy storage. *Chemical Engineering Journal* **2009,** *153* (1-3), 217-221.

74. Konuklu, Y.; Paksoy, H. O.; Unal, M., Nanoencapsulation of n-alkanes with poly(styrene-co-ethylacrylate) shells for thermal energy storage. *Applied Energy* **2015,** *150* (Supplement C), 335-340.

75. Fang, Y.; Wei, H.; Liang, X.; Wang, S.; Liu, X.; Gao, X.; Zhang, Z., Preparation and Thermal Performance of Silica/n-Tetradecane Microencapsulated Phase Change Material for Cold Energy Storage. *Energy & Fuels* **2016,** *30* (11), 9652-9657.

76. Fang, Y.; Zou, T.; Liang, X.; Wang, S.; Liu, X.; Gao, X.; Zhang, Z., Self-assembly Synthesis and Properties of Microencapsulated n-Tetradecane Phase Change Materials with a Calcium Carbonate Shell for Cold Energy Storage. *ACS Sustainable Chemistry & Engineering* **2017,** *5* (4), 3074-3080.

77. Han, P.; Qiu, X.; Lu, L.; Pan, L., Fabrication and characterization of a new enhanced hybrid shell microPCM for thermal energy storage. *Energy Conversion and Management* **2016,** *126* (Supplement C), 673-685.

78. Taguchi, Y.; Yokoyama, H.; Kado, H.; Tanaka, M., Preparation of PCM microcapsules by using oil absorbable polymer particles. *Colloids and Surfaces A: Physicochemical and Engineering Aspects* 2007, pp 41-47.

79. Jiang, Y.; Wang, D.; Zhao, T., Preparation, characterization, and prominent thermal stability of phase-change microcapsules with phenolic resin shell and n-hexadecane core. *Journal of applied polymer science* **2007,** *104* (5), 2799-2806.

80. Yafei, A.; Yong, J.; Jing, S.; Deqing, W., Microencapsulation of n-hexadecane as phase change material by suspension polymerization. *e-Polymers* **2007,** *7* (1), 1124-1132.

81. Onder, E.; Sarier, N.; Cimen, E., Encapsulation of phase change materials by complex coacervation to improve thermal performances of woven fabrics. *Thermochimica Acta* **2008,** *467* (1), 63-72.

82. Alay, S.; Alkan, C.; Göde, F., Synthesis and characterization of poly(methyl methacrylate)/n-hexadecane microcapsules using different cross-linkers and their application to some fabrics. *Thermochimica Acta* **2011,** *518* (1), 1-8.

83. Alay, S.; Göde, F.; Alkan, C., Synthesis and thermal properties of poly (n-butyl acrylate)/n-hexadecane microcapsules using different cross-linkers and their application to textile fabrics. *Journal of applied polymer science* **2011,** *120* (5), 2821-2829.

84. Tang, X.; Li, W.; Zhang, X.; Shi, H., Fabrication and performances of microencapsulated n-alkanes with copolymers having n-octadecyl side chains as shells. *Industrial & Engineering Chemistry Research* **2014,** *53* (4), 1678-1687.

85. Feczkó, T.; Kardos, A. F.; Németh, B.; Trif, L.; Gyenis, J., Microencapsulation of n-hexadecane phase change material by ethyl cellulose polymer. *Polymer Bulletin* **2014,** *71* (12), 3289-3304.

86. Zhang, Y.; Zheng, X.; Wang, H.; Du, Q., Encapsulated phase change materials stabilized by modified graphene oxide. *Journal of Materials Chemistry A* **2014,** *2* (15), 5304-5314.

87. Wu, B.; Zheng, G.; Chen, X., Effect of graphene on the thermophysical properties of melamine-urea-formaldehyde/N-hexadecane microcapsules. *RSC Advances* **2015,** *5* (90), 74024-74031.

88. Sarier, N.; Onder, E.; Ukuser, G., Silver incorporated microencapsulation of n-hexadecane and n-octadecane appropriate for dynamic thermal management in textiles. *Thermochimica Acta* **2015,** *613*, 17-27.

89. Alkan, C.; Aksoy, S. A.; Anayurt, R. A., Synthesis of poly(methyl methacrylate-co-acrylic acid)/n-eicosane microcapsules for thermal comfort in textiles. *Textile Research Journal* **2015,** *85* (19), 2051-2058.

90. Lashgari, S.; Arabi, H.; Mahdavian, A. R.; Ambrogi, V., Thermal and morphological studies on novel PCM microcapsules containing n-hexadecane as the core in a flexible shell. *Applied Energy* **2017,** *190* (Supplement C), 612-622.

91. Sarı, A.; Alkan, C.; Karaipekli, A., Preparation, characterization and thermal properties of PMMA/n-heptadecane microcapsules as novel solid–liquid microPCM for thermal energy storage. *Applied Energy* **2010,** *87* (5), 1529-1534.

92. He, F.; Wang, X.; Wu, D., Phase-change characteristics and thermal performance of form-stable n-alkanes/silica composite phase change materials fabricated by sodium silicate precursor. *Renewable Energy* **2015,** *74* (Supplement C), 689-698.

93. Li, W.; Zhang, X.-X.; Wang, X.-C.; Niu, J.-J., Preparation and characterization of microencapsulated phase change material with low remnant formaldehyde content. *Materials Chemistry and Physics* **2007,** *106* (2), 437-442.

94. Sarier, N.; Onder, E., The manufacture of microencapsulated phase change materials suitable for the design of thermally enhanced fabrics. *Thermochimica Acta* **2007,** *452* (2), 149-160.

95. Fei, B.; Lu, H.; Qi, K.; Shi, H.; Liu, T.; Li, X.; Xin, J. H., Multi-functional microcapsules produced by aerosol reaction. *Journal of Aerosol Science* **2008,** *39* (12), 1089-1098.

96. Zhang, H.; Wang, X., Fabrication and performances of microencapsulated phase change materials based on n-octadecane core and resorcinol-modified melamine–formaldehyde shell. *Colloids and Surfaces A: Physicochemical and Engineering Aspects* **2009,** *332* (2), 129-138.

97. Zhang, H.; Wang, X., Synthesis and properties of microencapsulated n-octadecane with polyurea shells containing different soft segments for heat energy storage and thermal regulation. *Solar Energy Materials and Solar Cells* **2009,** *93* (8), 1366-1376.

98. Gong, C.; Zhang, H.; Wang, X., Effect of shell materials on microstructure and properties of microencapsulated n-octadecane. *Iranian Polymer Journal* **2009,** *18* (6), 501-512.

99. Zhang, H.; Wang, X.; Wu, D., Silica encapsulation of n-octadecane via sol–gel process: A novel microencapsulated phase-change material with enhanced thermal conductivity and performance. *Journal of Colloid and Interface Science* **2010,** *343* (1), 246-255.

100. Zhang, H.; Sun, S.; Wang, X.; Wu, D., Fabrication of microencapsulated phase change materials based on n-octadecane core and silica shell through interfacial polycondensation. *Colloids and Surfaces A: Physicochemical and Engineering Aspects* **2011,** *389* (1), 104-117.

101. You, M.; Wang, X.; Zhang, X.; Zhang, L.; Wang, J., Microencapsulated n-Octadecane with

styrene-divinybenzene co-polymer shells. *Journal of Polymer Research* **2011,** *18* (1), 49-58.

102. Zhang, G. H.; Bon, S. A. F.; Zhao, C. Y., Synthesis, characterization and thermal properties of novel nanoencapsulated phase change materials for thermal energy storage. *Solar Energy* **2012,** *86* (5), 1149-1154.

103. Qiu, X.; Li, W.; Song, G.; Chu, X.; Tang, G., Microencapsulated n-octadecane with different methylmethacrylate-based copolymer shells as phase change materials for thermal energy storage. *Energy* **2012,** *46* (1), 188-199.

104. Supatimusro, D.; Promdsorn, S.; Thipsit, S.; Boontung, W.; Chaiyasat, P.; Chaiyasat, A., Poly(divinylbenzene) Microencapsulated Octadecane for Use as a Heat Storage Material: Influences of Microcapsule Size and Monomer/Octadecane Ratio. *Polymer-Plastics Technology and Engineering* **2012,** *51* (11), 1167-1172.

105. Qiu, X.; Li, W.; Song, G.; Chu, X.; Tang, G., Fabrication and characterization of microencapsulated n-octadecane with different crosslinked methylmethacrylate-based polymer shells. *Solar Energy Materials and Solar Cells* **2012,** *98* (Supplement C), 283-293.

106. Lone, S.; Lee, H. M.; Kim, G. M.; Koh, W.-G.; Cheong, I. W., Facile and highly efficient microencapsulation of a phase change material using tubular microfluidics. *Colloids and Surfaces A: Physicochemical and Engineering Aspects* **2013,** *422* (Supplement C), 61-67.

107. Wang, H.; Wang, J. P.; Wang, X.; Li, W.; Zhang, X., Preparation and Properties of Microencapsulated Phase Change Materials Containing Two-Phase Core Materials. *Industrial & Engineering Chemistry Research* **2013,** *52* (41), 14706-14712.

108. Qiu, X.; Song, G.; Chu, X.; Li, X.; Tang, G., Microencapsulated n-alkane with p(n-butyl methacrylate-co-methacrylic acid) shell as phase change materials for thermal energy storage. *Solar Energy* **2013,** *91* (Supplement C), 212-220.

109. Qiu, X.; Song, G.; Chu, X.; Li, X.; Tang, G., Preparation, thermal properties and thermal reliabilities of microencapsulated n-octadecane with acrylic-based polymer shells for thermal energy storage. *Thermochimica Acta* **2013,** *551* (Supplement C), 136-144.

110. Yu, S.; Wang, X.; Wu, D., Microencapsulation of n-octadecane phase change material with calcium carbonate shell for enhancement of thermal conductivity and serving durability: Synthesis, microstructure, and performance evaluation. *Applied Energy* **2014,** *114* (Supplement C), 632-643.

111. He, F.; Wang, X.; Wu, D., New approach for sol–gel synthesis of microencapsulated n-octadecane phase change material with silica wall using sodium silicate precursor. *Energy* **2014,** *67* (Supplement C), 223-233.

112. Qiu, X.; Lu, L.; Wang, J.; Tang, G.; Song, G., Preparation and characterization of microencapsulated n-octadecane as phase change material with different n-butyl methacrylate-based copolymer shells. *Solar Energy Materials and Solar Cells* **2014,** *128* (Supplement C), 102-111.

113. Qiu, X.; Lu, L.; Zhang, Z.; Tang, G.; Song, G., Preparation, thermal property, and thermal stability of microencapsulated n-octadecane with poly(stearyl methacrylate) as shell. *Journal of Thermal Analysis and Calorimetry* **2014,** *118* (3), 1441-1449.

114. Tang, X.; Li, W.; Zhang, X.; Shi, H., Fabrication and characterization of microencapsulated phase change material with low supercooling for thermal energy storage. *Energy* **2014,** *68* (Supplement C), 160-166.

115. Iamphaojeen, Y.; Siriphannon, P., Nanoencapsulation of n-Octadecane Phase Change Material in Self-Assembled Polyelectrolyte by Soft Solution Technique. *International Journal of Polymeric Materials and Polymeric Biomaterials* **2014,** *63* (17), 918-922.

116. Li, W.; Song, G.; Li, S.; Yao, Y.; Tang, G., Preparation and characterization of novel MicroPCMs (microencapsulated phase-change materials) with hybrid shells via the polymerization of two alkoxy silanes. *Energy* **2014,** *70* (Supplement C), 298-306.

117. Yuan, W.-J.; Wang, Y.-P.; Li, W.; Wang, J.-P.; Zhang, X.-X.; Zhang, Y.-K., Microencapsulation and characterization of polyamic acid microcapsules containing n-octadecane via electrospraying method. *Materials Express* **2015,** *5* (6), 480-488.

118. Qiu, X.; Lu, L.; Wang, J.; Tang, G.; Song, G., Fabrication, thermal properties and thermal stabilities of microencapsulated n-alkane with poly(lauryl methacrylate) as shell. *Thermochimica Acta* **2015,** *620*, 10-17.

119. Wu, Q.; Zhao, D.; Jiao, X.; Zhang, Y.; Shea, K. J.; Lu, X.; Qiu, G., Preparation, Properties, and Supercooling Prevention of Phase Change Material n-Octadecane Microcapsules with Peppermint Fragrance Scent. *Industrial & Engineering Chemistry Research* **2015,** *54* (33), 8130-8136.

120. Yang, Y.; Ye, X.; Luo, J.; Song, G.; Liu, Y.; Tang, G., Polymethyl methacrylate based phase change microencapsulation for solar energy storage with silicon nitride. *Solar Energy* **2015,** *115*, 289-296.

121. Zhu, Y.; Liang, S.; Chen, K.; Gao, X.; Chang, P.; Tian, C.; Wang, J.; Huang, Y., Preparation and properties of nanoencapsulated n-octadecane phase change material with organosilica shell for thermal energy storage. *Energy Conversion and Management* **2015,** *105* (Supplement C), 908-917.

122. Liang, S.; Li, Q.; Zhu, Y.; Chen, K.; Tian, C.; Wang, J.; Bai, R., Nanoencapsulation of n-octadecane phase change material with silica shell through interfacial hydrolysis and polycondensation in miniemulsion. *Energy* **2015,** *93* (Part 2), 1684-1692.

123. Tang, F.; Liu, L.; Alva, G.; Jia, Y.; Fang, G., Synthesis and properties of microencapsulated octadecane with silica shell as shape–stabilized thermal energy storage materials. *Solar Energy Materials and Solar Cells* **2017,** *160* (Supplement C), 1-6.

124. Zhao, L.; Wang, H.; Luo, J.; Liu, Y.; Song, G.; Tang, G., Fabrication and properties of microencapsulated n-octadecane with TiO2 shell as thermal energy storage materials. *Solar Energy* **2016,** *127* (Supplement C), 28-35.

125. Wang, H.; Zhao, L.; Chen, L.; Song, G.; Tang, G., Facile and low energy consumption synthesis of microencapsulated phase change materials with hybrid shell for thermal energy storage. *Journal of Physics and Chemistry of Solids* **2017,** *111* (Supplement C), 207-213.

126. Lu, S.; Shen, T.; Xing, J.; Song, Q.; Xin, C., Preparation, characterization, and thermal stability of double-composition shell microencapsulated phase change material by interfacial polymerization. *Colloid and Polymer Science* **2017,** *295* (10), 2061-2067.

127. Wu, G.; Hu, C.; Cui, J.; Chen, S.-C.; Wang, Y.-Z., Concurrent Superhydrophobicity and Thermal Energy Storage of Microcapsule with Superior Thermal Stability and Durability. *ACS Sustainable Chemistry & Engineering* **2017,** *5* (9), 7759-7767.

128. Wang, X.; Zhao, T., Effects of parameters of the shell formation process on the performance of microencapsulated phase change materials based on melamine-formaldehyde. *Textile Research Journal* **2017,** *87* (15), 1848-1859.

129. Zhao, J.; Yang, Y.; Li, Y.; Zhao, L.; Wang, H.; Song, G.; Tang, G., Microencapsulated phase change materials with TiO2-doped PMMA shell for thermal energy storage and UV-shielding. *Solar Energy Materials and Solar Cells* **2017,** *168* (Supplement C), 62-68.

130. Li, G.; Li, W., Synthesis and characterization of microencapsulated n-octadecane with hybrid shells containing

3-(trimethoxysilyl) propyl methacrylate and methyl methacrylate. *Journal of Thermal Analysis and Calorimetry* **2017,** *129* (2), 915-924.

131. Niu, X.; Xu, Q.; Zhang, Y.; Zhang, Y.; Yan, Y.; Liu, T., Fabrication and Properties of Micro-Nanoencapsulated Phase Change Materials for Internally-Cooled Liquid Desiccant Dehumidification. *Nanomaterials* **2017,** *7* (5), 96.

132. Huang, Y.-T.; Zhang, H.; Wan, X.-J.; Chen, D.-Z.; Chen, X.-F.; Ye, X.; Ouyang, X.; Qin, S.-Y.; Wen, H.-X.; Tang, J.-N., Carbon nanotube-enhanced double-walled phase-change microcapsules for thermal energy storage. *Journal of Materials Chemistry A* **2017,** *5* (16), 7482-7493.

133. Alay Aksoy, S.; Alkan, C.; Tözüm, M. S.; Demirbağ, S.; Altun Anayurt, R.; Ulcay, Y., Preparation and textile application of poly(methyl methacrylate-co-methacrylic acid)/n-octadecane and n-eicosane microcapsules. *The Journal of The Textile Institute* **2017,** *108* (1), 30-41.

134. Wang, H.; Luo, J.; Yang, Y.; Zhao, L.; Song, G.; Tang, G., Fabrication and characterization of microcapsulated phase change materials with an additional function of thermochromic performance. *Solar Energy* **2016,** *139* (Supplement C), 591-598.

135. Li, D.; Wang, J.; Wang, Y.; Li, W.; Wang, X.; Shi, H.; Zhang, X., Effect of N-isopropylacrylamide on the preparation and properties of microencapsulated phase change materials. *Energy* **2016,** *106* (Supplement C), 221-230.

136. Li, W.; Zong, J.; Huang, R.; Wang, J.; Wang, N.; Han, N.; Zhang, X., Design, controlled fabrication and characterization of narrow-disperse macrocapsules containing Micro/NanoPCMs. *Materials & Design* **2016,** *99* (Supplement C), 225-234.

137. Zhao, L.; Luo, J.; Wang, H.; Song, G.; Tang, G., Self-assembly fabrication of microencapsulated n-octadecane with natural silk fibroin shell for thermal-regulating textiles. *Applied Thermal Engineering* **2016,** *99*, 495-501.

138. Luo, J.; Zhao, L.; Yang, Y.; Song, G.; Liu, Y.; Chen, L.; Tang, G., Emulsifying ability and cross-linking of silk fibroin microcapsules containing phase change materials. *Solar Energy Materials and Solar Cells* **2016,** *147* (Supplement C), 144-149.

139. Sarı, A.; Alkan, C.; Biçer, A.; Altuntaş, A.; Bilgin, C., Micro/nanoencapsulated n-nonadecane with poly(methyl methacrylate) shell for thermal energy storage. *Energy Conversion and Management* **2014,** *86* (Supplement C), 614-621.

140. Moghaddam, M. K.; Mortazavi, S. M.; Khayamian, T., Preparation of calcium alginate microcapsules containing n-nonadecane by a melt coaxial electrospray method. *Journal of Electrostatics* **2015,** *73* (Supplement C), 56-64.

141. Kamali Moghaddam, M.; Mortazavi, S. M., Preparation, characterisation and thermal properties of calcium alginate/n-nonadecane microcapsules fabricated by electro-coextrusion for thermo-regulating textiles. *Journal of microencapsulation* **2015,** *32* (8), 737-744.

142. Alkan, C.; Sarı, A.; Karaipekli, A., Preparation, thermal properties and thermal reliability of microencapsulated n-eicosane as novel phase change material for thermal energy storage. *Energy Conversion and Management* **2011,** *52* (1), 687-692.

143. Phadungphatthanakoon, S.; Poompradub, S.; Wanichwecharungruang, S. P., Increasing the Thermal Storage Capacity of a Phase Change Material by Encapsulation: Preparation and Application in Natural Rubber. *ACS Applied Materials & Interfaces* **2011,** *3* (9), 3691-3696.

144. Fortuniak, W.; Slomkowski, S.; Chojnowski, J.; Kurjata, J.; Tracz, A.; Mizerska, U., Synthesis of a paraffin

phase change material microencapsulated in a siloxane polymer. *Colloid Polym Sci* **2013,** *291* (3), 725-733.

145. Jiang, F.; Wang, X.; Wu, D., Design and synthesis of magnetic microcapsules based on n-eicosane core and Fe3O4/SiO2 hybrid shell for dual-functional phase change materials. *Applied Energy* **2014,** *134* (Supplement C), 456-468.

146. Yu, S.; Wang, X.; Wu, D., Self-assembly synthesis of microencapsulated n-eicosane phase-change materials with crystalline-phase-controllable calcium carbonate shell. *Energy & Fuels* **2014,** *28* (5), 3519-3529.

147. Mohaddes, F.; Islam, S.; Shanks, R.; Fergusson, M.; Wang, L.; Padhye, R., Modification and evaluation of thermal properties of melamine-formaldehyde/n-eicosane microcapsules for thermo-regulation applications. *Applied Thermal Engineering* **2014,** *71* (1), 11-15.

148. Chai, L.; Wang, X.; Wu, D., Development of bifunctional microencapsulated phase change materials with crystalline titanium dioxide shell for latent-heat storage and photocatalytic effectiveness. *Applied Energy* **2015,** *138* (Supplement C), 661-674.

149. Li, F.; Wang, X.; Wu, D., Fabrication of multifunctional microcapsules containing n-eicosane core and zinc oxide shell for low-temperature energy storage, photocatalysis, and antibiosis. *Energy Conversion and Management* **2015,** *106* (Supplement C), 873-885.

150. Zhang, Y.; Wang, X.; Wu, D., Design and fabrication of dual-functional microcapsules containing phase change material core and zirconium oxide shell with fluorescent characteristics. *Solar Energy Materials and Solar Cells* **2015,** *133* (Supplement C), 56-68.

151. Jiang, B.; Wang, X.; Wu, D., Fabrication of microencapsulated phase change materials with TiO2/Fe3O4 hybrid shell as thermoregulatory enzyme carriers: A novel design of applied energy microsystem for bioapplications. *Applied Energy* **2017,** *201* (Supplement C), 20-33.

152. Zhang, Y.; Wang, X.; Wu, D., Microencapsulation of n-dodecane into zirconia shell doped with rare earth: Design and synthesis of bifunctional microcapsules for photoluminescence enhancement and thermal energy storage. *Energy* **2016,** *97* (Supplement C), 113-126.

153. Gao, F.; Wang, X.; Wu, D., Design and fabrication of bifunctional microcapsules for solar thermal energy storage and solar photocatalysis by encapsulating paraffin phase change material into cuprous oxide. *Solar Energy Materials and Solar Cells* **2017,** *168* (Supplement C), 146-164.

154. Liu, H.; Wang, X.; Wu, D., Fabrication of Graphene/TiO2/Paraffin Composite Phase Change Materials for Enhancement of Solar Energy Efficiency in Photocatalysis and Latent Heat Storage. *ACS Sustainable Chemistry & Engineering* **2017,** *5* (6), 4906-4915.

155. Zhang, X.; Wang, X.; Wu, D., Design and synthesis of multifunctional microencapsulated phase change materials with silver/silica double-layered shell for thermal energy storage, electrical conduction and antimicrobial effectiveness. *Energy* **2016,** *111* (Supplement C), 498-512.

156. Demirba, S.; Aksoy, S. A., Encapsulation of phase change materials by complex coacervation to improve thermal performances and flame retardant properties of the cotton fabrics. *Fibers and Polymers* **2016,** *17* (3), 408.

157. Genc, E.; Aksoy, S. A., FABRICATION OF MICROENCAPSULATED PCMs WITH NANOCLAY DOPED CHITOSAN SHELL AND THEIR APPLICATION TO COTTON FABRIC. *Tekst. Konfeksiyon* **2016,** *26* (2), 180-188.

158. Sarı, A.; Alkan, C.; Biçer, A., Thermal energy storage characteristics of micro-nanoencapsulated heneicosane and octacosane with poly(methylmethacrylate) shell. *Journal of Microencapsulation* **2016,** *33* (3), 221-228.

159. Alkan, C.; Sarı, A.; Karaipekli, A.; Uzun, O., Preparation, characterization, and thermal properties of microencapsulated phase change material for thermal energy storage. *Solar Energy Materials and Solar Cells* **2009,** *93* (1), 143-147.

160. De Castro, P. F.; Ahmed, A.; Shchukin, D. G., Confined-Volume Effect on the Thermal Properties of Encapsulated Phase Change Materials for Thermal Energy Storage. *Chemistry-A European Journal* **2016,** *22* (13), 4389-4394.

161. Li, J.; Liu, H.; Wang, X.; Wu, D., Development of Thermoregulatory Enzyme Carriers Based on Microencapsulated n-Docosane Phase Change Material for Biocatalytic Enhancement of Amylases. *ACS Sustainable Chemistry & Engineering* **2017,** *5* (9), 8396-8406.

162. Sarı, A.; Alkan, C.; Karaipekli, A.; Uzun, O., Microencapsulated n-octacosane as phase change material for thermal energy storage. *Solar Energy* **2009,** *83* (10), 1757-1763.

163. Fang, Y.; Liu, X.; Liang, X.; Liu, H.; Gao, X.; Zhang, Z., Ultrasonic synthesis and characterization of polystyrene/n-dotriacontane composite nanoencapsulated phase change material for thermal energy storage. *Applied Energy* **2014,** *132* (Supplement C), 551-556.

164. Sánchez, L.; Sánchez, P.; de Lucas, A.; Carmona, M.; Rodríguez, J. F., Microencapsulation of PCMs with a polystyrene shell. *Colloid and Polymer Science* **2007,** *285* (12), 1377-1385.

165. Jin, Z.; Wang, Y.; Liu, J.; Yang, Z., Synthesis and properties of paraffin capsules as phase change materials. *Polymer* **2008,** *49* (12), 2903-2910.

166. Fang, G.; Chen, Z.; Li, H., Synthesis and properties of microencapsulated paraffin composites with SiO2 shell as thermal energy storage materials. *Chemical Engineering Journal* **2010,** *163* (1), 154-159.

167. Sánchez-Silva, L.; Rodríguez, J. F.; Romero, A.; Borreguero, A. M.; Carmona, M.; Sánchez, P., Microencapsulation of PCMs with a styrene-methyl methacrylate copolymer shell by suspension-like polymerisation. *Chemical Engineering Journal* **2010,** *157* (1), 216-222.

168. Ma, S.; Song, G.; Li, W.; Fan, P.; Tang, G., UV irradiation-initiated MMA polymerization to prepare microcapsules containing phase change paraffin. *Solar Energy Materials and Solar Cells* **2010,** *94* (10), 1643-1647.

169. Wang, Y.; Shi, H.; Xia, T. D.; Zhang, T.; Feng, H. X., Fabrication and performances of microencapsulated paraffin composites with polymethylmethacrylate shell based on ultraviolet irradiation-initiated. *Materials Chemistry and Physics* **2012,** *135* (1), 181-187.

170. Chen, L.; Zhang, L. Q.; Tang, R. F.; Lu, Y. L., Synthesis and thermal properties of phase-change microcapsules incorporated with nano alumina particles in the shell. *Journal of Applied Polymer Science* **2012,** *124* (1), 689-698.

171. Zhang, M.; Tong, X. M.; Zhang, H.; Qiu, J. H., Preparation and Characterization of Poly (MMA-co-AA)/Paraffin Microencapsulated Phase Change Material for Thermal Energy Storage. *Energy Sources, Part A: Recovery, Utilization, and Environmental Effects* **2012,** *34* (5), 396-403.

172. Li, B.; Liu, T.; Hu, L.; Wang, Y.; Gao, L., Fabrication and Properties of Microencapsulated Paraffin@SiO2 Phase Change Composite for Thermal Energy Storage. *ACS Sustainable Chemistry & Engineering* **2013,** *1* (3), 374-380.

173. de Cortazar, M. G.; Rodríguez, R., Thermal storage nanocapsules by miniemulsion polymerization. *Journal of Applied Polymer Science* **2013,** *127* (6), 5059-5064.

174. Wei, J.; Li, Z.; Liu, L.; Liu, X., Preparation and characterization of novel polyamide paraffin MEPCM by interfacial polymerization technique. *Journal of Applied Polymer Science* **2013,** *127* (6), 4588-4593.

175. Chen, Z.; Cao, L.; Fang, G.; Shan, F., Synthesis and Characterization of Microencapsulated Paraffin Microcapsules as Shape-Stabilized Thermal Energy Storage Materials. *Nanoscale and Microscale Thermophysical Engineering* **2013,** *17* (2), 112-123.

176. Wang, J.; Sun, K.; Wang, J.; Guo, Y., Preparation of PLA-Coated Energy Storage Microcapsules and Its Application in Polyethylene Composites. *Polymer-Plastics Technology and Engineering* **2013,** *52* (12), 1235-1241.

177. Cao, L.; Tang, F.; Fang, G., Synthesis and characterization of microencapsulated paraffin with titanium dioxide shell as shape-stabilized thermal energy storage materials in buildings. *Energy and Buildings* **2014,** *72* (Supplement C), 31-37.

178. Park, S.; Lee, Y.; Kim, Y. S.; Lee, H. M.; Kim, J. H.; Cheong, I. W.; Koh, W.-G., Magnetic nanoparticle-embedded PCM nanocapsules based on paraffin core and polyurea shell. *Colloids and Surfaces A: Physicochemical and Engineering Aspects* **2014,** *450* (Supplement C), 46-51.

179. Silakhori, M.; Metselaar, H. S. C.; Mahlia, T. M. I.; Fauzi, H., Preparation and characterisation of microencapsulated paraffin wax with polyaniline-based polymer shells for thermal energy storage. *Materials Research Innovations* **2014,** *18* (sup6), S6-480-S6-484.

180. Xin, C.; Tian, Y.; Wang, Y.; Huang, X. a., Effect of curing temperature on the performance of microencapsulated low melting point paraffin using urea-formaldehyde resin as a shell. *Textile Research Journal* **2014,** *84* (8), 831-839.

181. Li, M.; Chen, M.; Wu, Z., Enhancement in thermal property and mechanical property of phase change microcapsule with modified carbon nanotube. *Applied Energy* **2014,** *127* (Supplement C), 166-171.

182. Qiu, X.; Lu, L.; Chen, Z., Preparation and characterization of flame retardant phase change materials by microencapsulated paraffin and diethyl ethylphosphonate with poly (methacrylic acid-co-ethyl methacrylate) shell. *Journal of Applied Polymer Science* **2015,** *132* (17).

183. Luo, R.; Wang, S.; Wang, T.; Zhu, C.; Nomura, T.; Akiyama, T., Fabrication of paraffin@SiO2 shape-stabilized composite phase change material via chemical precipitation method for building energy conservation. *Energy and Buildings* **2015,** *108* (Supplement C), 373-380.

184. Do, T.; Ko, Y. G.; Chun, Y.; Choi, U. S., Encapsulation of Phase Change Material with Water-Absorbable Shell for Thermal Energy Storage. *ACS Sustainable Chemistry & Engineering* **2015,** *3* (11), 2874-2881.

185. Giro-Paloma, J.; Konuklu, Y.; Fernández, A. I., Preparation and exhaustive characterization of paraffin or palmitic acid microcapsules as novel phase change material. *Solar Energy* **2015,** *112* (Supplement C), 300-309.

186. Yuan, K.; Wang, H.; Liu, J.; Fang, X.; Zhang, Z., Novel slurry containing graphene oxide-grafted microencapsulated phase change material with enhanced thermo-physical properties and photo-thermal performance. *Solar Energy Materials and Solar Cells* **2015,** *143* (Supplement C), 29-37.

187. Shi, J.; Wu, X.; Fu, X.; Sun, R., Synthesis and thermal properties of a novel nanoencapsulated phase change material with PMMA and SiO2 as hybrid shell materials. *Thermochimica Acta* **2015,** *617* (Supplement C), 90-94.

188. Zhang, L.; Yang, W.; Jiang, Z.; He, F.; Zhang, K.; Fan, J.; Wu, J., Graphene oxide-modified microencapsulated phase change materials with high encapsulation capacity and enhanced leakage-prevention performance. *Applied Energy* **2017,** *197* (Supplement C), 354-363.

189. Wan, X.; Guo, B.; Xu, J., A facile hydrothermal preparation for phase change materials microcapsules with a pliable self-recovering shell and study on its thermal energy storage properties. *Powder Technology* **2017,** *312* (Supplement C), 144-151.

190. Su, W.; Darkwa, J.; Kokogiannakis, G., Development of microencapsulated phase change material for solar thermal energy storage. *Applied Thermal Engineering* **2017,** *112* (Supplement C), 1205-1212.

191. Liu, J.; Chen, L.; Fang, X.; Zhang, Z., Preparation of graphite nanoparticles-modified phase change microcapsules and their dispersed slurry for direct absorption solar collectors. *Solar Energy Materials and Solar Cells* **2017,** *159* (Supplement C), 159-166.

192. Sun, N.; Xiao, Z., Synthesis and Performances of Phase Change Materials Microcapsules with a Polymer/BN/TiO2 Hybrid Shell for Thermal Energy Storage. *Energy & Fuels* **2017,** *31* (9), 10186-10195.

193. Zhang, J.; Zhao, T.; Chai, Y.; Wang, L., Preparation and Characterization of High Content Paraffin Wax Microcapsules and Micro/Nanocapsules with Poly Methyl Methacrylate Shell by Suspension-Like Polymerization. *Chinese Journal of Chemistry* **2017,** *35* (4), 497-506.

194. Şahan, N.; Paksoy, H., Determining influences of SiO2 encapsulation on thermal energy storage properties of different phase change materials. *Solar Energy Materials and Solar Cells* **2017,** *159* (Supplement C), 1-7.

195. Li-Ming, D.; Guang-Ling, P., The Influence of Interfacial Tension on the Properties of Phase Change Materials Microcapsules. *Journal of Polymer Materials* **2016,** *33* (4), 697.

196. Qiu, X.; Lu, L.; Han, P.; Tang, G.; Song, G., Fabrication, thermal property and thermal reliability of microencapsulated paraffin with ethyl methacrylate-based copolymer shell. *Journal of Thermal Analysis and Calorimetry* **2016,** *124* (3), 1291-1299.

197. Zhan, S.; Chen, S.; Chen, L.; Hou, W., Preparation and characterization of polyurea microencapsulated phase change material by interfacial polycondensation method. *Powder Technology* **2016,** *292* (Supplement C), 217-222.

198. Liu, C.; Rao, Z.; Li, Y., Composites enhance heat transfer in paraffin/melamine resin microencapsulated phase change materials. *Energy Technology* **2016,** *4* (4), 496-501.

199. Jiang, X.; Luo, R.; Peng, F.; Fang, Y.; Akiyama, T.; Wang, S., Synthesis, characterization and thermal properties of paraffin microcapsules modified with nano-Al2O3. *Applied Energy* **2015,** *137* (Supplement C), 731-737.

200. Al-Shannaq, R.; Farid, M.; Al-Muhtaseb, S.; Kurdi, J., Emulsion stability and cross-linking of PMMA microcapsules containing phase change materials. *Solar Energy Materials and Solar Cells* **2015,** *132* (Supplement C), 311-318.

201. Giro-Paloma, J.; Al-Shannaq, R.; Fernández, A.; Farid, M., Preparation and Characterization of Microencapsulated Phase Change Materials for Use in Building Applications. *Materials* **2016,** *9* (1), 11.

202. Rahman, A.; Dickinson, M. E.; Farid, M. M., Microencapsulation of a PCM through membrane emulsification and nanocompression-based determination of microcapsule strength. *Materials for Renewable and Sustainable Energy* **2012,** *1* (1).

203. Borreguero, A. M.; Valverde, J. L.; Rodríguez, J. F.; Barber, A. H.; Cubillo, J. J.; Carmona, M., Synthesis and characterization of microcapsules containing Rubitherm®RT27 obtained by spray drying. *Chemical Engineering Journal* **2011,** *166* (1), 384-390.

204. Chaiyasat, P.; Noppalit, S.; Okubo, M.; Chaiyasat, A., Innovative synthesis of high performance poly(methyl methacrylate) microcapsules with encapsulated heat storage material by microsuspension iodine transfer polymerization (ms ITP). *Solar Energy Materials and Solar Cells* **2016,** *157* (Supplement C), 996-1003.

205. Wang, T.; Wang, S.; Luo, R.; Zhu, C.; Akiyama, T.; Zhang, Z., Microencapsulation of phase change materials with binary cores and calcium carbonate shell for thermal energy storage. *Applied Energy* **2016,** *171* (Supplement C),

113-119.

206. Wang, T.; Wang, S.; Geng, L.; Fang, Y., Enhancement on thermal properties of paraffin/calcium carbonate phase change microcapsules with carbon network. *Applied Energy* **2016,** *179* (Supplement C), 601-608.

207. Fuensanta, M.; Paiphansiri, U.; Romero-Sánchez, M. D.; Guillem, C.; López-Buendía, Á. M.; Landfester, K., Thermal properties of a novel nanoencapsulated phase change material for thermal energy storage. *Thermochimica Acta* **2013,** *565* (Supplement C), 95-101.

208. Sarı, A.; Alkan, C.; Bilgin, C., Micro/nano encapsulation of some paraffin eutectic mixtures with poly (methyl methacrylate) shell: Preparation, characterization and latent heat thermal energy storage properties. *Applied Energy* **2014,** *136*, 217-227.

209. Sarı, A.; Alkan, C.; Döğüşcü, D. K.; Kızıl, Ç., Micro/nano encapsulated n-tetracosane and n-octadecane eutectic mixture with polystyrene shell for low-temperature latent heat thermal energy storage applications. *Solar Energy* **2015,** *115*, 195-203.

210. Sun, D.; Iqbal, K., Synthesis of functional nanocapsules and their application to cotton fabric for thermal management. *Cellulose* **2017,** *24* (8), 3525-3543.

211. Luo, W. S.; Yu, S. F.; Zhou, J. M. In *Effect of Core/Shell Ratio on Performance of Paraffin/Polyurea Phase Change Microencapsules*, Applied Mechanics and Materials, Trans Tech Publ: 2014; pp 32-35.

212. Al-Shannaq, R.; Kurdi, J.; Al-Muhtaseb, S.; Dickinson, M.; Farid, M., Supercooling elimination of phase change materials (PCMs) microcapsules. *Energy* **2015,** *87* (Supplement C), 654-662.

213. Wei, K.; Ma, B.; Wang, H.; Liu, Y.; Luo, Y., Synthesis and thermal properties of novel microencapsulated phase-change materials with binary cores and epoxy polymer shells. *Polymer Bulletin* **2017,** *74* (2), 359-367.

214. Ma, Y.; Chu, X.; Tang, G.; Yao, Y., Adjusting phase change temperature of microcapsules by regulating their core compositions. *Materials Letters* **2012,** *82*, 39-41.

215. Ma, Y.; Chu, X.; Li, W.; Tang, G., Preparation and characterization of poly(methyl methacrylate-co-divinylbenzene) microcapsules containing phase change temperature adjustable binary core materials. *Solar Energy* **2012,** *86* (7), 2056-2066.

216. Ma, Y.; Chu, X.; Tang, G.; Yao, Y., The effect of different soft segments on the formation and properties of binary core microencapsulated phase change materials with polyurea/polyurethane double shell. *Journal of Colloid and Interface Science* **2013,** *392* (Supplement C), 407-414.

217. Ma, Y.; Sun, S.; Li, J.; Tang, G., Preparation and thermal reliabilities of microencapsulated phase change materials with binary cores and acrylate-based polymer shells. *Thermochimica Acta* **2014,** *588* (Supplement C), 38-46.

218. Feczkó, T.; Trif, L.; Németh, B.; Horák, D., Silica-coated poly(glycidyl methacrylate-ethylene dimethacrylate) beads containing organic phase change materials. *Thermochimica Acta* **2016,** *641* (Supplement C), 24-28.

219. Schmidt, M., Phase Change Materials—latent heat storage for interior climate control. *BASF, Ludwigshafen, Germany* **2007**.

220. Uddin, M. S.; Zhu, H. J.; Hawlader, M. N. A., Effects of cyclic operation on the characteristics of a microencapsulated PCM storage material. *International Journal of Solar Energy* **2002,** *22* (3-4), 105-114.

221. Fabien, S. n., The manufacture of microencapsulated thermal energy storage compounds suitable for smart textile. In *Developments in heat transfer*, InTech: 2011.

222. Cao, F.; Yang, B., Supercooling suppression of microencapsulated phase change materials by optimizing shell

composition and structure. *Applied Energy* **2014,** *113*, 1512-1518.

223. Zhang, G. H.; Zhao, C.-Y., Thermal and rheological properties of microencapsulated phase change materials. *Renewable Energy* **2011,** *36* (11), 2959-2966.

224. Liu, L.; Alva, G.; Jia, Y.; Huang, X.; Fang, G., Dynamic thermal characteristics analysis of microencapsulated phase change suspensions flowing through rectangular mini-channels for thermal energy storage. *Energy and Buildings* **2017,** *134*, 37-51.

225. Giro-Paloma, J.; Oncins, G.; Barreneche, C.; Martínez, M.; Fernández, A. I.; Cabeza, L. F., Physico-chemical and mechanical properties of microencapsulated phase change material. *Applied energy* **2013,** *109*, 441-448.

226. Giro-Paloma, J.; Barreneche, C.; Martínez, M.; Šumiga, B.; Fernández, A. I.; Cabeza, L. F., Mechanical response evaluation of microcapsules from different slurries. *Renewable Energy* **2016,** *85*, 732-739.

227. Zhang, S.; Niu, J., Experimental investigation of effects of supercooling on microencapsulated phase-change material (MPCM) slurry thermal storage capacities. *Solar Energy Materials and Solar Cells* **2010,** *94* (6), 1038-1048.

228. Huang, M. J.; Eames, P. C.; McCormack, S.; Griffiths, P.; Hewitt, N. J., Microencapsulated phase change slurries for thermal energy storage in a residential solar energy system. *Renewable Energy* **2011,** *36* (11), 2932-2939.

229. Roberts, N. S.; Al-Shannaq, R.; Kurdi, J.; Al-Muhtaseb, S. A.; Farid, M. M., Efficacy of using slurry of metal-coated microencapsulated PCM for cooling in a micro-channel heat exchanger. *Applied Thermal Engineering* **2017,** *122* (Supplement C), 11-18.

230. Goel, M.; Roy, S.; Sengupta, S., Laminar forced convection heat transfer in microcapsulated phase change material suspensions. *International journal of heat and mass transfer* **1994,** *37* (4), 593-604.

231. Chen, L.; Wang, T.; Zhao, Y.; Zhang, X.-R., Characterization of thermal and hydrodynamic properties for microencapsulated phase change slurry (MPCS). *Energy Conversion and Management* **2014,** *79* (Supplement C), 317-333.

232. Chen, B.; Wang, X.; Zeng, R.; Zhang, Y.; Wang, X.; Niu, J.; Li, Y.; Di, H., An experimental study of convective heat transfer with microencapsulated phase change material suspension: Laminar flow in a circular tube under constant heat flux. *Experimental Thermal and Fluid Science* **2008,** *32* (8), 1638-1646.

233. Sabbah, R.; Farid, M. M.; Al-Hallaj, S., Micro-channel heat sink with slurry of water with micro-encapsulated phase change material: 3D-numerical study. *Applied Thermal Engineering* **2008,** *29* (2), 445-454.

234. Qiu, Z.; Ma, X.; Li, P.; Zhao, X.; Wright, A., Micro-encapsulated phase change material (MPCM) slurries: Characterization and building applications. *Renewable and Sustainable Energy Reviews* **2017,** *77* (Supplement C), 246-262.

235. Song, S.; Shen, W.; Wang, J.; Wang, S.; Xu, J., Experimental study on laminar convective heat transfer of microencapsulated phase change material slurry using liquid metal with low melting point as carrying fluid. *International Journal of Heat and Mass Transfer* **2014,** *73* (Supplement C), 21-28.

236. Kong, M.; Alvarado, J. L.; Terrell Jr, W.; Thies, C., Performance characteristics of microencapsulated phase change material slurry in a helically coiled tube. *International Journal of Heat and Mass Transfer* **2016,** *101*, 901-914.

237. Zhang, S.; Niu, J., Two performance indices of TES apparatus: Comparison of MPCM slurry vs. stratified water storage tank. *Energy and Buildings* **2016,** *127* (Supplement C), 512-520.

238. Qiu, Z.; Ma, X.; Zhao, X.; Li, P.; Ali, S., Experimental investigation of the energy performance of a novel

Micro-encapsulated Phase Change Material (MPCM) slurry based PV/T system. *Applied Energy* **2016,** *165*, 260-271.

239. Kong, M.; Alvarado, J. L.; Thies, C.; Morefield, S.; Marsh, C. P., Field evaluation of microencapsulated phase change material slurry in ground source heat pump systems. *Energy* **2017,** *122*, 691-700.

240. Cabeza, L. F.; Castellon, C.; Nogues, M.; Medrano, M.; Leppers, R.; Zubillaga, O., Use of microencapsulated PCM in concrete walls for energy savings. *Energy and Buildings* **2007,** *39* (2), 113-119.

241. Aguayo, M.; Das, S.; Maroli, A.; Kabay, N.; Mertens, J. C.; Rajan, S. D.; Sant, G.; Chawla, N.; Neithalath, N., The influence of microencapsulated phase change material (PCM) characteristics on the microstructure and strength of cementitious composites: Experiments and finite element simulations. *Cement and Concrete Composites* **2016,** *73*, 29-41.

242. Cao, V. D.; Pilehvar, S.; Salas-Bringas, C.; Szczotok, A. M.; Rodriguez, J. F.; Carmona, M.; Al-Manasir, N.; Kjøniksen, A.-L., Microencapsulated phase change materials for enhancing the thermal performance of Portland cement concrete and geopolymer concrete for passive building applications. *Energy Conversion and Management* **2017,** *133*, 56-66.

243. Wei, Z.; Falzone, G.; Wang, B.; Thiele, A.; Puerta-Falla, G.; Pilon, L.; Neithalath, N.; Sant, G., The durability of cementitious composites containing microencapsulated phase change materials. *Cement and Concrete Composites* **2017,** *81*, 66-76.

244. Young, B. A.; Wei, Z.; Rubalcava-Cruz, J.; Falzone, G.; Kumar, A.; Neithalath, N.; Sant, G.; Pilon, L., A general method for retrieving thermal deformation properties of microencapsulated phase change materials or other particulate inclusions in cementitious composites. *Materials & Design* **2017,** *126*, 259-267.

245. Nelson, G., Application of microencapsulation in textiles. *International journal of pharmaceutics* **2002,** *242* (1), 55-62.

246. You, M.; Zhang, X. X.; Li, W.; Wang, X. C., Effects of MicroPCMs on the fabrication of MicroPCMs/polyurethane composite foams. *Thermochimica Acta* **2008,** *472* (1), 20-24.

247. Borreguero, A. M.; Valverde, J. L.; Peijs, T.; Rodríguez, J. F.; Carmona, M., Characterization of rigid polyurethane foams containing microencapsulated Rubitherm® RT27. Part I. *Journal of Materials Science* **2010,** *45* (16), 4462-4469.

248. Borreguero, A. M.; Rodríguez, J. F.; Valverde, J. L.; Arevalo, R.; Peijs, T.; Carmona, M., Characterization of rigid polyurethane foams containing microencapsulated Rubitherm® RT27: catalyst effect. Part II. *Journal of Materials Science* **2011,** *46* (2), 347-356.

249. Borreguero, A. M.; Rodríguez, J. F.; Valverde, J. L.; Peijs, T.; Carmona, M., Characterization of rigid polyurethane foams containing microencapsulted phase change materials: microcapsules type effect. *Journal of Applied Polymer Science* **2013,** *128* (1), 582-590.

250. Serrano, A.; Borreguero, A. M.; Garrido, I.; Rodríguez, J. F.; Carmona, M., Reducing heat loss through the building envelope by using polyurethane foams containing thermoregulating microcapsules. *Applied Thermal Engineering* **2016,** *103* (Supplement C), 226-232.